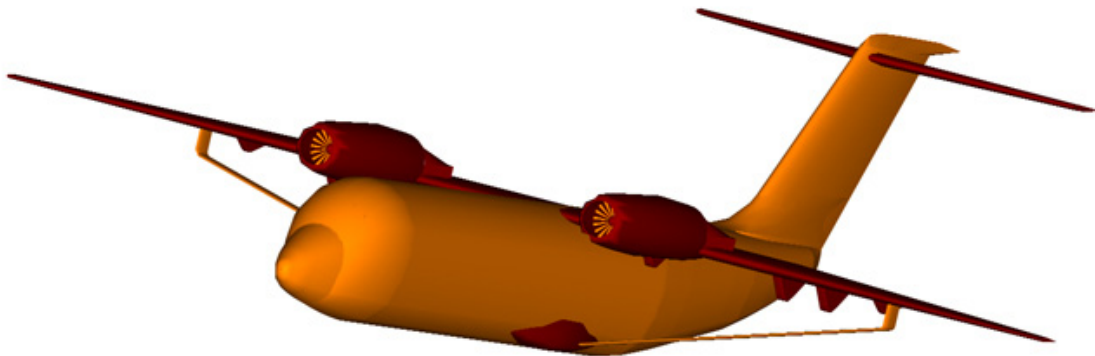


Volant

**An Airport Adaptive Regional Transport
with a Secondary Role to Support
Homeland Security**



**2003-2004 AIAA Undergraduate
Team Aircraft Design**

Volant

“Moving quickly or nimbly...and apt to fly”



Volant Team Roster Spring 2004

Member	AIAA Number	Signature
Steve Froehlich	236946	_____
Heidi Kent	236838	_____
Matt Long	188397	_____
Dzelal Mujezinovic	196933	_____
Andrew Parker	192803	_____
Mike Reilly	200113	_____
Amy Sloan	240759	_____
Jessica Bowen	242047	_____
Faculty Advisor		
Dr. W. H. Mason		_____

Executive Summary

Team Volant presents the Firefly as a solution to the 2003-2004 AIAA Team Undergraduate Design Competition Request for Proposal (RFP) for an Airport Adaptive Regional Transport with a Secondary Role to Support Homeland Security.

The main drivers for this proposal were Short Takeoff and Landing (STOL) capability and cruise efficiency. STOL capability tends to come at the expense of cruise efficiency and, by extension, operational costs. A study of comparator aircraft revealed that current regional jets fail to meet the takeoff and landing distances of 2,500 ft required by the RFP, prompting the need for a powered lift design. Three powered lift systems were identified for investigation: Externally Blown Flaps (EBF), Internally Blown Flaps (IBF), and Upper Surface Blowing (USB). Preliminary analysis and research were conducted for all three systems in the areas of weight, cost, materials, and structures. This process was used to select USB as the high lift system for the Firefly.

The Firefly is a twin engine regional transport, which can be converted to fulfill the secondary role of a government operated emergency vehicle. This aircraft has strut braced, high mounted wings with a slight forward sweep and composite control surfaces. The strut braced design allows for a decreased wing thickness and controls the wing structural divergence caused by the forward sweep. The engines are 3.8% scaled down versions of the GE CF34-8C1 high bypass turbofan and are mounted above the wings to accommodate the USB high lift system. The fuselage has a conventional wedge tail design and a composite skin that utilizes Glare to decrease weight and increase strength. The T-tail is designed with double hinged elevators and rudder composed of carbon-fiber epoxy for greater control authority at low speeds. The landing gear is in a dual tandem configuration with triple pivoting retraction that is accomplished with titanium struts and shocks. The interior layout is designed to hold 49 passengers comfortably, with the ability to accommodate aircraft growth to 65 and 81 passenger models. This layout can also be modified for government use in the secondary missions.

In addition to STOL capability, the Firefly is able to conduct a Simultaneous Non-interfering (SNI) approach, which consists of a 1-nm diameter spiral descent from 5000 ft. This approach allows the Firefly to utilize runways with approach corridors that would normally interfere with the approach or departure corridors or larger runways. By operating from these currently unused runways, the Firefly will alleviate congestion at major airports. Large control surfaces give the Firefly enough control authority to continue the SNI approach even with an engine failure. In addition, the Firefly will employ an automatic flight control system that uses inertial measurement units and differential GPS to estimate position and velocity, and use this information to fly the SNI approach without pilot input if necessary, allowing the Firefly to complete the approach in IMC Cat 3C conditions (zero visibility).

The performance of the Firefly is above and beyond that of a typical regional jet with a combination of USB, forward swept wings, composite materials, and an overall optimized design. The minimum takeoff distance of 2204 ft will reduce the need for larger, overused runways. The composite control surfaces and stall speed of 50 knots allow for operation in a minimal amount of air space. The Firefly combines optimal design with unparalleled performance capability to effectively fill the STOL regional jet and emergency government requirements.

VOLANT PROUDLY PRESENTS...THE FIREFLY.

TYPE: Twin engine regional transport/Government operated emergency vehicle.

WINGS: Forward swept, strut-based, high wing monoplane.

FUSELAGE: Wedge tailed conventional design which utilizes Glare to reduce overall weight and add strength.

TAILS: T-tail design with double hinged elevators and rudder composed of Carbon-fiber epoxy.

LANDING GEAR: Triple pivoting retraction system, braced by Titanium struts and shocks.

POWERPLANT: A 3.77% scaled down version of the GE CF34-8C1 high bypass turbofan engine. Critical high lift generated via upper surface blowing.

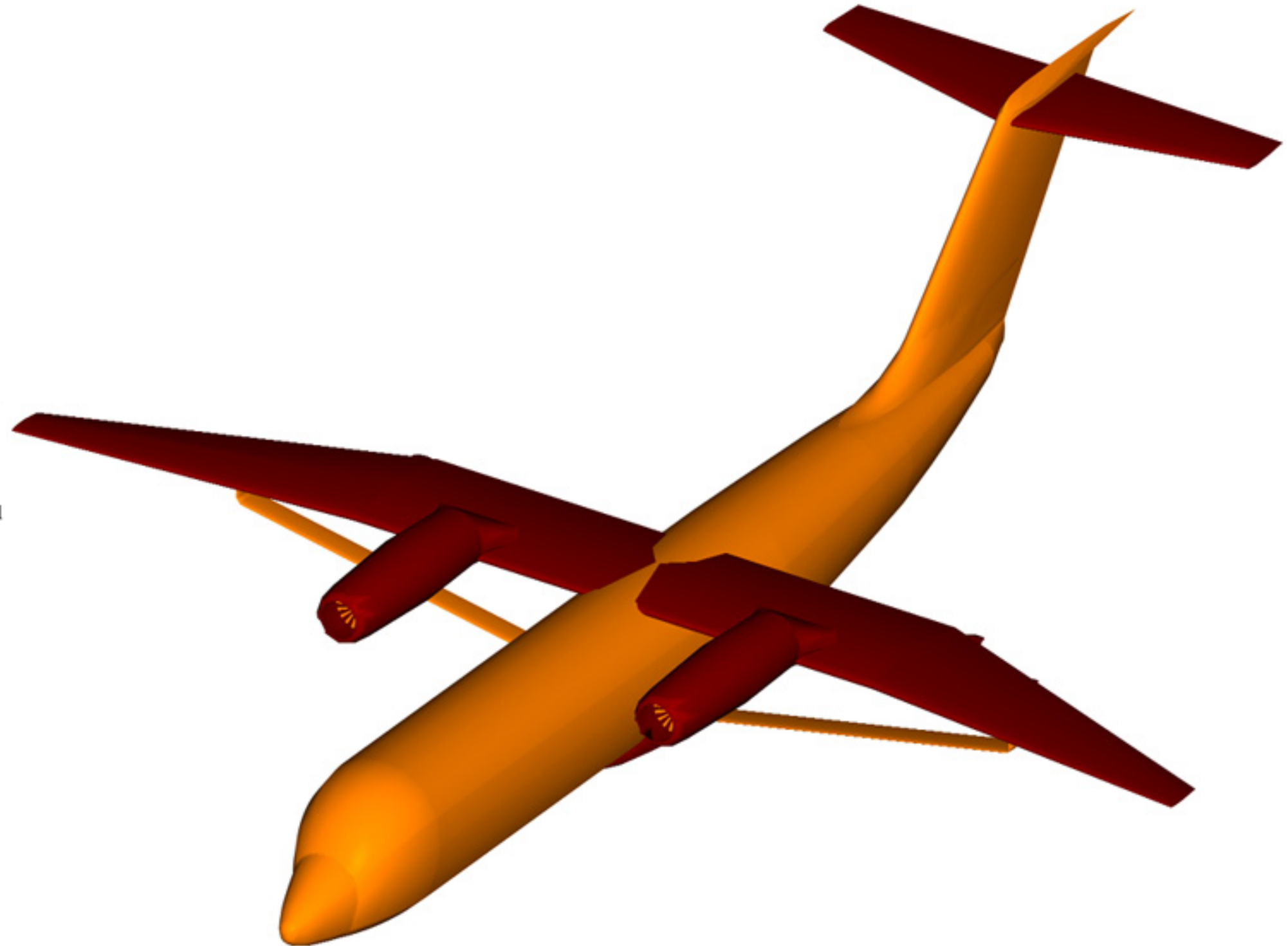
ACCOMODATIONS: An interior layout to hold 49 passengers comfortably. Designed with growth in mind, expandable to 65 and 81 passenger models. Also readily available for government use for the Civil Reserve Fleet.

DIMENSIONS:

Wingspan: 89'-6"
Overall Length: 100'-8"
Overall Height: 29'-11"
Cabin Length: 51'-3"
TOGW (Primary): 53082 lbs.
TOGW (Secondary): 47482 lbs.

PERFORMANCE:

Cruise Speed: 425 kts.
Rate of Climb(S.L.): 8454 fpm
Stall Speed: 50 kts.
Minimum Takeoff Distance: 2204 ft.
Range with Reserves: 1500 nmi.



DRAWING TITLE:

FIREFLY 3D MODEL

DESIGNED BY: **TEAM VOLANT**

DRAFTED BY: **MATT LONG**

SCALE: **NTS**

DATE: **5/7/04**

Table of Contents

Executive Summary	iii
Table of Contents	vi
Index of Tables	viii
Index of Figures	ix
Index of Acronyms	x
Index of Acronyms	x
Index of Symbols	xi
1 Introduction and RFP	1
1.1 Introduction	1
1.2 Request for Proposal Requirements	2
2 Design Drivers	5
2.1 STOL Requirements	5
2.2 Mission Flexibility	8
3 Conceptual Designs	8
3.1 Concept 1 – Externally Blown Flaps	8
3.1.1 Externally Blown Flaps	9
3.1.2 Aft-Swept Wings	9
3.1.3 T-Tail	10
3.1.4 Winglets	10
3.2 Concept 2 – Internally Blown Flaps	11
3.2.1 Internally Blown Flaps	11
3.2.2 Conventional Tail	12
3.3 Concept 3 – Upper Surface Blowing	12
3.3.1 Upper Surface Blowing	13
3.3.2 Strut Braced Wing	14
3.3.3 Forward Swept Wings	14
3.3.4 H-Tail	15
3.4 Selection Criteria and Decision	15
3.5 Sizing Carpet Plot	17
3.6 Selected Configuration	18
3.6.1 Wing Design	20
3.6.2 Aircraft Exits	20
3.6.3 Interior Configurations	20
3.7 Future Expansion	25
4 Aerodynamics	26
4.1 Maximum Attainable Lift	26
4.2 Wing Geometry	30
4.3 Airfoil Analysis	32
4.4 Drag Buildup	34
4.5 Speed Brake	38
4.6 Wing Strut Pylon Juncture	38
5 Propulsion	40
5.1 Engine Selection	40
5.2 Inlet Sizing	42
5.3 Exit Nozzle	43
5.4 Engine Removal	45
5.5 Noise	45
6 Stability and Control	45
6.1 Design Philosophy	46

6.2	Tail Design	46
6.3	Control Surfaces	46
6.4	Stability and Control Derivatives	47
6.5	Dynamic Response and Handling Qualities	48
6.6	SNI Approach	49
6.7	Engine Out and Crosswind	50
6.8	Trim at C_{Lmax}	51
7	Performance	51
7.1	Takeoff and Landing Performance	52
7.2	Rate of Climb, Absolute & Service Ceiling and Time to Climb	53
7.3	Cruise Performance and Level Flight Envelope	55
7.4	Endurance and Loiter Endurance	57
8	Materials and Structures	58
8.1	Material Selections	58
8.2	Structural Requirements	61
8.3	Structural Design	62
8.3.1	Wing Design	64
8.3.2	Strut Design	64
8.3.3	Fuselage Design	65
8.3.4	Tail Design	65
8.3.5	Landing Gear	66
9	Systems	68
9.1	Basic Layout	68
9.2	Cockpit	69
9.3	Flight Controls	71
9.4	Aircraft Lighting and Deicing	72
9.5	Cabin environment	73
9.6	Altitude Warning	73
9.7	Electrical System	73
9.8	Fuel System	74
10	Aircraft Weight Analysis	75
10.1	Aircraft Component Weight	75
10.2	Aircraft Center of Gravity	77
11	Aircraft Cost Analysis	79
11.1	Aircraft Cost Method and Cost Breakdown	79
11.2	Research, Development, Test and Evaluation Cost	79
11.3	Manufacturing Cost	80
11.4	Total Flyaway Cost	81
11.5	Differentiating Consumer and Government Cost	81
12	Conclusion	83
	References	84

Index of Tables

Table 1-1: Main RFP Requirements	2
Table 2-1: Current RJ Specifications and Comparison to RFP Requirements (Ref. 2-1).....	5
Table 2-2: Other RJ Specifications of Interest (Ref. 2-1)	5
Table 3-1: Selection Criteria	16
Table 3-2: Comparison of Concept 3 with Current RJs (Ref. 3-12)	16
Table 4-1: Firefly Cruise Build Up Summary (M = 0.74)	35
Table 4-2: Lift To Drag Ratios	37
Table 4-3: Strut Dimensions	39
Table 5-1: Engine Comparison	41
Table 5-2: Engine Sizing Geometry.....	41
Table 5-3: Inlet Sizing Geometry.....	43
Table 6-1: Flight Conditions for Stability and Control Evaluation.....	47
Table 6-2: Stability and Control Derivatives	47
Table 6-3: Class A and C, Level 1 Handling Qualities.....	48
Table 6-4: Class B, Level 1 Handling Qualities	48
Table 6-5: Necessary Control Deflections	50
Table 7-1: Performance Requirements	52
Table 7-2: BFL Takeoff Length for different surfaces at 5000 ft.....	52
Table 7-3: Landing Distance for different surfaces at 5000 ft.....	53
Table 7-4: Maximum Rate of Climb and Climb Angle	55
Table 7-5: Maximum Range and Optimum Cruise Speed	57
Table 8-1: Material Specifications (Ref. 8-6)	60
Table 8-2: Material Placement.....	61
Table 10-1: Weights and CG for Primary and Secondary Mission.....	76
Table 10-2: Estimated Moments of Inertia	77
Table 11-1: RDT&E Cost Breakdown (in millions of year 2004 USD).....	80
Table 11-2: Manufacturing Cost (in millions of year 2004 USD)	81
Table 11-3: Flyaway Cost (in millions of year 2004 USD).....	81
Table 11-4: Government and Airline Acquisition Costs per Unit (in millions of year 2004 USD)	82
Table 11-5: Breakdown of Operational Costs between Airline and Government (in year 2004 USD).....	82
Table 12-1: Major RFP Requirements	83

Index of Figures

Figure 1-1: Primary Mission Profile and Requirements	3
Figure 1-2: Secondary Mission Profile and Requirements	4
Figure 2-1: Carpet Plot of Stall Speed as a Function of Wing Loading and C_{Lmax}	6
Figure 2-2: Carpet Plot of Landing Distance as a Function of Wing Loading and C_{Lmax}	7
Figure 3-1: Concept 1 (Externally Blown Flaps).....	9
Figure 3-2: Concept 2 (Internally Blown Flaps).....	11
Figure 3-3: Concept 3 (Upper Surface Blowing).....	13
Figure 3-4: Carpet Plot used to Optimize Final Sizing.....	17
Figure 3-5: Firefly General Arrangements.....	19
Figure 3-6: Regional Jet Inboard Profile.....	22
Figure 3-7: Regional Jet Cross Section.....	23
Figure 3-8: Inboard Profile for Firefighter Mission.....	24
Figure 3-9: Cross section for firefighter mission	25
Figure 3-10: Firefly-100, -200, and -300 Series Aircraft.....	26
Figure 4-1: Firefly Wing Cross section, showing USB flap and slat extended	27
Figure 4-2: NASA USB Wind Tunnel Data, $\delta f = 50^\circ$ $\delta s = 40^\circ$, 4 Engines Operating (Ref. 4-1).....	29
Figure 4-3: NASA Wind Tunnel Data, $\delta f = 50^\circ$ $\delta s = 40^\circ$, Outboard Engines Only (Ref. 4-1).	29
Figure 4-4: QSRA Lift Coefficient with a 50° flap deflection (Ref. 4-2)	30
Figure 4-5: Drag Divergence Mach Number	31
Figure 4-6: Firefly Selected Airfoils a) Wing b) Strut c) Vertical Tail d) Horizontal Tail.....	32
Figure 4-7: Firefly Pressure Distribution at Cruise.....	33
Figure 4-8: Skin Friction of the SC(2)-0612 at Cruise Conditions	33
Figure 4-9: Airfoil Drag Divergence	34
Figure 4-10: Firefly Full Configuration Cruise Drag Polar	36
Figure 4-11: Drag Mach Number Relationship	36
Figure 5-1: 3.77% scaled CF34-8C1 Thrust _{Available} /Thrust _{SL-Static} vs. Altitude for Mach 0.74 (Ref. 5-2)	42
Figure 5-2: 3.77% scaled CF34-8C1 Thrust Available vs. Altitude for Mach 0.74 (Ref. 5-2).....	42
Figure 5-3: Engine Exit nozzle Geometry	44
Figure 5-4: Engine Removal	45
Figure 6-1: Feedback Control Loop.....	50
Figure 6-2: Elevator Deflection Required to Trim at C_{Lmax} at Max. Throttle	51
Figure 7-1: Hodograph Diagram.....	54
Figure 7-2: Absolute and Service Ceiling.....	54
Figure 7-3: Specific Range at Various Altitudes for Primary Mission.....	56
Figure 7-4: Specific Range at Various Altitudes for Secondary Mission	56
Figure 7-5: 1-g Operating Envelop	57
Figure 8-1: Material Distribution.....	60
Figure 8-2: V-n Diagram	62
Figure 8-3: Structural Layout.....	63
Figure 8-4: Strut Dampening System.....	65
Figure 8-5: Landing Gear Retraction and Specifications.....	67
Figure 9-1: Aircraft Systems Layout	68
Figure 9-2: Cockpit Dash.....	69
Figure 9-3: Overhead Panel	70
Figure 9-4: Center Console.....	71
Figure 9-5: Fuel Tank Locations.....	74
Figure 10-1: CG Locations	77
Figure 10-2: CG Travel for Primary Mission	78
Figure 10-3: CG Travel for Secondary Mission	78
Figure 11-1: RDT&E Cost Percentage	80

Index of Acronyms

AEECS	All Electrical Environmental Climate System
AIAA	American Institute of Aeronautics and Astronautics
AGL	Above Ground Level
APU	Auxiliary Power Unit
DFW	Dallas Fort Worth Airport
EBF	Externally Blown Flaps
EESS	Electro Expulsive Separation System
EGPWS	Enhanced Ground Proximity Warning System
FAR	Federal Aviation Regulation
IBF	Internally Blown Flaps
IMC	Instrument Meteorological Conditions
LAAS	Local Area Augmentation System
MSL	Mean Sea Level
OEM	Original Equipment Manufacturing
QSRA	Quiet Short-haul Research Aircraft
RDT&E	Research, Development, Testing and Engineering
RFP	Request for Proposal
RJ	Regional Jet
SBW	Strut Braced Wing
SFC	Specific Fuel Consumption
SNI	Simultaneous Non-Interfering
STOL	Short Take-Off Landing
TOGW	Takeoff Gross Weight
USB	Upper Surface Blowing

Index of Symbols

C_L	Lift coefficient
C_{Lmax}	Maximum lift coefficient
C_D	Drag coefficient
C_{D0}	Parasite drag coefficient
C_M	Pitching moment coefficient
R	Total landing distance
R_a	Obstacle clearing distance
t/c	Thickness ratio
κ_α	Airfoil technology factor
Λ	Wing sweep angle
M_{cr}	Critical Mach number
ρ	Air density
σ	Density ratio
V_{stall}	Stall speed
W/S	Wing loading
T/W	Thrust to weight ratio
AR	Aspect Ratio
L/D	Lift to drag ratio
C_μ	Thrust coefficient
MAC	Mean aerodynamic chord
δe	Elevator deflection
δr	Rudder deflection
δa	Aileron deflection
δf	Flap deflection
δs	Slat deflection
α	Angle-of-attack
β	Sideslip angle
q	Dynamic pressure

1 Introduction and RFP

1.1 Introduction

Regional jets have proven to be extremely useful for promoting the growth of the airline industry. Carrying anywhere from 30-100 passengers over a range of 500-2000 nm, the flexibility of these aircraft has spurred the expansion of hub-and-spoke operations and the creation of new routes to bypass high-density hubs.

However, regional jets pose a problem to the airline industry because they are designed to use the same runways as larger transport jets, adding to the congestion at major airports. While flights by regional jets made up 40-50% of the total number of flights in 2000, they accounted for only 4% of the commercial aviation revenue (Ref. 1-1).

There is clearly a desire to move the majority of regional arrivals and departures from the long runways to shorter, underused runways. Currently there are only 600 airports that can support commercial air traffic, but there are an additional 6000 airports with runways 3000-8000 ft long (Ref. 1-2). Flying regional jets into these smaller airports would free up many of the currently congested runways for the larger transports and allow for additional growth of the air travel industry without having to build more airports or runways. To utilize these short runways, new regional jets will have to meet challenging restrictions on takeoff and landing distances, as well as use unique approach trajectories to avoid commercial traffic going into current airports.

In addition, the formation of the new Department of Homeland Security requires an increased emphasis on preparation for speedy reaction to a national emergency. The U.S. government currently maintains a Civil Air Reserve Fleet for the primary purpose of transporting military troops, but these aircraft could also be used to perform a variety of missions in times of homeland security crises. An aircraft already designed to takeoff and land in a short distance while carrying about 50 or more passengers would be capable of flying first responders from the surrounding region into the crisis area using the civil reserve fleet.

1.2 Request for Proposal Requirements

The AIAA Request for Proposal (RFP) calls for an Airport Adaptive Regional Transport to serve primarily in a regional jet role and be capable of carrying 49 passengers over a block range of 1500 nm more efficiently and economically than current regional jet designs. To relieve congestion at major airports, the aircraft must be able to land and takeoff from relatively short underused runways of 2500 ft or less and be capable of conducting a Simultaneous Non-Interfering (SNI) approach into a major airport.

This aircraft will also serve in the civil reserve fleet and be available for the government to commandeer in times of homeland security crisis. In this homeland security role, the aircraft will be used to transport people and equipment to “remote, high, hot areas with minimal runway length for takeoff and landing.” The RFP provides a specific example of a secondary mission in which the aircraft will be used to transport 20 firefighters in response to a wildfire. Table 1-1 lists the main RFP requirements for the two different missions, and a detailed description of the mission requirements is shown in Figures 1-1 and 1-2.

An aircraft capable of meeting the requirements of both missions would be expected to be more expensive than an aircraft designed for one mission. Since the airlines would be using the aircraft solely in the regional jet role, they would prefer to pay only for the cost of a regional jet. Consequently, it is necessary to identify any increments in flyaway and operational costs that would be necessary to meet the requirements of the secondary mission. This additional cost will be paid by the government, on the condition that the aircraft could be commandeered during times of crisis. This arrangement has no effect on the amount paid by the airlines for an aircraft to fulfill the regional jet role. For the government, this arrangement is an economical alternative to procuring and maintaining its own fleet of aircraft.

Table 1-1: Main RFP Requirements

	Primary Mission	Secondary Mission (Wildfire)	
		Outbound	Inbound
Takeoff Distance (BFL)	2,500 ft	2,500 ft	2,000 ft
Landing Distance (BFL)	2,500 ft	2,000 ft	2,500 ft
Range	1,500 nm	750 nm	750 nm
Cruise Speed	400 knots	400 knots	400 knots
Passengers	49	20	0
Crew	3	3	3

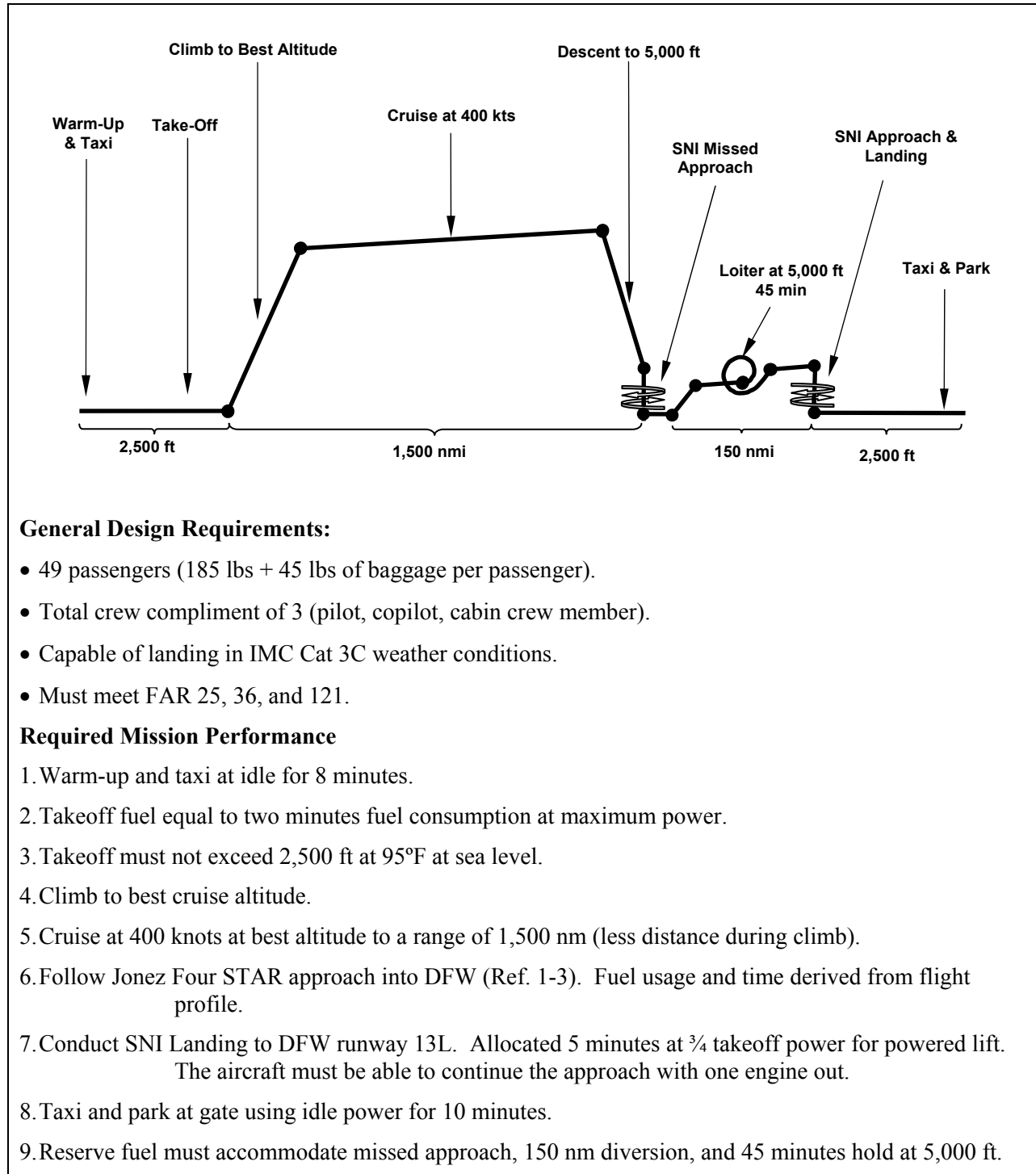


Figure 1-1: Primary Mission Profile and Requirements

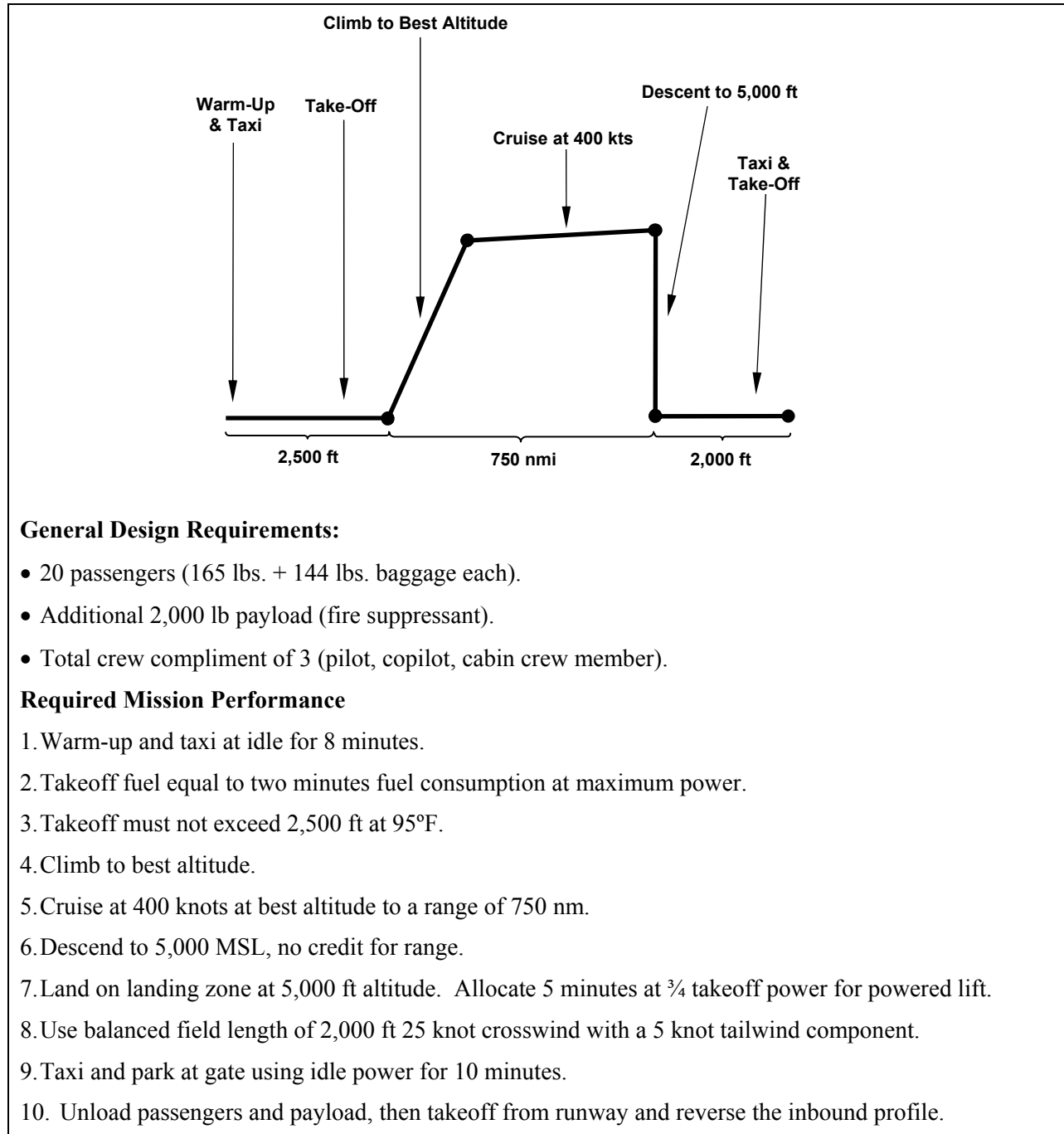


Figure 1-2: Secondary Mission Profile and Requirements

2 Design Drivers

The main design drivers for the RFP are STOL capability and mission flexibility. Meeting the STOL requirements while also designing for mission flexibility will come at the expense of cruise efficiency, additional weight, and operational cost. The best design will meet the RFP requirements for STOL and mission flexibility while minimizing the adverse effect on cruise efficiency.

2.1 STOL Requirements

Before considering a new aircraft design, a study was performed of current regional jets to identify how they compare to the requirements in the RFP. Table 2-1 shows how two current 50 passenger aircraft perform for the regional jet role, as well as additional specifications of interest.

Table 2-1: Current RJ Specifications and Comparison to RFP Requirements (Ref. 2-1)

SPECIFICATIONS	Embraer ERJ-145	Bombardier CRJ200	RFP Requirements	
Takeoff Distance	5,775	6,336	2,500	ft
Landing Distance	4,257	4,884	2,500	ft
Passengers	50	50	49	-
Range	1,540	2,325	1500	nm
Cruise Speed	446.74	430	400	knots
Approach Speed	119	113	65	knots

Table 2-2: Other RJ Specifications of Interest (Ref. 2-1)

SPECIFICATIONS	Embraer ERJ-145	Bombardier CRJ200	Units
SFC	0.36	0.346	lbs/hr
T/W	0.31	0.3	lbs/hr
W/S	87.26	118.71	lbs/ft ²
C_{Lmax}	1.823	2.75	-
TOGW	47,995	61,730	lbs
Cruise Altitude	32,000	41,000	ft
C_{Lcruise}	0.37	0.81	-
Total Thrust	14,890	18,390	lbs
Length	98.6	88.3	ft
Height	22.3	20.5	ft
Wingspan	66	70	ft
Wing Area	550	520	ft ²
AR	7.9	9.4	-

The most significant difference between the regional jet described by the RFP and current RJs are the short landing and takeoff distances. Current RJs also fail to meet the approach speed, but this is mostly a function of the landing distance requirement. Clearly, there is a need to design a new aircraft to meet these RFP requirements.

Before proceeding to conceptual design, the suitability of typical high lift and powered lift systems was studied. Figure 2-1 shows how wing loading and C_{Lmax} affect the aircraft's stall speed at sea level, based on the equation:

$$V_{Stall} = \sqrt{\frac{2\left(\frac{W}{S}\right)}{\rho_{sl} C_{Lmax}}} \quad (2.1)$$

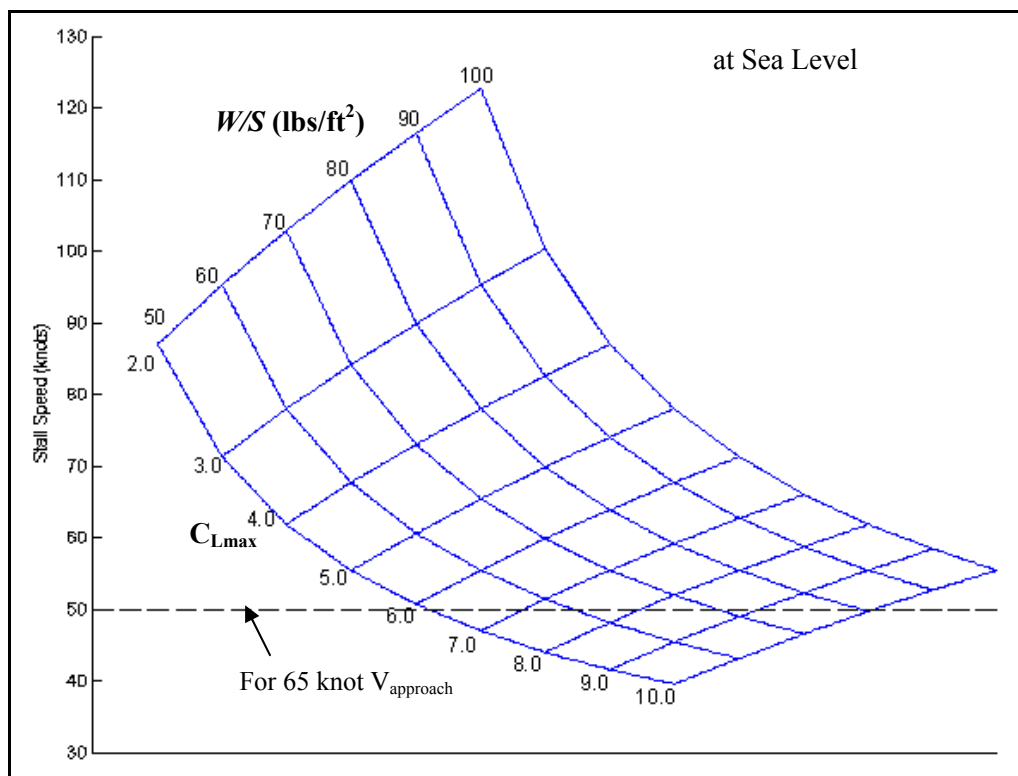


Figure 2-1: Carpet Plot of Stall Speed as a Function of Wing Loading and C_{Lmax}

Only wing loadings greater than 50 lbs/ft² were considered because this is the minimum wing loading that would be adequate for acceptable cruise performance (comparator RJs have wing loadings of 80-120 lbs/ft²). For the primary mission, the aircraft is required to have an approach speed of 65 knots, corresponding to a stall speed of 50 knots. As shown in Figure 2-1, even with a wing loading as low as

50 lbs/ft², the aircraft would need a C_{Lmax} of 6.0. Since even the best purely mechanical high lift devices do not produce a C_{Lmax} above 4.0, it is evident that powered lift will be necessary. Figure 2-2 shows a similar analysis for landing in a balanced field length of 2,000 ft at an altitude of 5,000 ft MSL, which is the landing requirement for the secondary mission. The landing distance was calculated using Equation 2.2, from Ref. 2-2:

$$R = 1.67 \cdot \left[80 \left(\frac{W}{S} \right) \left(\frac{1}{\sigma C_{Lmax}} \right) + R_a \right] \quad (2.2)$$

Where R is the landing distance, R_a is the obstacle clearance distance, set as 450 ft for a STOL approach angle of -7° , and σ is the density ratio.

To meet the constraints in Figure 2-1 and Figure 2-2 while flying with reasonable cruise efficiency, it is desirable to have the highest wing loading possible. The figures show that to get the highest wing loading, the highest C_{Lmax} will be desirable. By using powered lift systems, C_{Lmax} values on the range of 7-10 can be achieved (Ref 2-3).

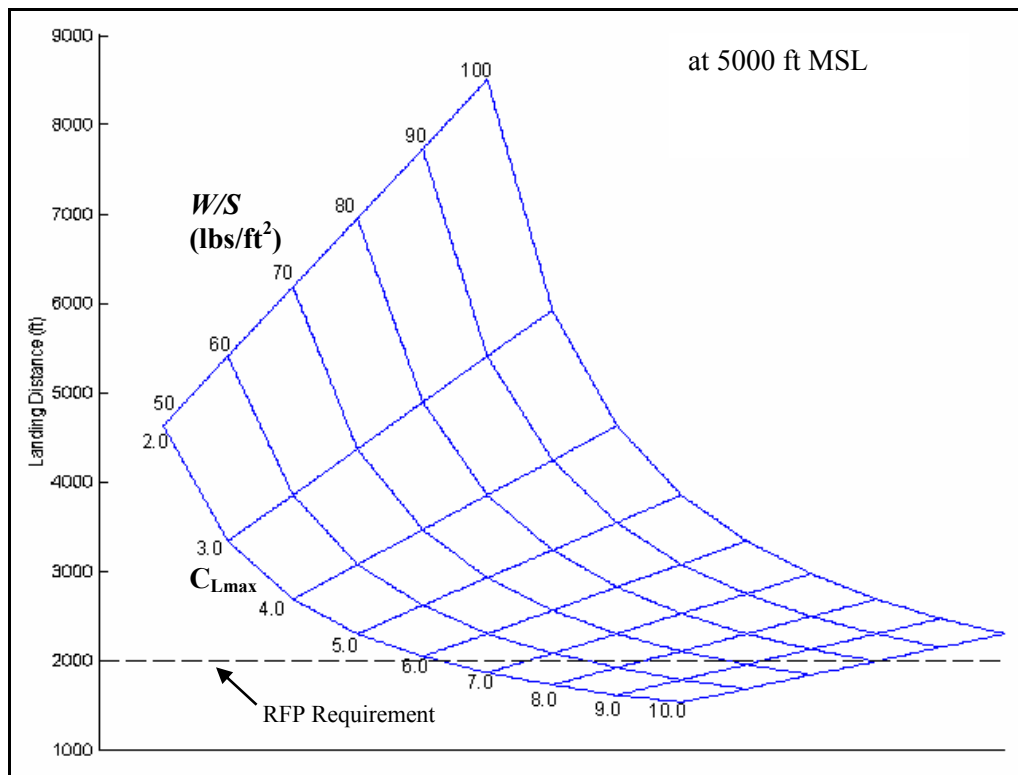


Figure 2-2: Carpet Plot of Landing Distance as a Function of Wing Loading and C_{Lmax}

2.2 Mission Flexibility

Another design driver that is contained in the RFP is the airplane's ability to serve in different roles for the government in times of crisis. Additional systems will be necessary so that the aircraft can be outfitted in a variety of configurations and perform in a range of environments. These systems include interior features such as removable seats and over head compartments to make room for emergency equipment, as well as exterior features, such as strengthened landing gear to improve the aircraft survivability in hostile environments. These additional systems result in penalties in production and operational costs. It is important to balance the flexibility of the aircraft against the feasibility of these additional systems.

3 Conceptual Designs

Having determined that powered lift would be necessary to meet the landing requirements set forth in the RFP, three powered lift systems were chosen for further investigation: externally blown flaps (EBF), internally blown flaps (IBF), and upper surface blowing (USB). These three powered lift systems served as the core around which three conceptual designs were created. Preliminary weight approximations were used to generate initial sizing and performance estimates.

3.1 Concept 1 – Externally Blown Flaps

Concept 1, shown in Figure 3-1, is based on the C-17 and utilizes externally blown flaps to produce the amount of lift required to meet the landing and takeoff requirements. Four engines are required to produce the amount of thrust needed. The aircraft includes a slightly aft swept wing, winglets, and a T-tail. The features of Concept 1 are described below.

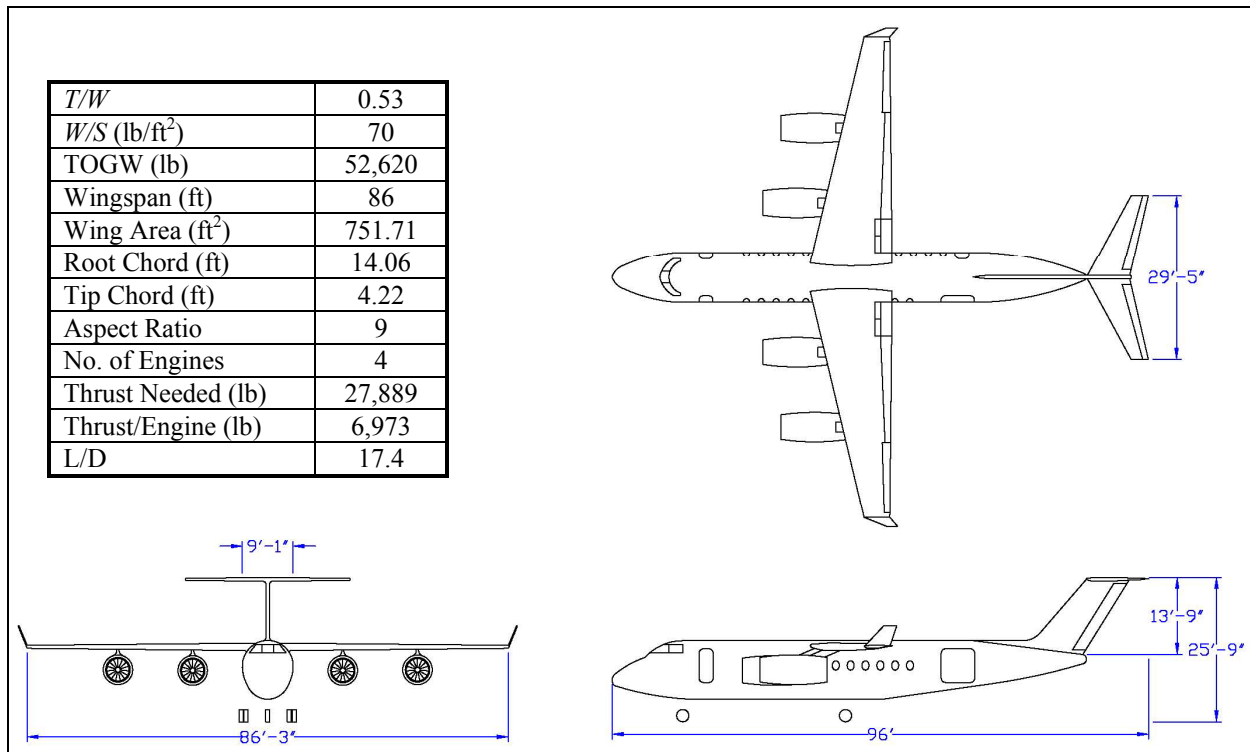


Figure 3-1: Concept 1 (Externally Blown Flaps)

3.1.1 Externally Blown Flaps

One popular method of powered lift in use today is the concept of externally blown flaps. This makes use of the exhaust from under-wing pylon-mounted engines impinging directly on conventional slotted flaps such that the flow is directed downward to augment the wing lift. The additional lift from the EBF system could as much as double the lift of the conventional configuration. Externally blown flaps are employed on the C-17, currently in service with the Air Force. The C-17's wings are configured with sets of double-slotted flaps that are extended downward directly into the exhaust flow of its engines. Part of the exhaust is directed downward by the flaps while the rest is passed through and then downward over the flaps. This uses the Coanda effect, which involves air turning on the convex side of an aerodynamic surface. The EBF system used on the C-17 was able to produce a C_{Lmax} value as high as 5.0 (Ref. 3-1).

3.1.2 Aft-Swept Wings

In the 1930s it was discovered that a swept wing results in a delay in transonic drag rise because of compressibility effects that are associated with the Mach number normal to the leading edge of the wing.

The critical conditions are reached only when normal Mach number has been locally accelerated to the local sonic speed. Wing sweep will add some structural weight (Ref 3-2), however the normal Mach number is reduced so transonic effects are delayed allowing for a more efficient cruise.

Supercritical airfoils are used in combination with wing sweep to minimize supersonic flow, resulting in weak shock formation and low compressibility drag over the wing. However, excessive wing sweep of the trailing edge can reduce the effectiveness of high-lift devices and control surfaces.

The aircraft specified in the RFP is required to fly at 0.7 Mach. This speed is at the lower limit of the transonic flow region. Consequently, significant wing sweep is not required to reduce the critical Mach number and minimize supersonic flow over the wing. Accordingly, the wing was swept only 10°.

3.1.3 T-Tail

One of the advantages of having a T-tail is that the placement of the horizontal stabilizer at the top of the rudder has a tendency to increase the rudder's effectiveness. This is referred to as the endplate effect. By putting the horizontal stabilizer on top of the vertical stabilizer, this places an added stress on the tail of the aircraft, and requires added structural weight. However since the moment arm is greater using a swept T-tail, the surface area of the horizontal stabilizer can be smaller and lighter than a conventional horizontal tail. This will produce less trim drag (Ref. 3-3).

3.1.4 Winglets

Winglets are used to reduce drag due to lift. Winglets reduce drag by harnessing the upward flow, acting like sails on a sailboat, thus producing a forward force and additional thrust (Ref. 3-4).

By reducing drag and augmenting the thrust force, winglets allow for increased speed while using the original amount of power. Lower power requirements for a mission will save in fuel consumption and will make the aircraft more efficient.

Winglets are roughly similar to a wingspan extension. By increasing wing span, the aspect ratio is also increased and will lead to a higher lift to drag ratio, allowing for a more efficient flight. Adding a

winglet to the aircraft increases the bending moments at the wing root. This requires a stronger structure and increased weight, but not as much as a straight span extension. It is important to determine if the reduction in drag is worth the increase in weight.

3.2 Concept 2 – Internally Blown Flaps

Concept 2, shown in Figure 3-2, utilizes internally blown flaps to produce the required lift necessary for the RFP requirements. Like Concept 1, a slightly swept wing with winglets is used to reduce drag and improve the wing efficiency. The primary difference between Concept 1 and 2, aside from the powered lift system, is the tail; concept 2 uses a conventional tail as opposed to a T-tail, primarily for the savings in structural weight. Concept 2 also only requires two engines because of the relative high efficiency of IBF.

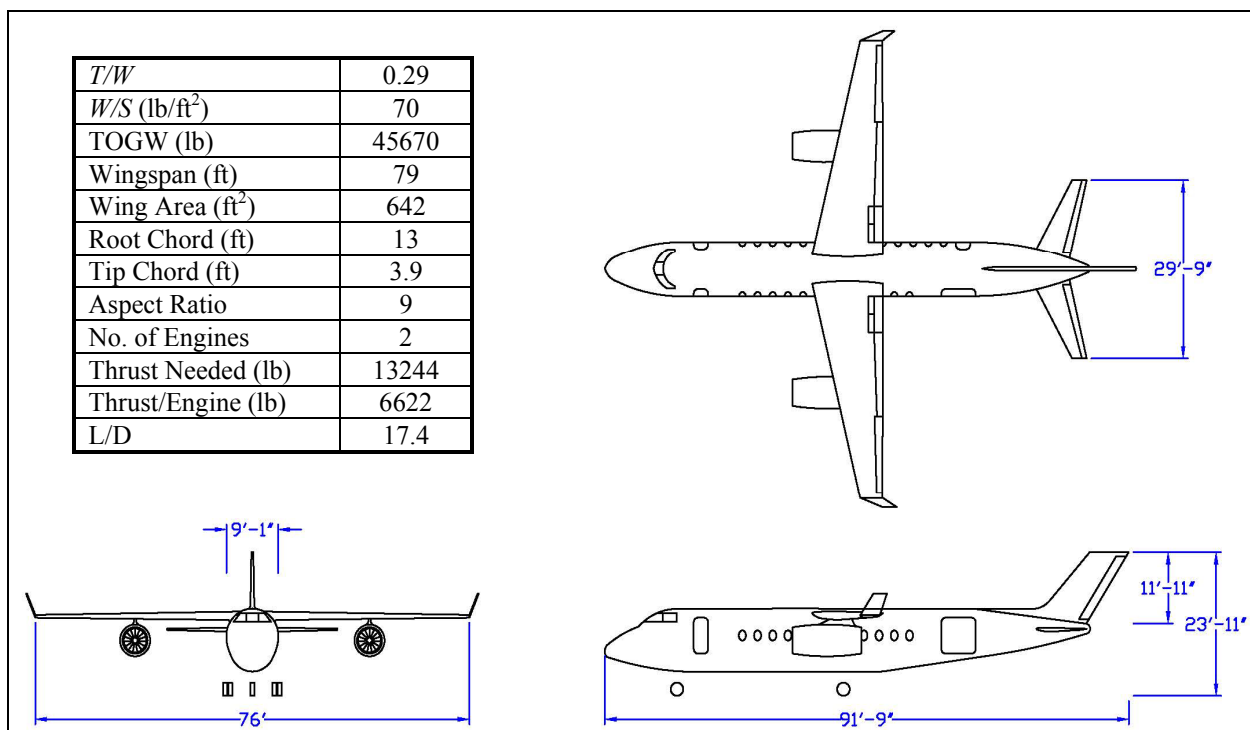


Figure 3-2: Concept 2 (Internally Blown Flaps)

3.2.1 Internally Blown Flaps

Internally blown flaps (IBF) are one of the most efficient forms of powered lift, requiring the least amount of mass flow to produce high C_L s (Ref. 3-5). This design incorporates an engine mounted

underneath the wing with all or part of the jet exhaust being ducted from the engine, through the wing, and exhausted over the trailing edge. There is also a crossover duct that allows one engine to blow exhaust over both wings. This solves the control problem when there is one engine out, but it presents more problems due to the extra weight and complicated structural arrangement. One drawback of internally blown flaps is that the air flowing through the narrow gaps in the wing and flaps produces much more noise than other powered lift systems (Ref. 3-5)

3.2.2 Conventional Tail

The conventional tail is the lightest tail currently available, due mainly to its simplicity. The main concern when using a conventional tail is rudder sizing. The rudder and stabilizer must be large enough to provide the necessary yawing moment to keep the aircraft in straight flight under engine out and crosswind conditions.

3.3 Concept 3 – Upper Surface Blowing

Concept 3, shown in Figure 3-3, uses Upper Surface Blowing (USB) to produce the lift required to meet the takeoff and landing requirements of the RFP. This aircraft uses forward swept wings, which reduce drag at transonic speeds and potentially has larger regions of laminar flow than an aft swept wing. The wings will be supported by a strut, allowing for the design of thinner, higher aspect ratio wings. A streamlined blister was added to the bottom of the fuselage of Concept 3 to accommodate the additional structure required for the strut, as well as the landing gear. Concept 3 uses an H-tail because of the better horizontal tail performance at high angles of attack, which will be useful for the short takeoff and landing.

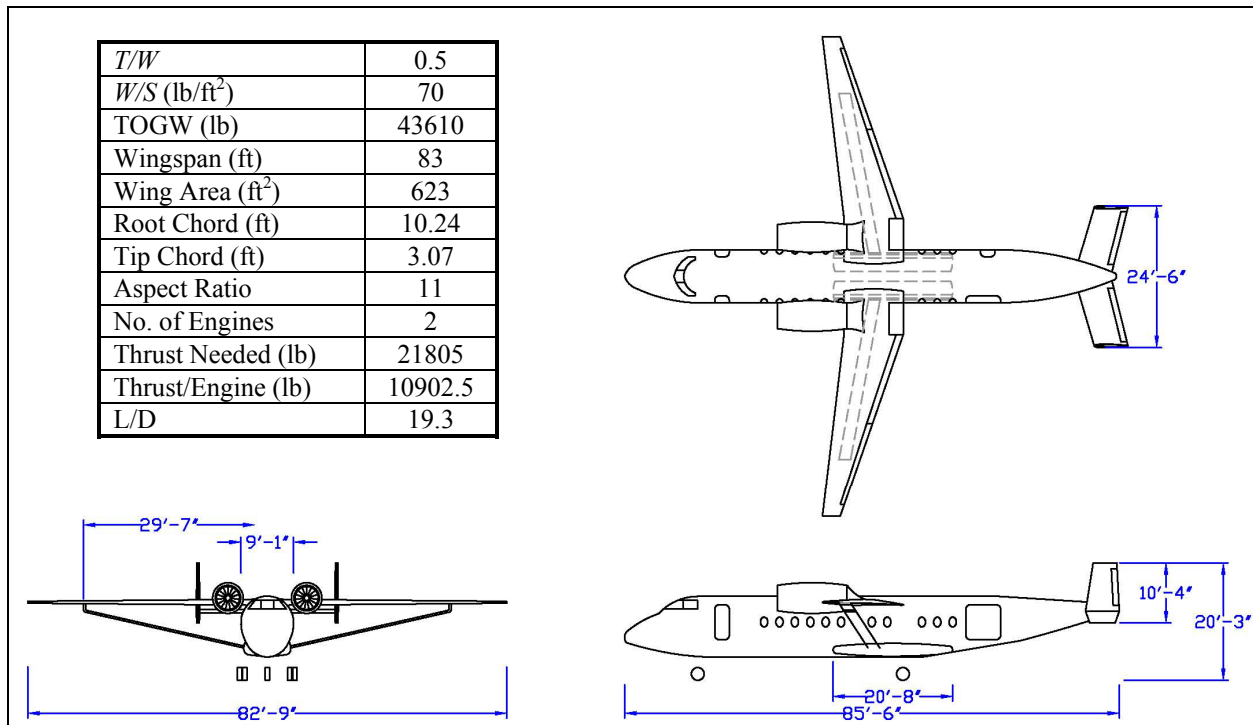


Figure 3-3: Concept 3 (Upper Surface Blowing)

3.3.1 Upper Surface Blowing

Upper surface blowing is another powered lift concept which incorporates the Coanda effect to maximize the lift produced by the aircraft (Ref.3-5). Engines are mounted forward and above the wing such that the exhaust blows over the upper surface of the wing and flaps to create more lift.

The USB high lift system has been flown in a number of aircraft. The YC-14 employed a USB configuration with two engines mounted above and forward of the wings. This configuration also gave the aircraft a quieter noise footprint. The exhaust was spread out over the wing to enhance circulation and lift augmentation during STOL operations (Ref. 3-6).

Another significant USB program was the Quiet Short Haul Research Aircraft (QSRA) program by NASA Ames. The QSRA was a deHavilland C-8 Buffalo aircraft, modified with 4 upper surface blowing engines. The program was able to demonstrate stability at C_L 's as high as 10. The aircraft also had a very small noise footprint, much smaller than a conventional jet transport. (Ref. 3-7)

The Japanese ASKA used USB in addition to vortex generators on the wing to keep the exhaust stream attached to the flaps. A Boundary Layer Control system was used to bleed high pressure air from

the leading edge of the wing (Ref. 3-8). USB is also used on the Antonov An-72, a Russian made STOL transport (Ref. 3-9).

In most cases the penalty of using USB is high fuel consumption during cruise, as a result of additional drag produced by wing overblowing, which leads to a decreased lift-to-drag ratio in cruise.

3.3.2 Strut Braced Wing

The strut-braced wing (SBW) has long been an integral part of the design of small general aviation prop planes such as the Cessna 172. The strut is attached to the wing by a pylon, and pinned to the fuselage. The loads carried by the strut help reduce the root bending moment. This makes it possible to use a lighter and more efficient wing. While struts have been an element of the design of primarily low-speed aircraft, the benefits associated with employing a strut are equally applicable to higher-speed aircraft.

While the strut works very well during flight (when it is in tension), problems can develop when the aircraft is subjected to negative loads, especially during landing. A strut load damping system will be required to reduce the loads carried on the strut during landing to reduce this problem.

Virginia Tech, under the support of NASA Langley Research Center, has conducted extensive research on the SBW concept for a transonic transport aircraft. Early work by Joel Grasmeyer, et al, (Ref. 3-10) found that the payoffs of the transonic SBW include reduced aircraft weight and improved cruise performance due to the synergistic effects from the higher aspect ratio, reduced thickness, and reduced sweep angle of the wing.

3.3.3 Forward Swept Wings

The advantages in drag of aft swept wings are also present in forward swept wings. Until recently forward swept wings have not been used often due to problems with aeroelastic divergence. Unlike aft sweep wings, forward swept wings tend to twist up at the tips when under aerodynamic loads. At the divergence speed, the twisting at the wingtips becomes so large that the wing continues twisting until it

fails. By using composite materials and struts this problem can be avoided by raising the divergence speed above the achievable speed of the aircraft.

Forward swept wings are ideal in the case of flight at transonic speeds or high angles of attack. When flying at transonic speeds a shock can form on the upper surface of the wing. To minimize drag the shock wave needs to form close to the trailing edge and be weak as possible. This results in a more highly swept shock and a lower drag penalty for a forward swept wing when compared to an aft swept wing. It is suggested that a forward swept wing may be capable of supporting a laminar attachment-line flow at a much higher free-stream Reynolds number than a corresponding swept-back wing because flow contamination due to the fuselage is eliminated(Ref. 3-11).

Flow over the upper surface of an aft swept wing has a component in the spanwise direction toward the wing tips. This leads to a thicker boundary layer at the tip and will cause tip stall at high angles of attack, reducing aileron effectiveness. When using forward swept wings the span wise flow is toward the root, causing stall to begin at the wing root for high angles of attack. Blowing air over the wing root with USB will help prevent stall at the root. In the case of aft swept wings, the turbulent boundary layer of the fuselage can spread along the wing leading edge. When using forward swept wings no disturbances from the fuselage will contaminate the leading edge (Ref. 3-11).

3.3.4 H-Tail

The H-tail is primarily used to place the vertical tails in the undisturbed air while flying at high angles of attack and increasing yawing moment for engine out performance and small radius turns. The H-tail tends to be heavier than the conventional tail, but as a result of the placement of the vertical tail, more flow is forced over the vertical stabilizer and allows the horizontal tail to be smaller (Ref. 3-3).

3.4 Selection Criteria and Decision

Table 3-1 shows a comparison of the three concepts, from which one preferred concept was selected. The categories in Table 3-1 were given a weighting factor from 1 to 9, with 9 being the most important. The most important categories were selected to be weight, cost, and safety. Each concept was ranked

with a value of 1-9 for each category, again with 9 as the best performer. These rankings were based on analysis of the concepts and consideration of the technologies used in each concept. From this ranking method, concept 3 proved to be the preferred concept.

Table 3-1: Selection Criteria

Selection Criteria	Weight	Concept 1 (EBF)	Concept 2 (ISB)	Concept 3 (USB)
TOGW	x9	5	7	9
Cruise Performance	x7	7	7	9
Safety	x9	9	7	7
Materials	x5	7	5	5
Operational Cost (/year)	x9	5	9	9
Acquisition Cost (/year)	x9	5	7	9
Marketability	x5	7	5	5
Total Score		335	369	419

Table 3-2 provides a comparison of some of the major design elements between the preferred concept and two representative 50-passenger regional jets. The fundamental differences between the new aircraft and current RJs are the C_{Lmax} , wing loading, and thrust to weight ratio. The relatively high C_{Lmax} and low wing loading are required to fly slowly enough on approach to land in the short distance required by the RFP, which is almost half the landing distance of the two comparator aircraft. The higher thrust to weight ratio is necessary since powered lift is being used to achieve such a high C_{Lmax} . The low wing loading translates into a larger wing area and wingspan. However, the use of struts will allow for a more efficient wing design with a higher aspect ratio, resulting in an overall lighter aircraft.

Table 3-2: Comparison of Concept 3 with Current RJs (Ref. 3-12)

	Concept 3 (USB)	Embraer ERJ-145	Bombardier CRJ200	Units
Takeoff Distance	< 2,500	5,775	6,336	ft
Landing Distance	< 2,500	4,257	4,884	ft
Wingspan	83	66	70	ft
Wing Area	623	550	520	ft ²
AR	11	7.9	9.4	
TOGW	43,610	47,995	61,730	lbs
C_{Lmax}	8.5	1.823	2.75	-
W/S	70	87	119	lbs/ft ²
T/W	0.43	0.31	0.3	-
No. of Engines	2	2	2	-
Thrust	21,805	14,890	18,390	lbs
Thrust/Engine	10,903	7,445	9,195	lbs

3.5 Sizing Carpet Plot

The carpet plot shown in Figure 3-4 was used to determine the final size of the aircraft. The plot shows TOGW as a function of T/W and W/S . The values for weight were determined from a statistical review of similar aircraft, taking into consideration the weight savings expected by the use of composites and strut. The constraint lines reflect the relationship between T/W and W/S required for climb. This relationship is especially important since powered lift is used to produce the necessary lift during takeoff and landing. The specific relationship between W/S and thrust-required for the constraint lines is discussed in greater detail in Chapter 4.

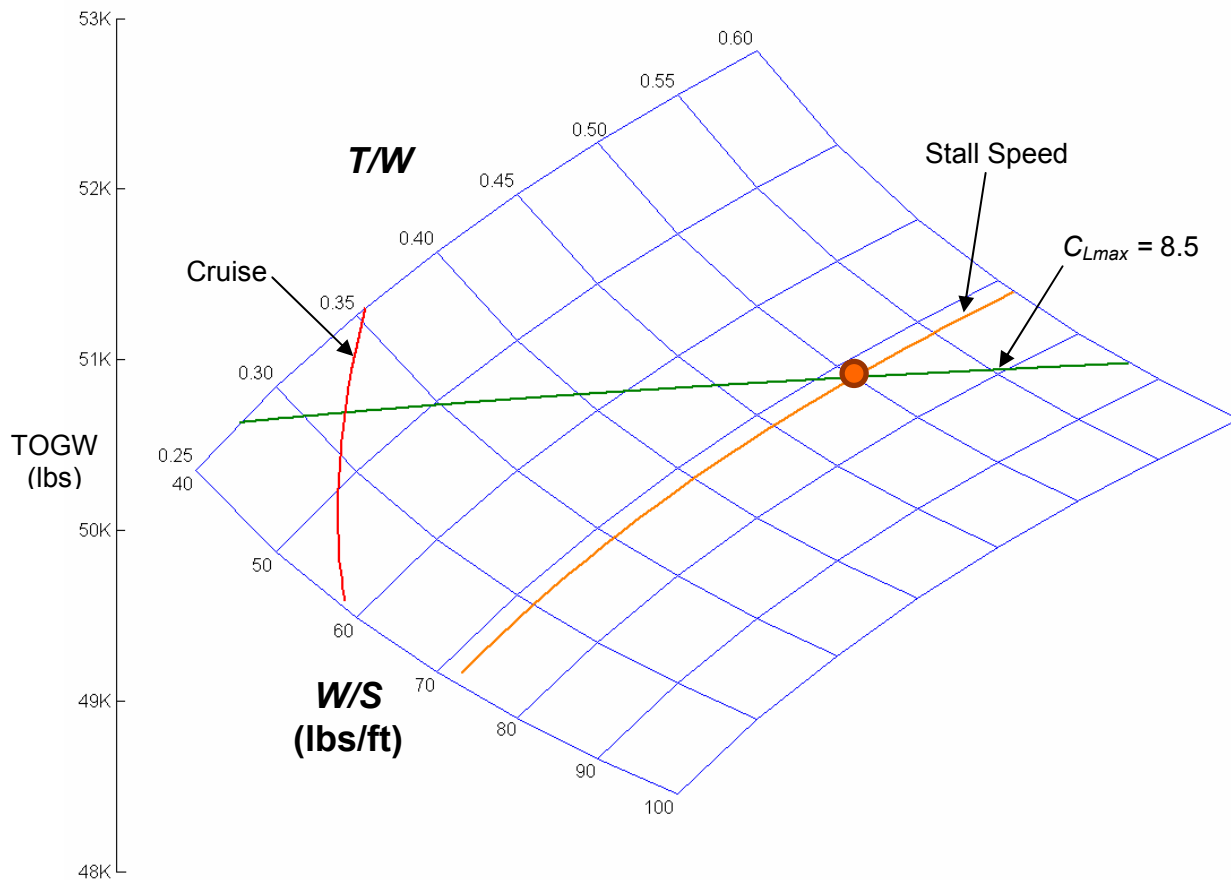


Figure 3-4: Carpet Plot used to Optimize Final Sizing

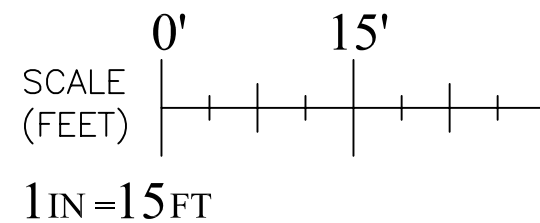
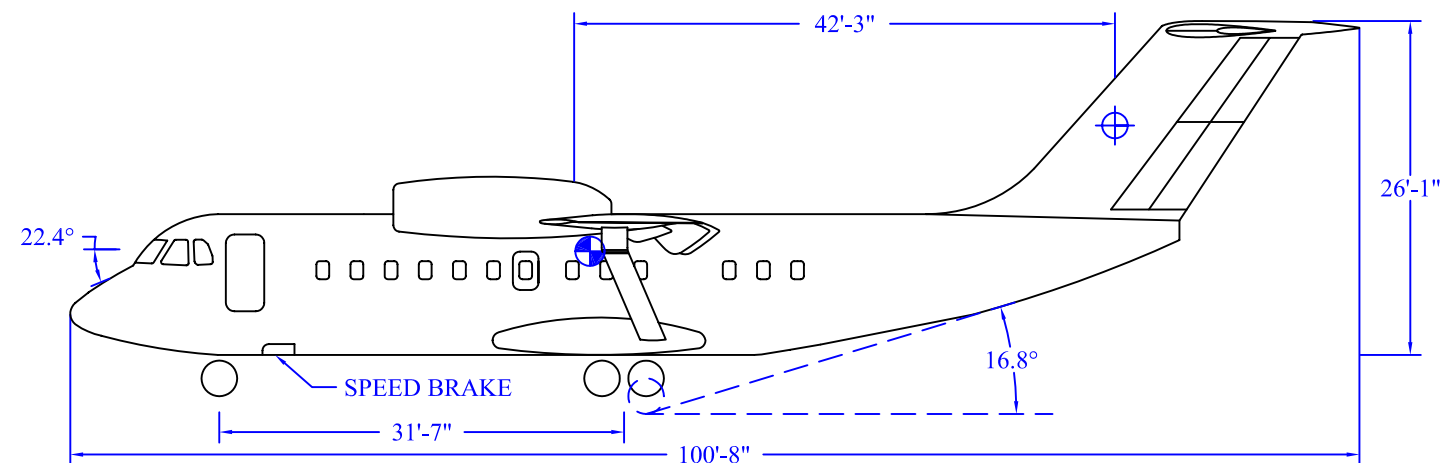
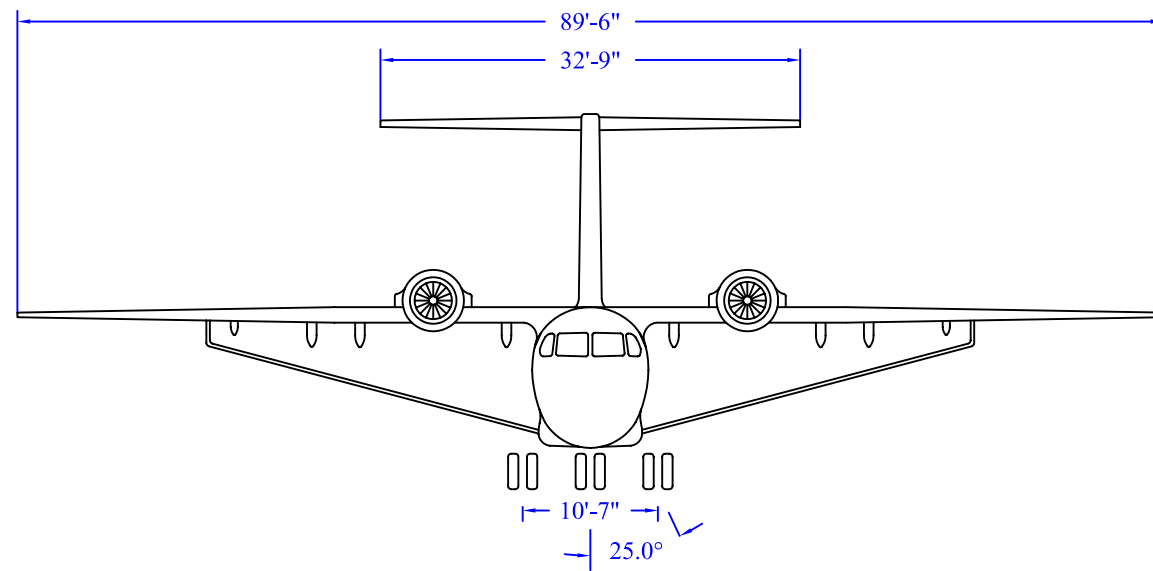
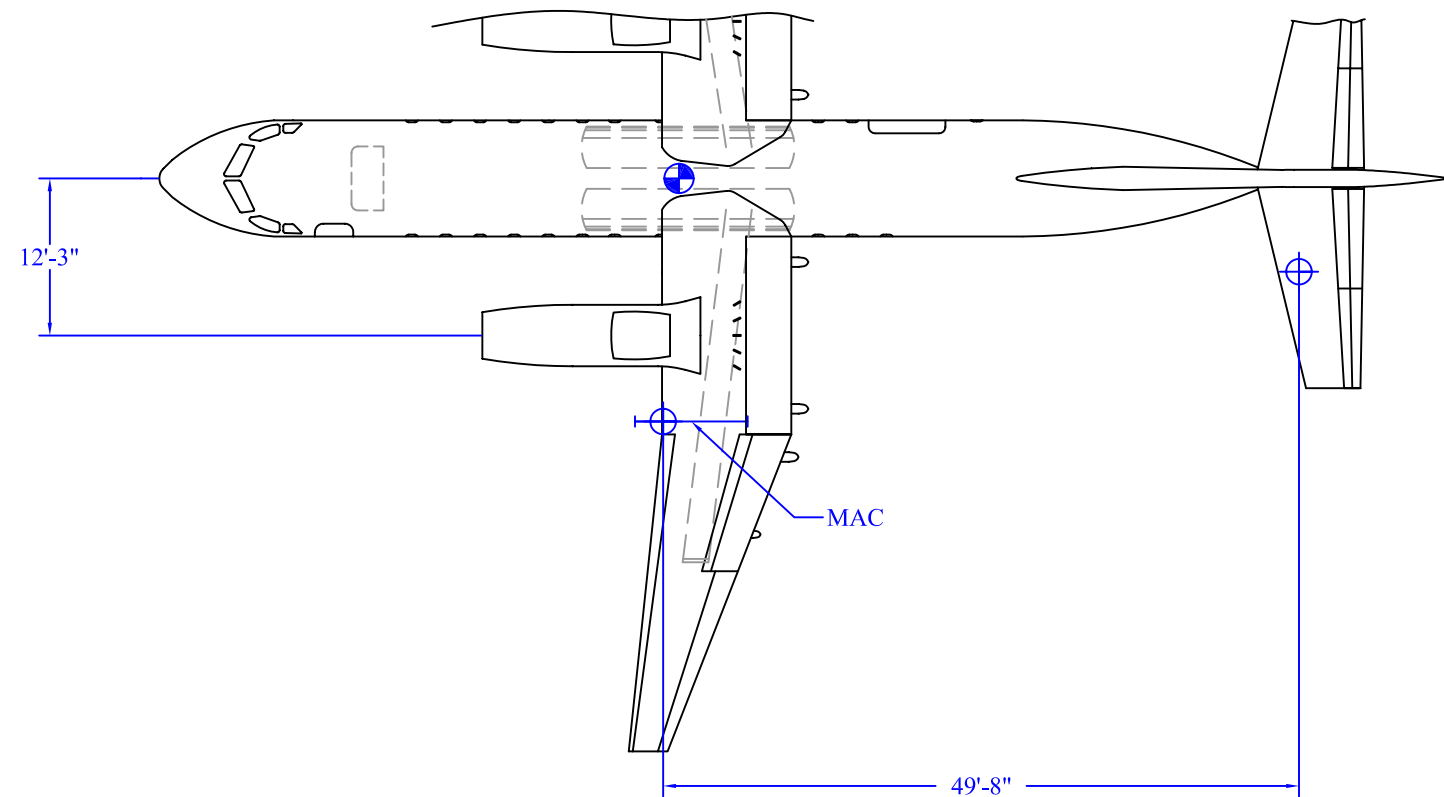
The $C_{L_{max}}$ constraint represents the T/W needed for a given wing loading to achieve a C_L of 8.5. A $C_{L_{max}}$ of 8.5 was chosen based on experimental results, as discussed in section 4.1. This constraint appears to have little effect on the TOGW of the aircraft, since less thrust is needed with a smaller wing loading. Moving along this line from the intersection with the climb constraint to the intersection with the stall speed constraint represents a change of 230 lbs. However, as discussed in Chapter 2, a higher wing loading is desirable for improving efficiency and ride quality in turbulence. The point at the intersection of $C_{L_{max}}$ and stall speed constraint. The base aircraft was therefore selected at a W/S of 72 lbs/ft², a T/W of 0.50, and a TOGW of 51000 lbs. The TOGW is an initial estimate at this point and more detailed analysis of the component weights is given in Chapter 10.

3.6 Selected Configuration

Team Volant presents the Firefly, a 49-passenger regional jet that utilizes Upper Surface Blowing to augment the lift generated by the wing, allowing for greatly reduced takeoff and landing distances. The twin high-bypass jet engines are mounted on top of the high wing, such that the exhaust blows over the trailing edge of the wing. The wings are supported by a strut that attaches at 66% of the wing semi-span. The strut provides additional support to the wing, allowing the wing to have a higher aspect ratio, and making it possible to support a thicker wing. The strut connection to the fuselage is housed in a blister on the bottom of the fuselage that also holds the landing gear. The landing gear for the Firefly is more robust than the landing gear of a standard regional jet, because the Firefly will be expected to encounter more hazardous runway conditions during its secondary role, as an aircraft in the Civil Reserve Fleet.

The final configuration of the Firefly is shown in Figure 3.5. The only major conceptual difference between the final configuration and Concept 3 is that a T-tail was used instead of an H-tail. More detailed sizing of components and control surfaces was done to develop the final configuration, and is discussed in the remaining chapters. The unswept portion of the wing was expanded, and the engines were moved farther outboard to increase the amount of blown wing area.

COMPILED DATA	APPENDAGE		
	WING	HORIZONTAL TAIL	VERTICAL TAIL
REF. AREA (sq ft.)	728.5	206.27	204.65
ASPECT RATIO	11.0	5.14	1.18
TAPER RATIO	.30	.50	.75
SPAN (ft.)	89.5	32.75	15.59
ROOT CHORD (ft.)	10.09	8.5	15.0
TIP CHORD (ft.)	3.03	4.25	11.25
MAC (ft.)	8.8	6.61	13.21
L.E. SWEEP (deg)	-6.0	13.6	41.9
1/4 CHORD SWEEP (deg)	-10.0	10.0	40.0
VOL. COEFFICIENT	-	1.61	.137
T/W RATIO	.50		
PRIMARY MISSION TOGW (lbs)	53,082		
SECONDARY MISSION TOGW (lbs)	47,917		



DRAWING TITLE:		
FIREFLY GENERAL ARRANGEMENTS		
DESIGNED BY: TEAM VOLANT		
DRAFTED BY: MATT LONG		
SCALE: AS SHOWN	DATE: 4/15/04	DWG NO. FIG. 3-5

3.6.1 Wing Design

The Firefly was designed as a high wing aircraft. The motivation for this placement originated mainly from the secondary mission requirement. More times than not, when flying in a secondary role the aircraft will be landing in rough and littered clearings. Fear of foreign material being sucked into the engine made a high wing design more desirable. As a secondary benefit ground noise is lessened during takeoff and landing. The wings extend unswept for a distance of 20ft from the centerline of the fuselage. At that point the wings are swept forward at a quarter chord sweep angle of 10°. A more detailed description of the wing design is given in section 4.2.

3.6.2 Aircraft Exits

Adhering to the FAR requirements, the Firefly was designed with a total of 4 exits. The forward most exit is a Type I exit and located on the port side. It serves as the main crew and passenger access way. The next two exits lie opposite each other on either side of the cabin just forward of the leading edge of the wings. Both of these exits are Type III emergency exits. The final exit is on the starboard side adjacent to the aft end of the cabin. This exit is 6 ft x 6ft and serves as a cargo/conversion door. For the transition between the primary and secondary missions this door will be used to transfer the interiors of the plane to and from the cabin. During the secondary mission the exit will be used to load government personnel as well as any cargo which may be needed for the mission.

3.6.3 Interior Configurations

As a result of the variety of roles the Firefly could be asked to fulfill for the government, two entirely separate interior configurations had to be designed to complement not only passengers in the regional jet role, but also the government employees flying in times of crises.

The cross section of the aircraft was designed in order to allow the wing structure to pass through the fuselage above the cabin. This was done to decrease any drag that may occur from having the wings

placed above the fuselage. Maintaining this constant cross section also allots space for the wiring of the various aircraft systems.

3.6.3.1 Primary Mission Configuration

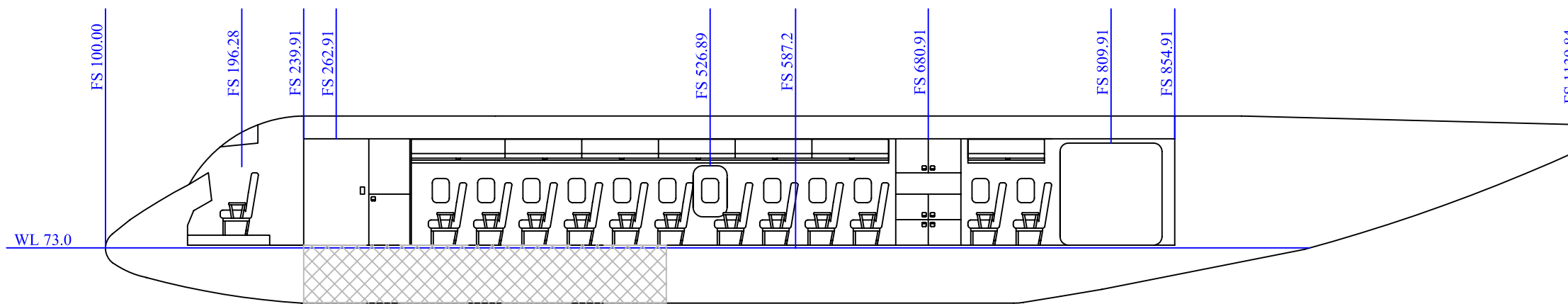
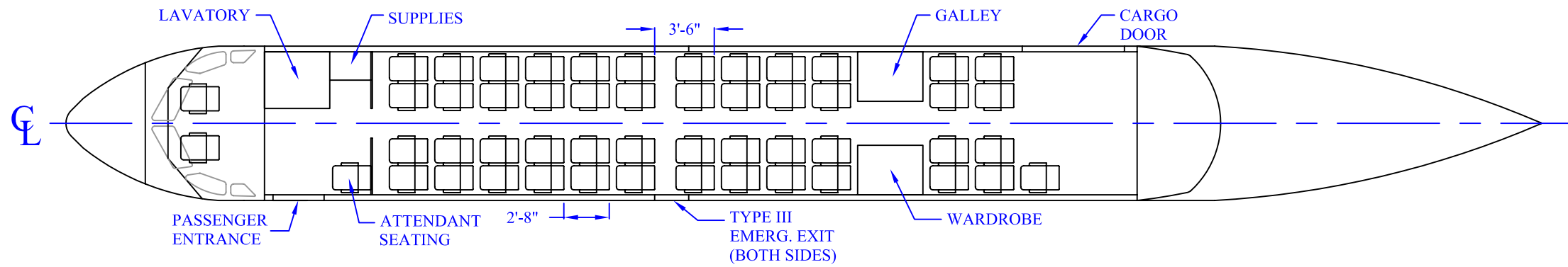
3.6.3.1.1 Seating

Figure 3.6 shows the interior configuration and inboard profiles of the Firefly in its regional jet role. Figure 3.7 shows the corresponding cross section for this role. The third crew member's seat is situated on the port side in the forward section of the cabin. The 49 passenger seats are positioned in a 32" pitch, and are situated four abreast.

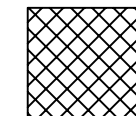
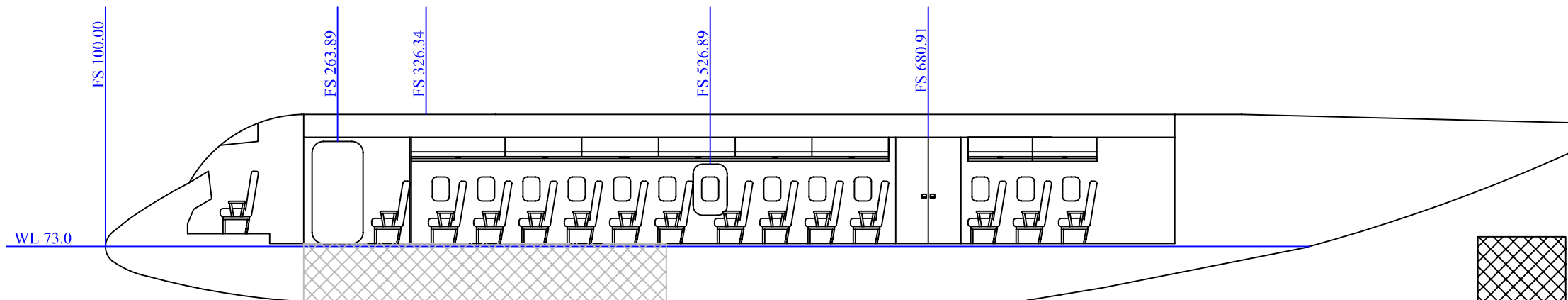
3.6.3.1.2 Amenities

The cabin includes 200 ft³ of overhead baggage, with an additional 326 ft³ of baggage storage available underneath the cabin in the belly of the aircraft.

The placement of a lavatory, galley, and wardrobe was carefully considered. The lavatory was placed forward, just aft of the cockpit, so that plumbing would not have to be removed when the aircraft is called to serve in the Civil Reserve Fleet. The galley and wardrobe were placed in the cabin such that they lined up with the trailing edge of the wing. Flight tests of various aircraft that use USB have shown that the trailing edge was a significant source of noise inside the cabin. By placing these fixtures at the trailing edge of the wing, passengers are further distanced from the noise.

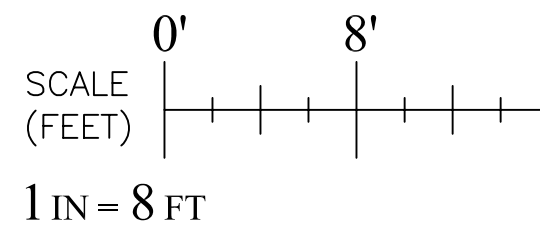


VIEW FROM PORT SIDE



UNDER FLOOR BAGGAGE AREA

VIEW FROM STARBOARD SIDE



DRAWING TITLE: FIREFLY INBOARD PROFILE (PRIMARY MISSION)		
DESIGNED BY: TEAM VOLANT		
DRAFTED BY: MATT LONG		
SCALE: AS SHOWN	DATE: 4/15/04	DWG NO. FIG. 3-6

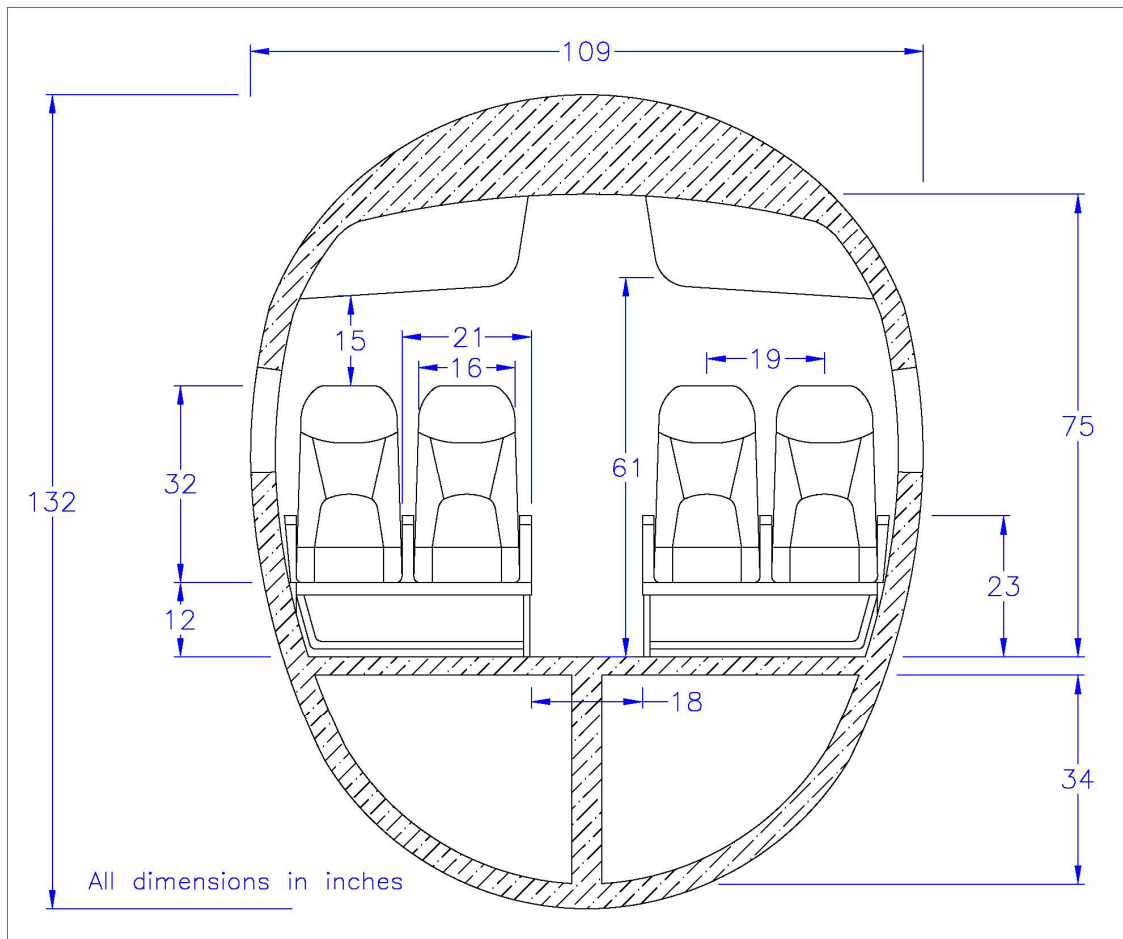
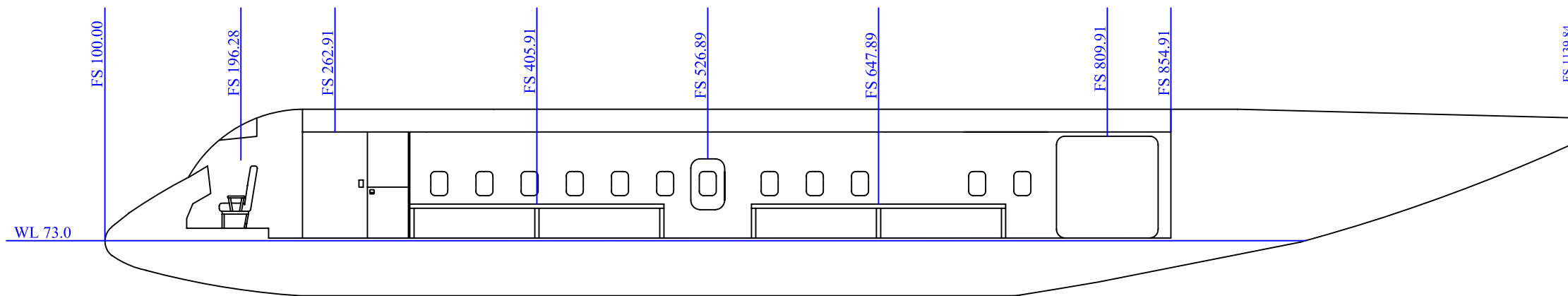
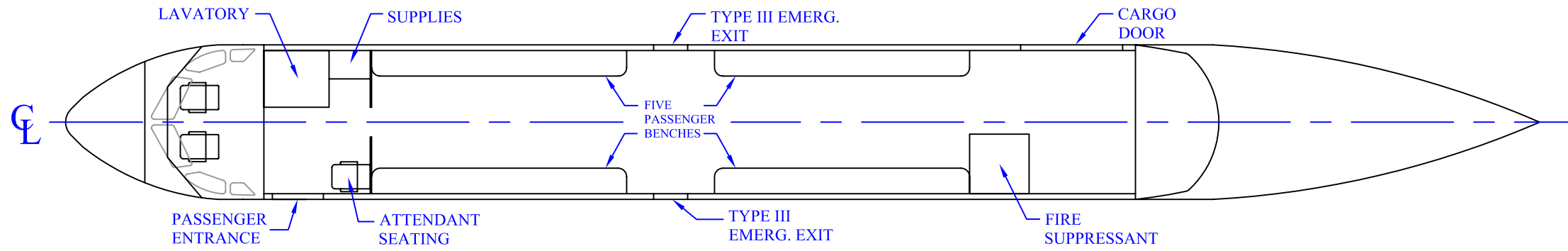


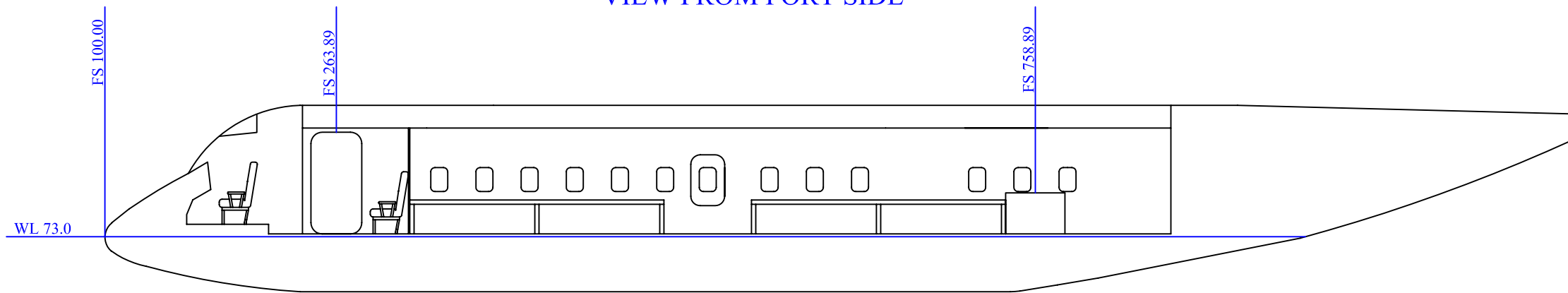
Figure 3-7: Regional Jet Cross Section

3.6.3.2 Secondary Mission

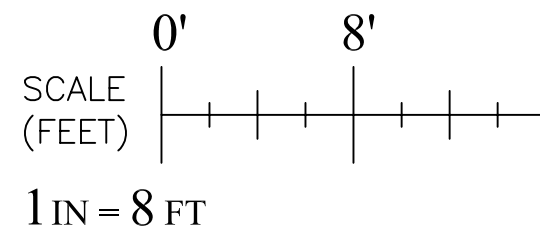
The interior configuration and inboard profiles for the secondary mission are shown in Figure 3-8. The cross section is shown in Figure 3-9. Upon being commandeered by the government, all of the passenger seats are removed from the cabin and replaced with four inboard facing mesh benches to accommodate 20 firefighters. The decision to remove the seats was made to preserve the upholstery of the airline seats, and to free up room so the firefighters could easily move around the cabin. Overhead compartments are removed, along with the galley and the wardrobe. The fire suppressant specified in the RFP will be carried on the port side of the aft section in the cabin. The cargo door will allow for easy loading and unloading of the seats, fire suppressant, and other bulky firefighting equipment.



VIEW FROM PORT SIDE



VIEW FROM STARBOARD SIDE



DRAWING TITLE: FIREFLY INBOARD PROFILE (SECONDARY MISSION)		
DESIGNED BY: TEAM VOLANT		
DRAFTED BY: MATT LONG		
SCALE: AS SHOWN	DATE: 4/15/04	DWG NO. FIG. 3-8

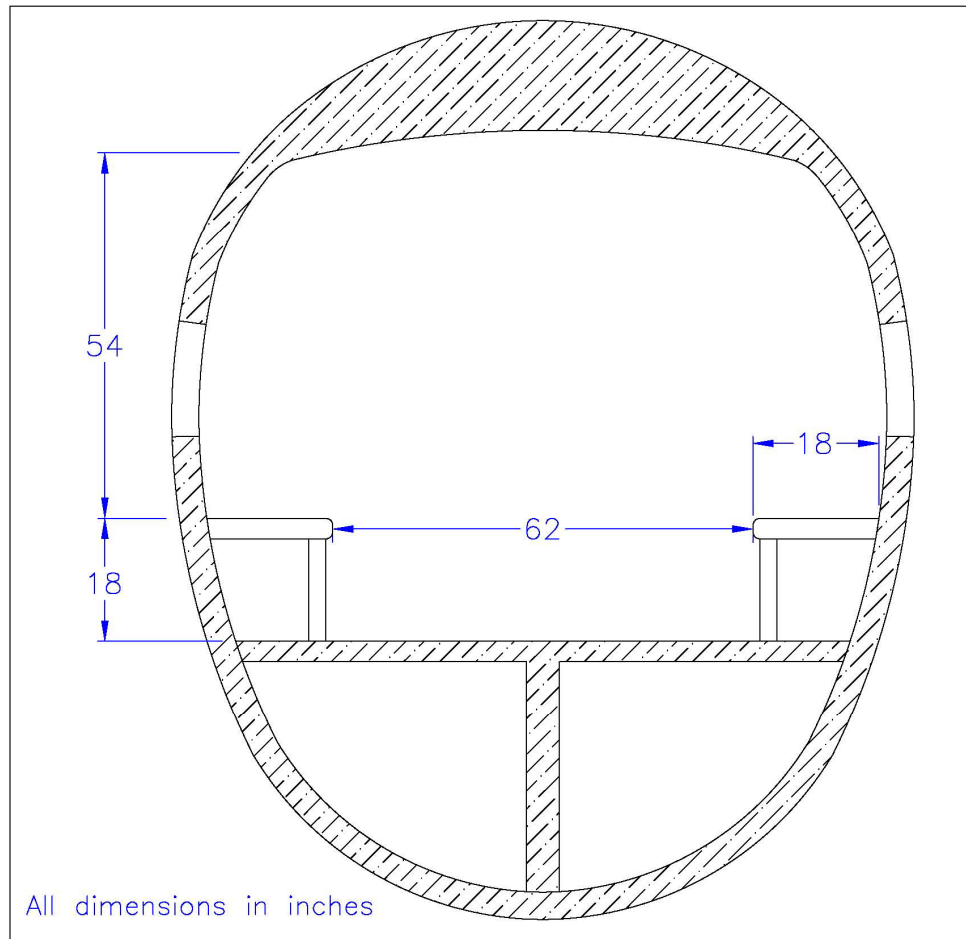


Figure 3-9: Cross section for firefighter mission

3.7 Future Expansion

The standard practice in the aerospace industry is to build a family of aircraft, as opposed to designing and developing a unique design for each size. In this vein, extended versions of the Firefly will include a 65 passenger -200 series and an 81 passenger -300 series. To stretch the original cabin, eight seats will be added to the fuselage forward and aft of the CG. This will maintain the CG position, so that the landing gear will not have to be adjusted. The extended cabins are shown in figure 3-10. For the -200 series, the aircraft will have a tail scrape angle of 14.1°. The -300 series will have a tail scrape angle of 12.1°.

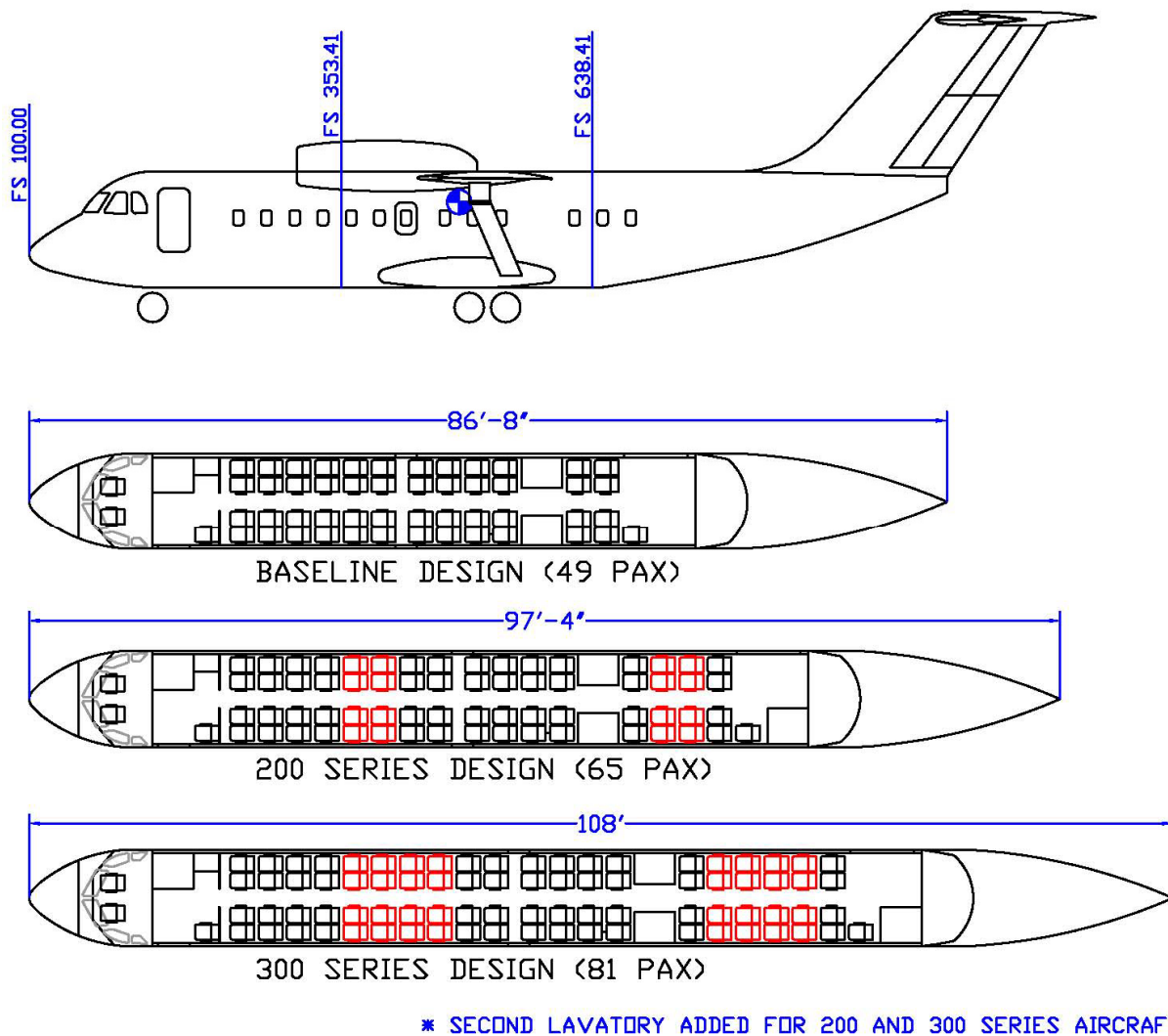


Figure 3-10: Firefly-100, -200, and -300 Series Aircraft

4 Aerodynamics

4.1 Maximum Attainable Lift

As stated in the mission drivers, the most difficult task is achieving a nominal balanced field take-off and landing requirement of 2500 ft. Typical RJ's are currently taking off in 4000 to 5000 ft (see Table 2-1). To accomplish high lift capability the use of Upper Surface Blowing (USB) is incorporated into the design of the Firefly. Based on the approach speed specified in the RFP of 65 knots and the take-off and landing requirement we calculated our required stall speed to be 50 knots. The two carpet plots in Figures 2-1 and 2-2 show wing loading as a function of C_{Lmax} , stall speed and landing distance, this gives us a

gives us a wing loading of 72 lb/ft^2 where S_{ref} is 728 ft^2 . By using USB we can achieve a $C_{L_{\text{max}}}$ of 8.5 at stall speed, as can be proven by experimental data obtained by NASA (Ref. 4-1).

Upper Surface Blowing powered lifting systems have been proven to work on the YC-14 by Boeing and the experimental Quiet Short-Haul Research Aircraft (QSRA) by NASA Ames Research Center. USB provides STOL capabilities due to a higher attainable lift coefficient than standard mechanical high lift flap systems. By mounting the engines forward and above the wing we are able to utilize the Coanda effect and blow the engine exhaust over the upper surface of the wing and flaps. The technique behind USB provides high levels of lift at low noise levels (Ref. 4-2). Quieter aircraft are desired in the commercial setting where noise levels are important to residential zones located close to airports.

In the 1970s NASA Langley conducted low speed wind-tunnel investigations of a four-engine upper surface blown model. The investigation was carried out in the Langley V/STOL tunnel to determine the power on static turning characteristics of the simulated engine flow and the powered lift aerodynamic performance of the four-engine upper surface blown transport configuration having a 30° swept wing (Ref. 4-1). Using a partial-span 35-percent-chord double slotted flap system, NASA engineers found the USB performed best with the flap deflected at 50° with a 40° leading edge slat deflection. The Firefly was designed with a similar flap system, shown in figure 4-1. The USB flaps are supported by wing fairings.

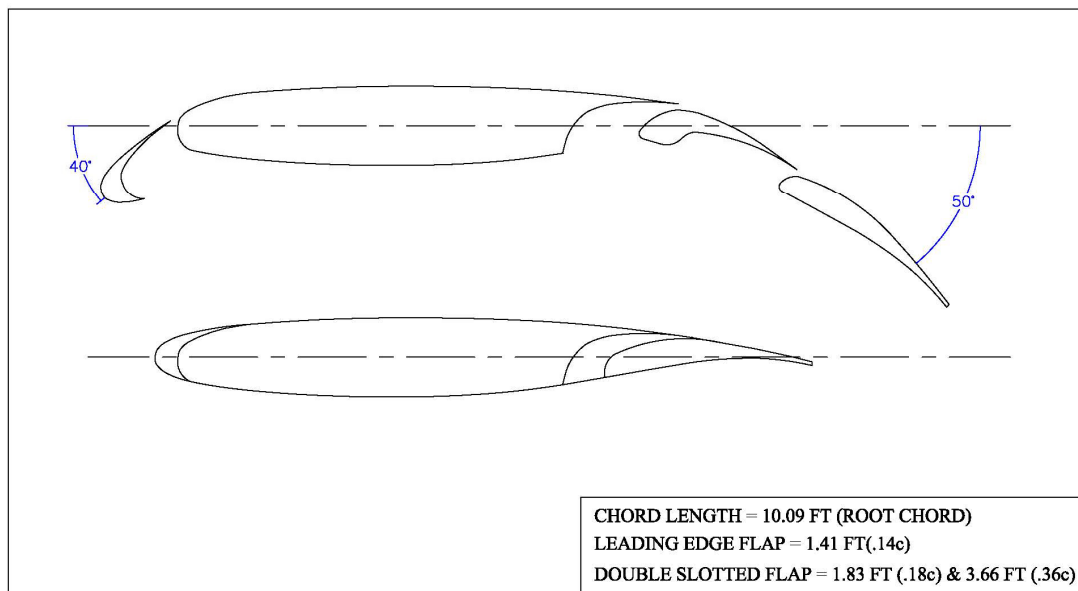


Figure 4-1: Firefly Wing Cross section, showing USB flap and slat extended

There is currently no reliable computational method for predicating the performance of a USB system, so wind tunnel and flight test data must serve as the basis for the thrust required to produce a C_{Lmax} of 8.5.

A summary of the NASA wind tunnel data with two and four engines can be seen in Figures 4-2 and 4-3 (from Ref. 4-1). Comparing these two data sets suggests that the model with two engines required 150% more thrust to generate the same C_L values as the model with four engines.

In 1978 NASA Ames began the Quiet Short-Haul Research Aircraft (QSRA) program. This aircraft also utilized USB with four engines to take-off and land in exceptionally short distances (Ref. 4-2). As shown in Figure 4-4, the QSRA was able to produce a C_L of 8.5 by using a T/W of 0.38. Since the QSRA had a W/S of 81 lbs/ft², and the Firefly has a W/S of 72 lbs/ft², it was determined that we would need a T/W of 0.33, if we had 4 engines. However, since we only have two engines, this value must be scaled up by 150% to obtain a T/W of 0.50.

The YC-14 was, like the Firefly, a twin-engine USB aircraft. Although specific information on the maximum lift coefficients of the YC-14 is not available, the aircraft was able to achieve takeoff and landing performance similar to that dictated by the RFP with a T/W of 0.57 and a wing loading of 85 lbs/ft². This number was scaled down based on wing loading to get a T/W of 0.48, similar to the number derived from the QSRA data.

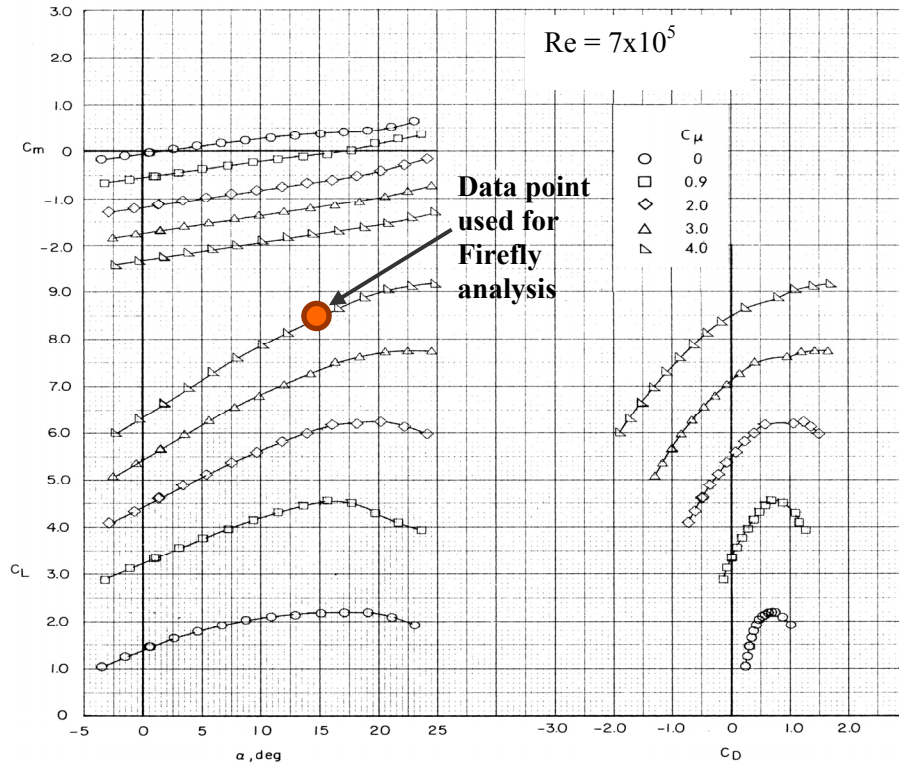


Figure 4-2: NASA USB Wind Tunnel Data, $\delta f = 50^\circ$ $\delta s = 40^\circ$, 4 Engines Operating (Ref. 4-1)

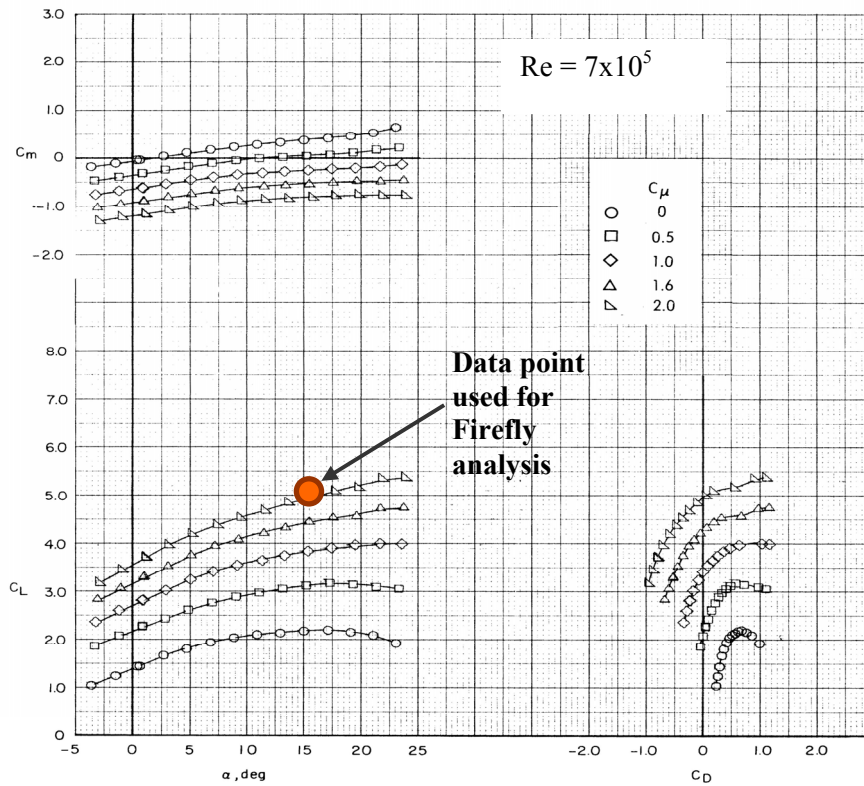


Figure 4-3: NASA Wind Tunnel Data, $\delta f = 50^\circ$ $\delta s = 40^\circ$, Outboard Engines Only (Ref. 4-1).

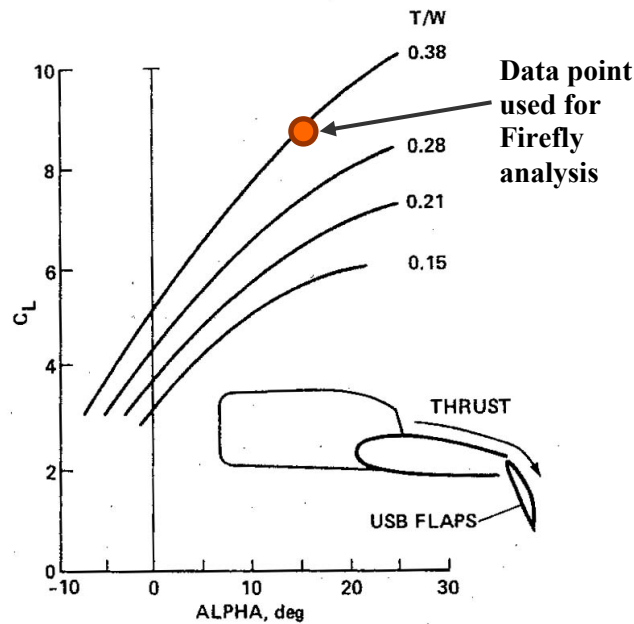


Figure 4-4: QSRA Lift Coefficient with a 50° flap deflection (Ref. 4-2)

4.2 Wing Geometry

As the RFP states the Firefly is required to cruise at a speed of at least 400 knots, which is Mach 0.69 at a cruise altitude of 38,500ft. Since Mach 0.69 is very close to the transonic region a supercritical SC(2)-0612 airfoil is used for the wing. After analysis, Section 4-3 will show that this airfoil at cruise conditions is efficient up to the drag divergent Mach number, $M_{dd} = 0.74$. The strut and pylon airfoils will be the symmetrical SC(2)-0010 airfoil. The horizontal and vertical tail airfoils will be respectively symmetrical SC(2)-0012 and SC(2)-0013 airfoils, based on the design of the YC-14 and C-17 aircrafts.

The average cruise weight is determined to be 47238.5 lb by taking the TOGW and accounting for loss in fuel weight. Using this weight to cruise at steady level flight C_{Ltrim} is calculated to be 0.40. To reduce the drag experienced at transonic speeds the wing will have a forward sweep angle of 10° at the quarter-chord; this will reduce the normal Mach number. Since we are able to attain a C_{Lmax} of 8.5, from Figure 2-2 we determined our wing loading to be 72 lbs/ft². The use of a strut allows us to use a wing with an aspect ratio wing of 11, improving the Firefly's performance at cruise.

The Korn equation is a method to estimate drag-divergence Mach numbers as a function of lift coefficient, wing sweep angle and wing thickness (Ref. 4-3). By choosing the critical Mach number to be close to the cruise speed, drag due to supersonic flow will be minimized and the aircraft will be more efficient during. Using the cruise Mach number of 0.74 along with the Korn Equation (Equation 4-1), Figure 4-5 shows that with a thickness ratio of 12%, and the wing quarter chord sweep to be 10°, the cruise Mach number is close to the drag divergence Mach number. Since the wing is designed with supercritical airfoil the technology factor κ_α was chosen to be 0.95.

$$M_{dd} = \frac{\kappa_\alpha}{\cos \Lambda} - \frac{(t/c)}{\cos^2 \Lambda} - \frac{C_l}{10 \cos^3 \Lambda} \quad (4-1)$$

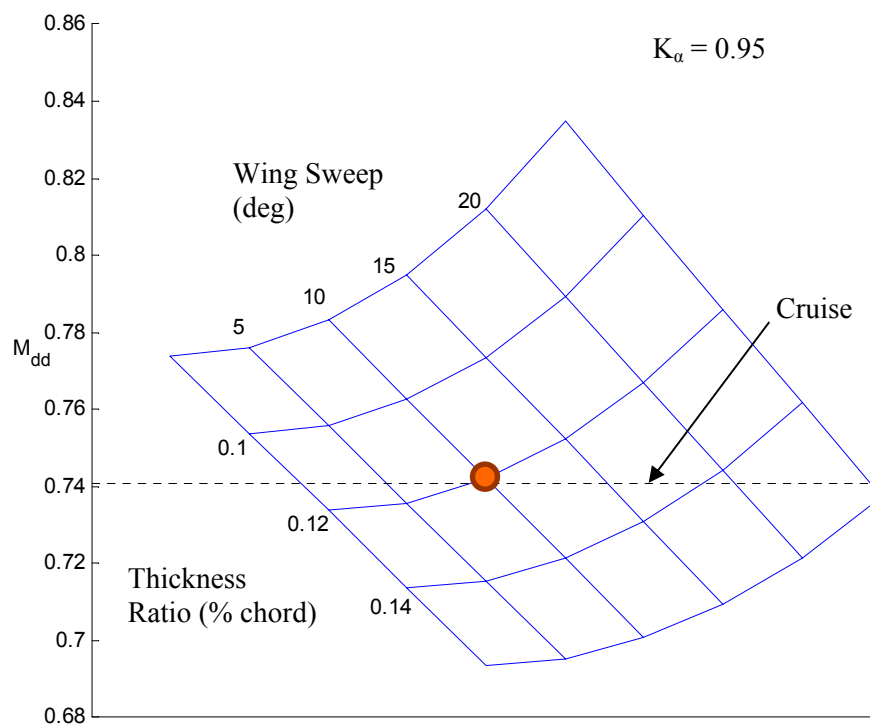


Figure 4-5: Drag Divergence Mach Number

The forward swept outer panel will provide excellent aileron control, as well as prevent the wing tip from stalling. The upper surface blowing propulsion system will prevent stall occurring at the root as a

result of detached flow. The strut is used to prevent wing divergence during cruise and increase overall efficiency of the aircraft (Ref. 4-4).

4.3 Airfoil Analysis

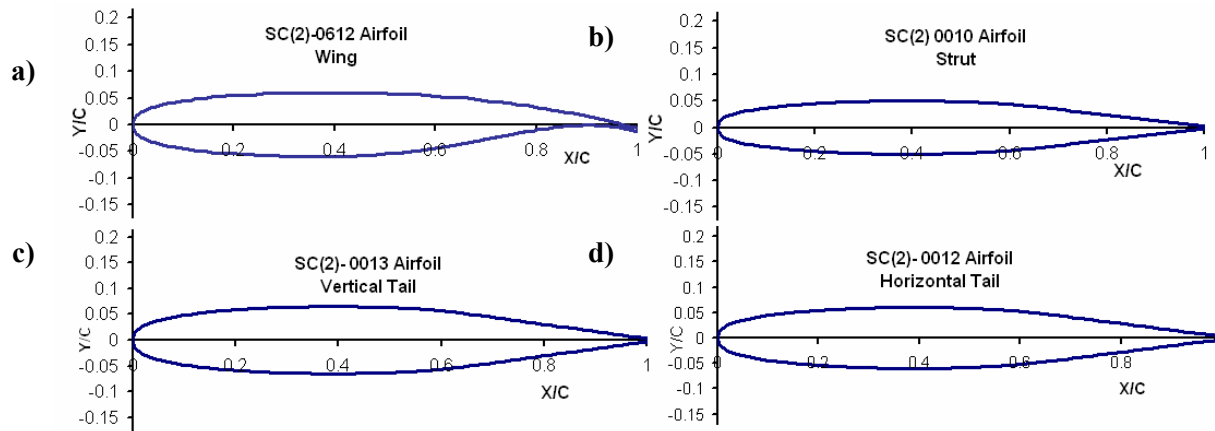


Figure 4-6: Firefly Selected Airfoils a) Wing b) Strut c) Vertical Tail d) Horizontal Tail

To minimize supersonic flow over the wing the SC(2)-0612 airfoil is used, analysis on this airfoil was carried out using MSES (Ref. 4-5). MSES is a computational fluid mechanics code that allows the user to analyze, modify and optimize single and multi element airfoils for a range of Mach and Reynolds numbers.

There should be no separation on top or bottom surfaces of the airfoil at cruise conditions. By looking at Pressure Distribution shown in Figure 4-7, it is apparent there is a very small shock at about 10% chord on the top surface. To get a better understanding of what's happening at this point, the skin friction plot, Figure 4-8 shows there is transition from laminar to turbulent boundary layer, but no separation. On the lower surface of the airfoil transition occurs at about 50% chord. This transition is due to the cusp near the trailing edge of this particular supercritical airfoil as can be seen in Figure 4-6a.

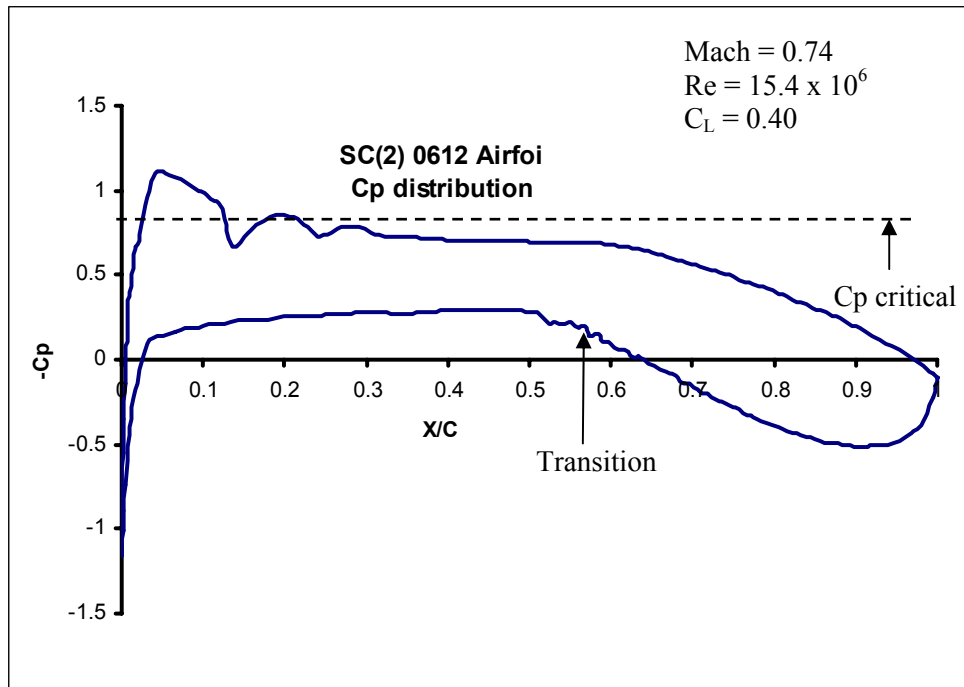


Figure 4-7: Firefly Pressure Distribution at Cruise

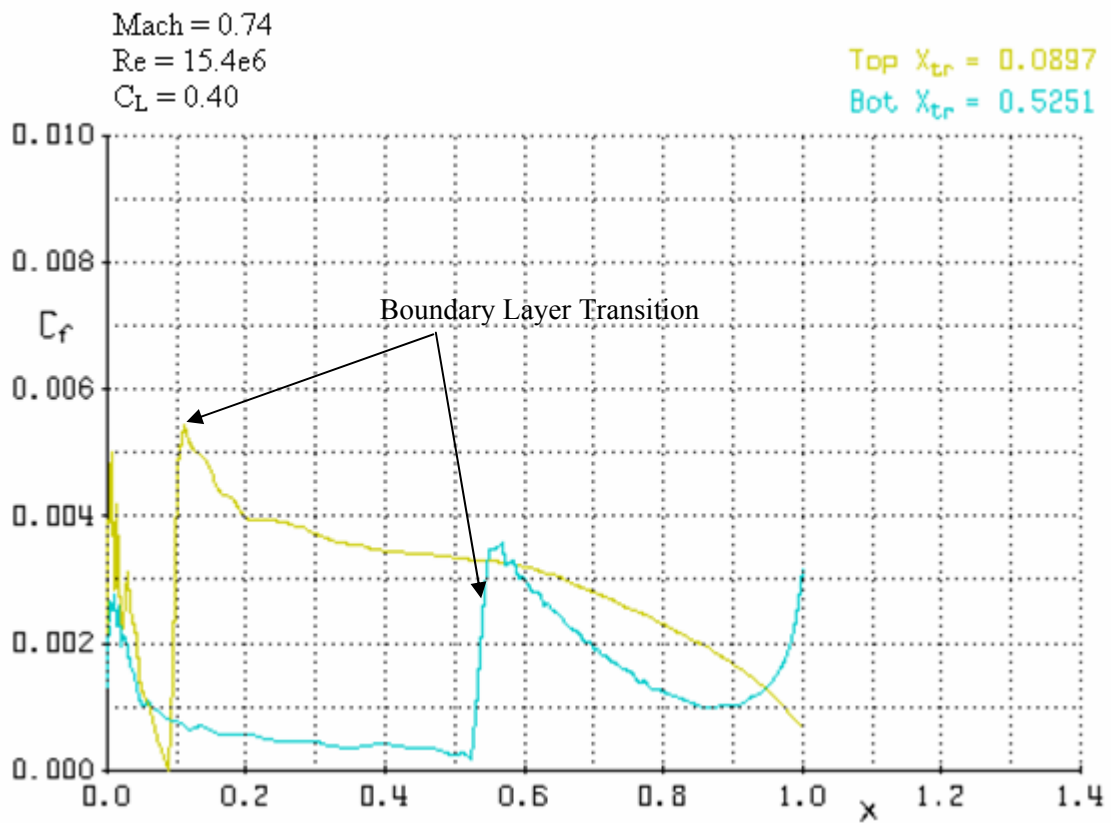


Figure 4-8: Skin Friction of the SC(2)-0612 at Cruise Conditions

The plot of airfoil drag versus freestream Mach number (Figure 4-9) also shows that this particular airfoil is not being pushed to its fullest potential at cruise conditions, and is capable of being just as efficient at higher speeds, up to Mach 0.74 as mentioned in Section 4-2. This is the normal Mach number, the freestream Mach number is 0.73. Note Figure 4-9 only shows only the airfoil drag divergence; this is not the same as the total aircraft drag divergence.

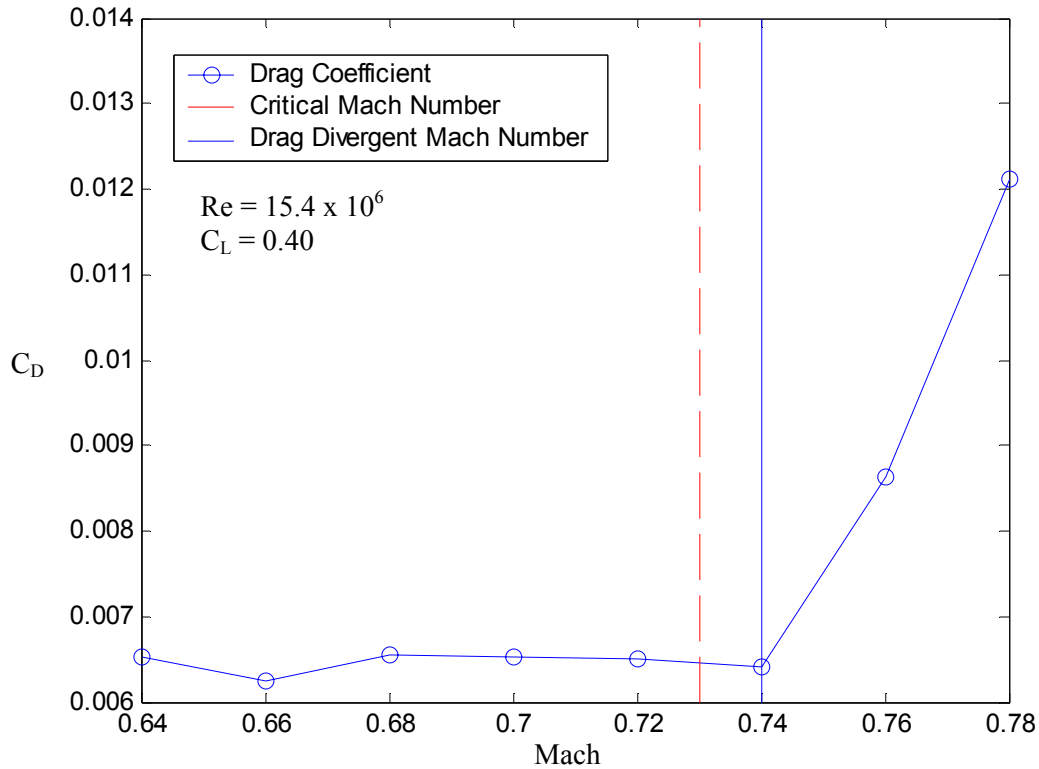


Figure 4-9: Airfoil Drag Divergence

4.4 Drag Buildup

Drag build up was calculated by the method described in Raymer (Ref. 4-6). The parasite drag is based on many components: fuselage, wing, strut, strut pylon, nacelle, blister, horizontal and vertical stabilizers. Since at cruise conditions the flow very briefly reaches supersonic speeds just past the leading edge, then quickly goes subsonic again wave drag is negligible in this analysis.

Total aircraft drag is based on the following equation:

$$C_D = C_{D0} + \frac{1}{\pi A \text{Re}} C_L^2 \quad (4-2)$$

Where the aspect ratio is 11 and the Oswald efficiency factor was calculated to be 0.73 (equation 12-49 Ref. 4-6).

Table 4-1: Firefly Cruise Build Up Summary (M = 0.74)

	Characteristic Length	Re	M	C _f	FF	S _{wet}	C _{D0}
Fuselage	87.58	1.3E+08	0.74	0.0019	1.0910	2700	0.0078
Wing	9.745	14621532	0.74	0.0026	1.5297	1233.68	0.0069
Strut	1.58	2370498	0.74	0.0036	1.4668	300	0.0030
Strut Pylon	1.58	2370498	0.74	0.0036	1.4726	18.78	0.0001
Nacelle	10.33	15503203	0.74	0.0026	1.1222	640.88	0.0036
Horizontal Stab	6.58	9877023	0.74	0.0028	1.5173	463.52	0.0028
Vertical Stab	13.20	19816653	0.74	0.0025	1.4413	454.58	0.0023
Blister	16.5	23650654	0.74	0.0025	1.0450	70	0.0003
						C_{D0} total	0.02738
						C_D total	0.0337

At cruise conditions using a C_L of 0.40 and equation 4-2 the total aircraft drag coefficient is found to be 0.0337. Using the method described in Roskam (Ref. 4-7) the maximum lift to drag ratio is found to be 15.18, and the cruise lift to drag ratio is found to be 11.48 at 38,500 ft.

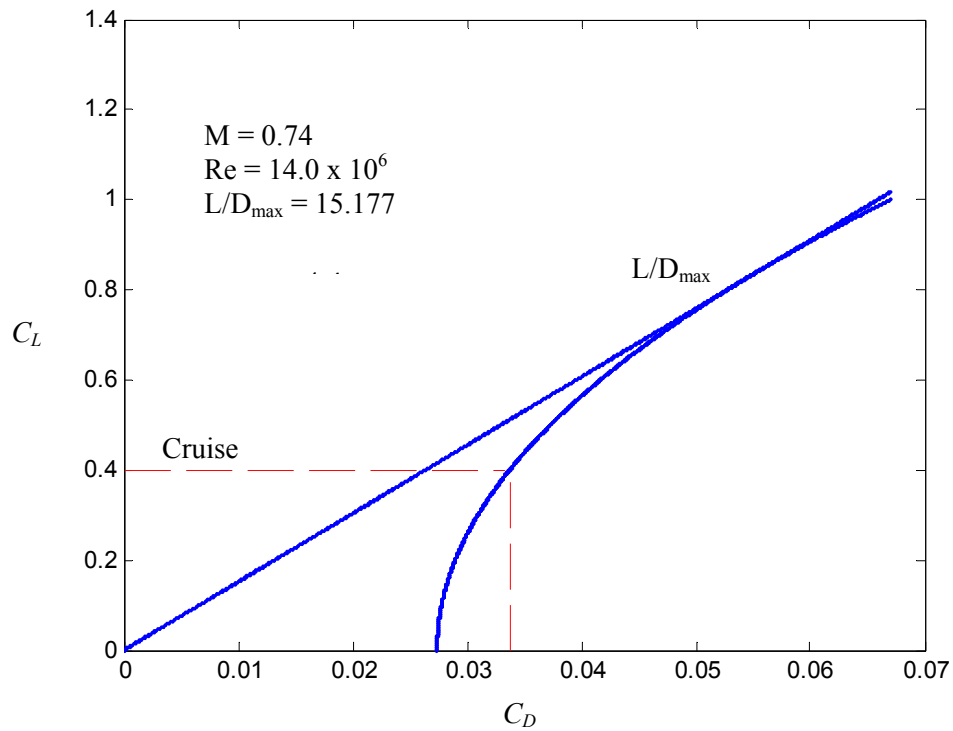


Figure 4-10: Firefly Full Configuration Cruise Drag Polar

To determine the thrust need during steady level flight a plot Figure 4-11 shows that 3,951 lbs of thrust are required to maintain steady the level flight at cruise conditions.

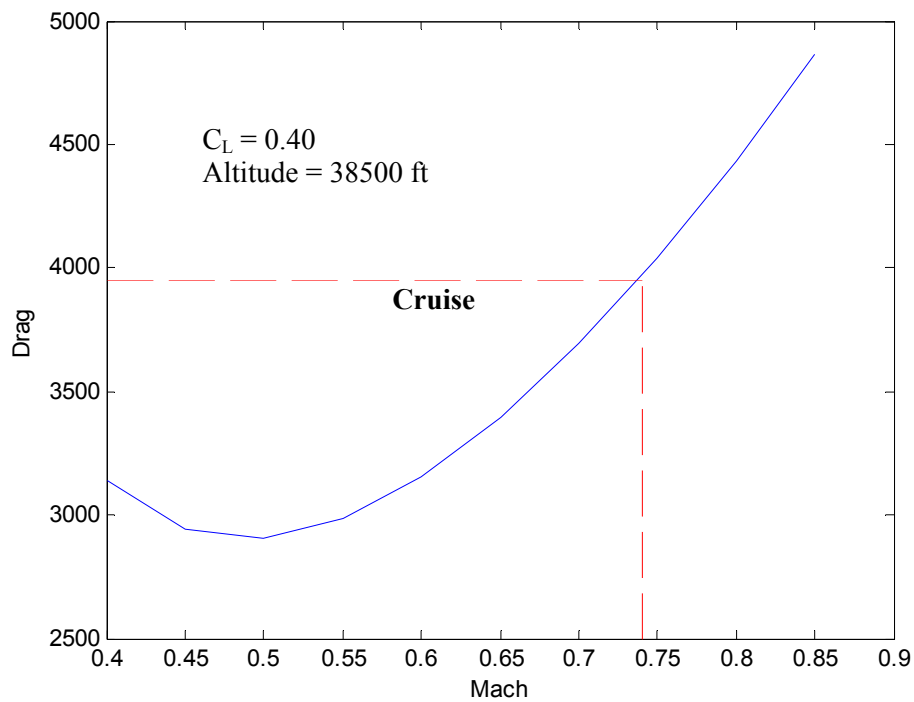


Figure 4-11: Drag Mach Number Relationship

Takeoff and landing drag coefficients are found to be respectively 2.99 and 0.39, using the same method as above, however when the aircraft is take-off and landing configuration the flaps are deflected as well as the landing gear deployed. The lift to drag ratios for takeoff and landing are found to be 1.85 and 7.69. Figures 4-12, 4-13, and Tables 4-3 and 4-4 below summarize this information.

Table 4-2: Lift To Drag Ratios

	Primary Mission				Secondary Mission			
	Takeoff	Cruise	Landing	Stall	Takeoff	Cruise	Landing	Stall
Weight (lbs)	53,082	47,238	41,395	52,200	47,917	42,073	36,230	52,200
Altitude (ft)	S.L.	38,000	S.L.	S.L.	5,000	38,500	5,000	5,000
C_L	5.528	0.4	2.99	8.5	4.99	0.38	2.62	8.5
C_D	2.994	0.033	0.389	2.898	1.02	0.032	0.3062	2.898
Velocity (knots)	62.5	425	65	50	62.5	425	65	50
L/D	1.846	11.48	7.686	2.933	4.89	12	8.56	2.933
L/Dmax		15.177				15.177		

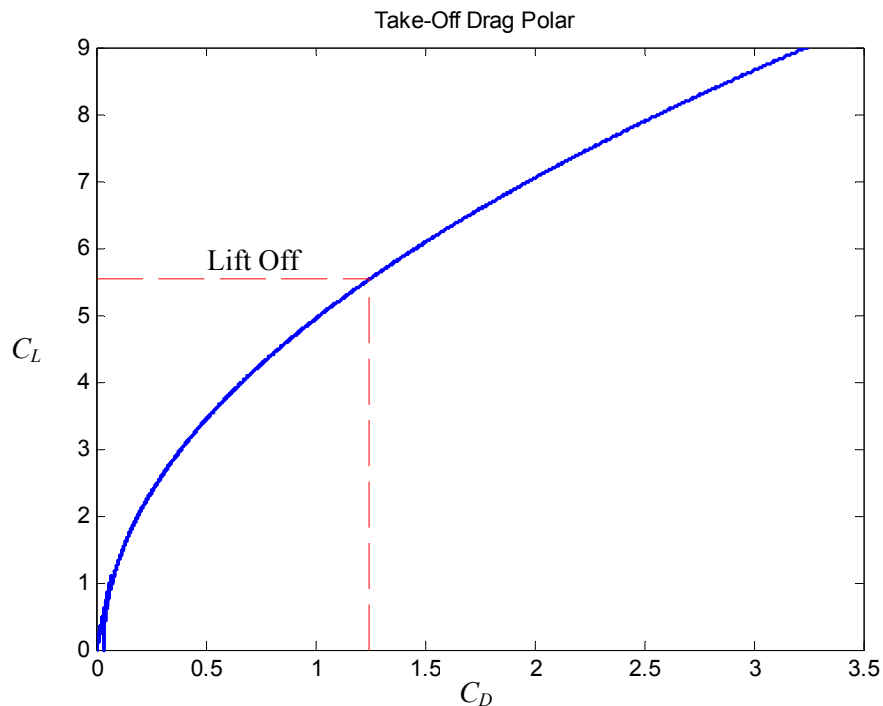


Figure 4-12: Firefly Landing Configuration Drag Polar

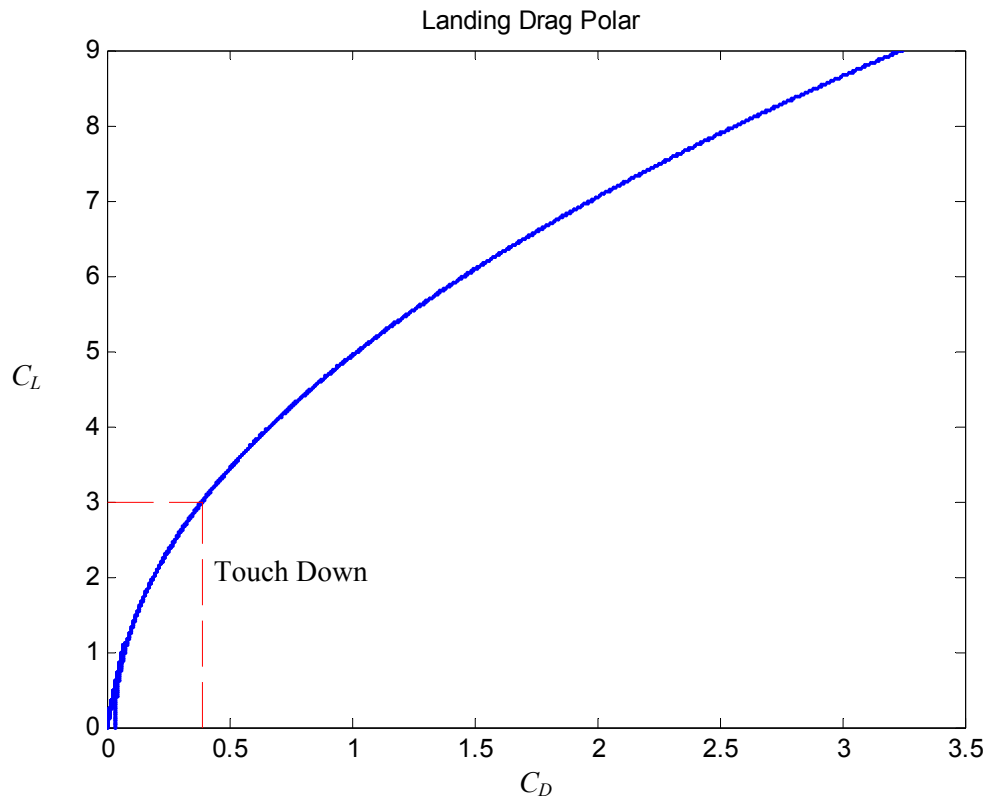


Figure 4-13: Firefly Take-Off Configuration Drag Polar

4.5 Speed Brake

A speed brake is located just aft of the nose landing gear. The main function of the speed brake is to provide additional drag for landing and approach. When Firefly is configured for approach/landing powered lift is required to maintain the necessary C_L . Since the powered lifting system on the Firefly is upper surface blowing and depends on additional thrust for increased lift, the speed brakes will be required to counter act the added thrust and keep the aircraft at the desired speed.

4.6 Wing Strut Pylon Juncture

Struts are designed to reduce the loads on the wing at cruise as well as landing conditions. While in flight the strut will be in tension with the purpose of reducing the effect of wing twist. Forward Swept wings tend to twist up at tips and cause premature stall. When the aircraft is landing the strut is compressed and reduces some of the bending moment at the root. Studies show that strut-braced wing

(SBW) configurations have had up to 19% savings in TOGW, 25% savings in fuel weight and a 28% increase in L/D when compared to its cantilevered wing counterpart (Ref. 4-4).

The location of the strut is designed to gain optimal structural reinforcement as well as aerodynamic efficiency. The pylon is located at 67% semi-span location of the wing as extends 4.1% semi-span below the wing. A super critical airfoil SC(2)-0010 is chosen for the strut, based on the A7 SBW design, a Virginia Tech experimental model (Ref. 4-4).

Table 4-3: Strut Dimensions

Airfoil	SC(2)-0010
Semi-span location	29.9 ft
Vertical drop down distance	1.83 ft
Strut chord	1.58 ft
Strut t/c	0.12
Strut Λ_{LE}	6°

One of the problems commonly encountered with SBW in transonic flight is the formation of shocks at the point of minimum area. The strut and wing juncture act like a 2-D nozzle and can cause choked flow as pictured in Figure 4-14. To reduce this effect equation 4-4 is used, where A is the inlet area and A^* is the minimum area:

$$\frac{A^*}{A} = \left(\frac{\gamma + 1}{2} \right)^{\frac{\gamma + 1}{2(\gamma - 1)}} M \left(1 + \frac{\gamma + 1}{2} \right)^{\frac{\gamma + 1}{2(\gamma - 1)}} \quad (4-3)$$

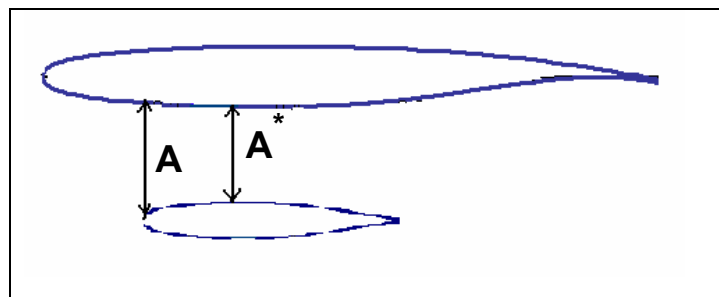


Figure 4-14: 2-D representation of nozzle effect between the strut and the wing

At cruise conditions using a free stream Mach number of 0.73, the inlet to throat area ratio must be greater than or equal to 2.66 to minimize compressibility and drag due to choked flow. To make this possible the top surface of the strut is flattened near the pylon. This reduces the thickness by half, from 10% to 5% t/c , leaving the rest of the strut symmetric.

5 Propulsion

5.1 Engine Selection

A Thrust to Weight ratio of 0.5 with a TOGW of 53,082 lbs gives a required thrust of 13270.5 lbs per engine to takeoff and land in the required distance. An engine with a high bypass ratio is needed to maximize the static thrust.

GE engines were first examined for each concept, in particular the CF line because of their proven success with the TF34. The CF-34-3A was ideal for our 3 and 4 engine concepts, but would need to be scaled too much for our 3rd and final concept with only 2 engines (Ref 5-1). To meet the higher thrust per engine needed for the final concept, the CF-34-8C1 was found to be a good match to our thrust requirements and specific fuel consumption (SFC) requirements. This engine only needs to be scaled down by a small percentage.

For a higher maximum thrust engine, the CFM-56 was considered, but is not practical because of the large scaling factor needed (Ref 5-2). Honeywell has designed two engines for short runways, noise restrictions, and short field performance; the ALF502 and the LF507. These two engines were attractive due to their small size and weight and were well suited for concepts 1 and 2, but would need to be scaled up too much for concept 3 (Ref 5-3).

Two additional engines were considered. These are the Rolls Royce AE 3007, and the Pratt and Whitney PW 300. The AE 3007 produces 7580 lbs of thrust and has a bypass ratio of 5 (Ref. 5-4). The PW 300 produces a thrust of 8000 lbs (Ref.5-5). These two options were also discarded once concept 3 was selected because of the scaling factor that would have been required.

For the preferred concept, the selected engines were two General Electric CF34-8C1s, based on the past performance of its predecessor, the TF34. The TF34 is a dependable, combat proven engine used in the A-10 and S-3A military aircraft. The TF34 evolved into the CF34, a commercial engine with excellent performance, durability and reliability. This will be important when used in remote areas while performing its civil defense role. The government's use of the TF34 engine in the past will give them confidence in its reliability and performance. The characteristics for the engines examined are shown in Table 5-1. As shown, the CF-34-8C1 allows for the smallest scale factor while still maintaining a high bypass ratio. Table 5-2 shows the scaled up versions of the CF34-3A1 and the CF34-8C1 compared to the off-the-shelf model. While scaled to the same thrust required, the CF34-8C1 model has a lower weight, front face area and diameter, with only a slightly longer length compared to the scaled up CF34-3A1 model. Figure 5-2 shows the thrust changes at altitude with respect to sea-level static thrust. As altitude increases, thrust goes down from the less dense air. Figure 5-3 is the thrust available in pounds at varying altitude.

Table 5-1: Engine Comparison

Engine	Maker	Thrust (lbs)	SFC	Diameter (in)	Length (in)	Weight (lbs)	Bypass ratio	scale % req'd
CF-34-3A	GE	9220	0.357	49	103	1650	6.2	43.93
CF-34-8C1	GE	13790	0.358	52	128	2350	6.1	3.77
CFM-56	GE	27300	0.38	65	98.7	5205	5.1	48.86
BR 710	Rolls Royce	14750	0.38	48	134	3600	4.2	10.03

Table 5-2: Engine Sizing Geometry

Specification	CF34-3A1	CF-34 scaled	CF34-8C1	CF34-8C1 scaled
Thrust (lbs)	9220	13270.5	13790	13270.5
Length (in)	103	119.15	128	126.05
Diameter	49	58.79	52	51.01
Weight	1650	2462.95	2350	2252.80
Front Face Area (in ²)	1885.74	2714.17	2123.72	2043.71
Scale factor (%)		-43.93		3.77

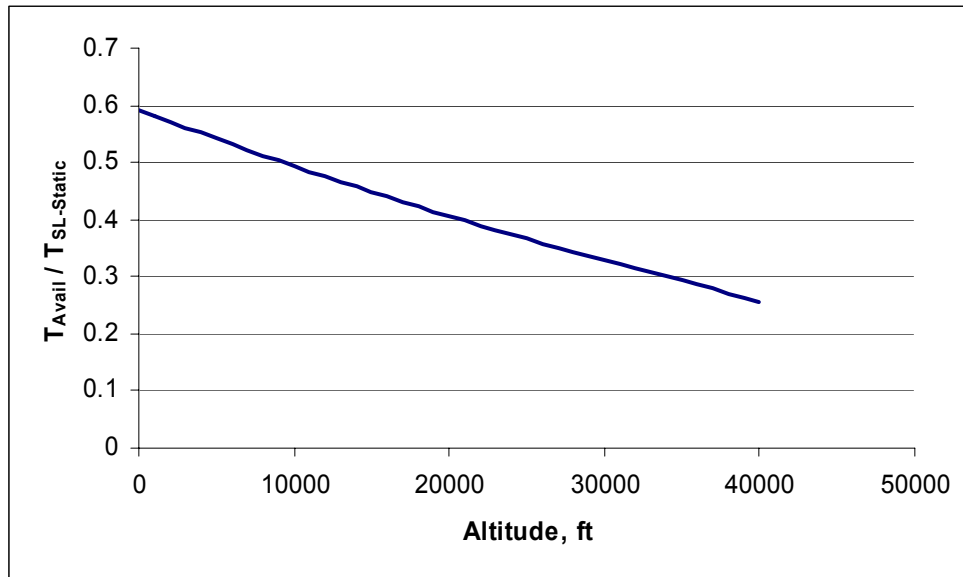


Figure 5-1: 3.77% scaled CF34-8C1 Thrust_{Available}/Thrust_{SL-Static} vs. Altitude for Mach 0.74 (Ref. 5-2)

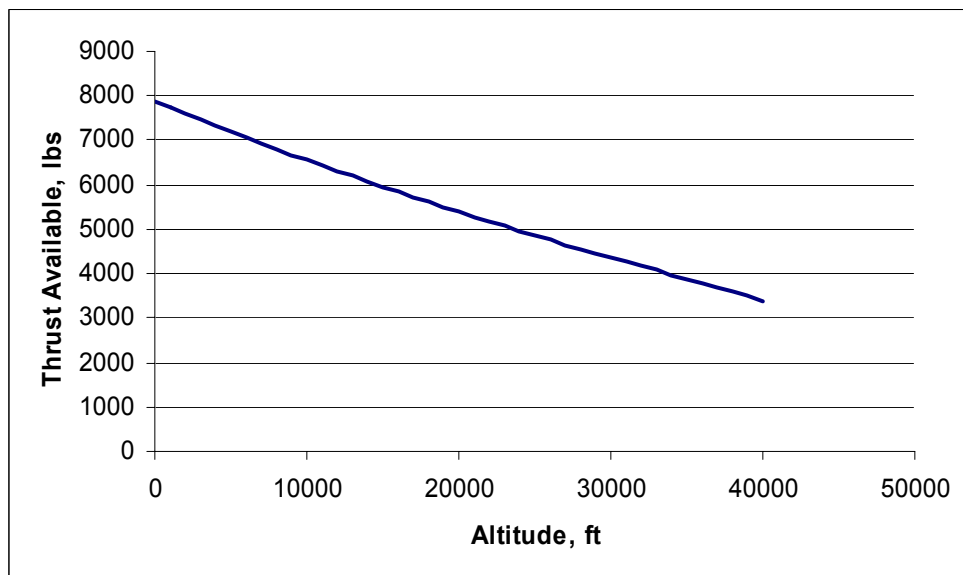


Figure 5-2: 3.77% scaled CF34-8C1 Thrust Available vs. Altitude for Mach 0.74 (Ref. 5-2)

5.2 Inlet Sizing

For a design Mach number of 0.74, a normal inlet is used to slow the flow to prevent the compressor blade tips from reaching Mach 1. A large lip radius provides additional air needed for take-off thrust at

slow speeds. The over-wing podded nacelles reduce the landing-gear height and reduce noise on the ground. Placing the inlets forward of the wing minimize distortion. The downside to this is the placement makes it difficult to access for maintenance. Table 5-3 shows the changes in the inlet geometry from the off-the-shelf CF34-8C1 engine and our 3.77% scaled version.

Table 5-3: Inlet Sizing Geometry

Engine	CF34-8C1	CF34-8C1 scaled 3.77%
Throat Area	1592.79	1532.78
Inlet radius	22.52	22.09
Lip radius	18.01	17.67

5.3 Exit Nozzle

An exit nozzle configuration was needed to guide the exhaust flow over the wing and flaps. A D-nozzle was considered initially. According to NASA research (Ref. 5-6), the turning radius of an aircraft with a USB system with a D-nozzle is too small to maintain attached flow of the relatively thick jet exhaust.

A 6:1 aspect ratio nozzle was chosen for our aircraft as shown in Figure 5-3. The converging internal cross-sectional area distribution, from the circular internal shape to the rectangular nozzle exit, was selected to match the internal area characteristics of a D-nozzle to reduce the tendency for the internal flow to separate. Exit nozzle doors were added based on results from the YC-14 program. These doors fold flat against the outside of the exit nozzle during STOL operations, to allow the exhaust to spread along the wing. During cruise however, these doors fold in to the flow, directing the flow straight out of the nozzle.

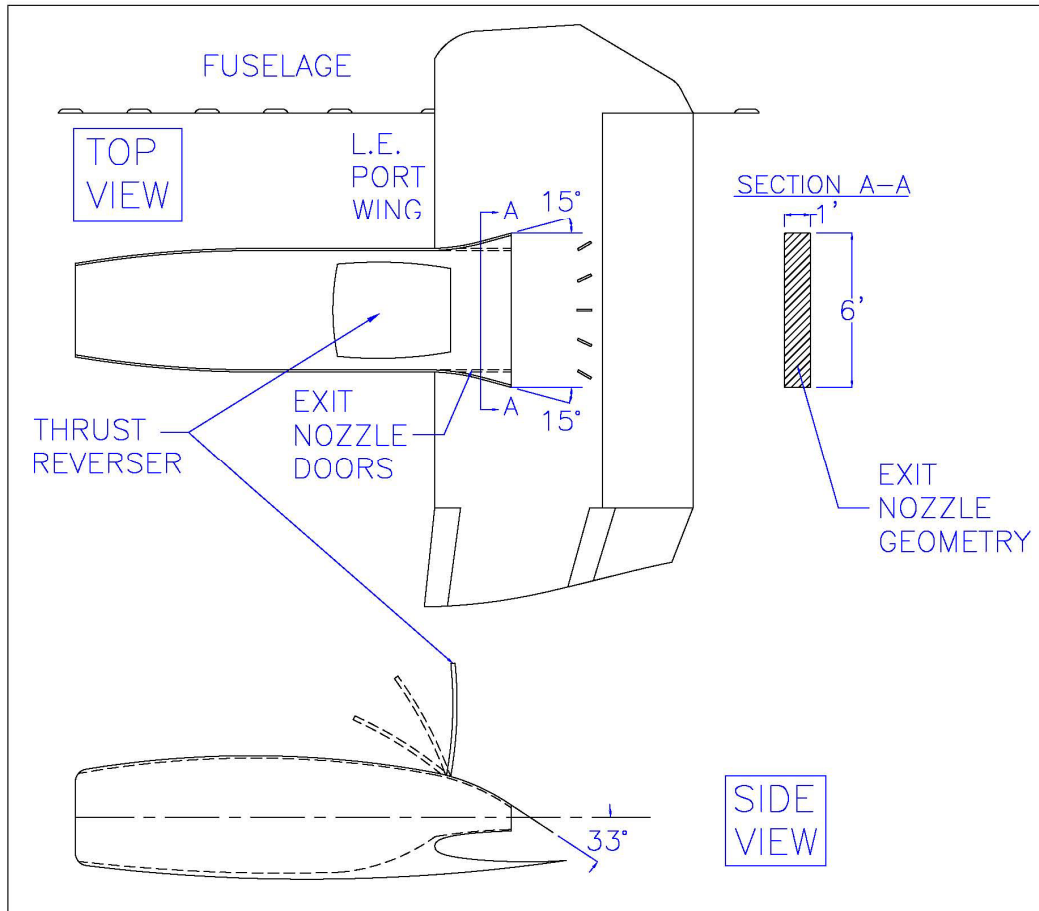


Figure 5-3: Engine Exit nozzle Geometry

Vortex Generators are placed along the trailing edge of the wing behind the nozzle to mix the exhaust flow with the local boundary layer, which will cause the flow to go against the pressure gradients downstream along the flaps. They extend out of the wing only when the USB flaps are fully deployed and retract during cruise (Ref 5-6).

Reversers are used to assist the aircraft in slowing down after touchdown. The upper rear surface of the nacelle is deflected up causing the flow to turn forward, as shown in Figure 5-3. A layer of carbon-fiber epoxy is placed on the surface of the wing where the exhaust is flowing over in case of an engine fire on engine start with full fuel tanks in the wings. This heat shield is faired out to meet with the surface of the wing to reduce its effect on aerodynamics.

5.4 Engine Removal

Ease of engine replacement and maintenance was a driving factor in designing this aircraft. Using the Upper Surface Blowing high lift system required the engine be placed in front of the wing to allow the exhaust to be blown over it. An added benefit to this was that it allowed for the engine to be dropped straight down out of its supports by opening the removal hatches shown in Figure 5-4.

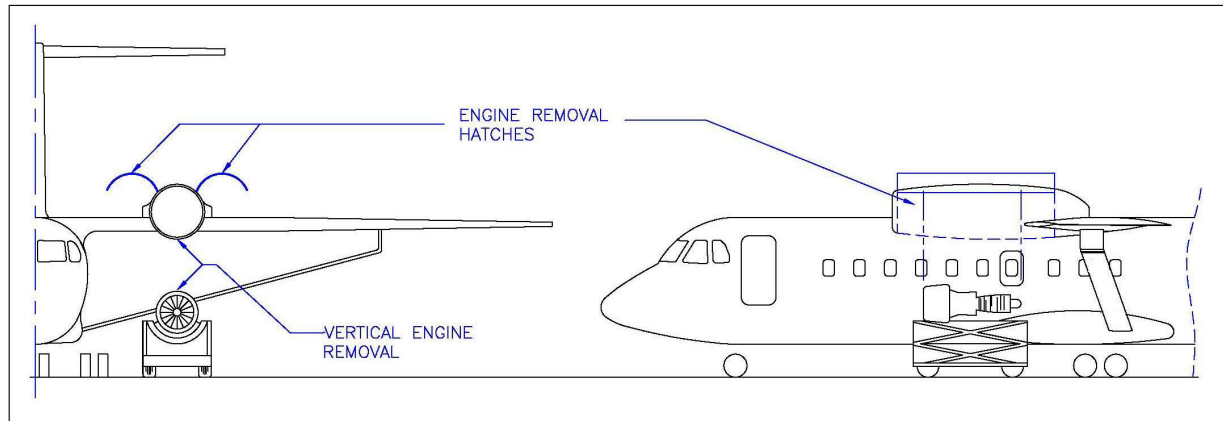


Figure 5-4: Engine Removal

5.5 Noise

A variety of studies have been done to investigate the noise characteristics of aircraft that use USB to provide additional lift during takeoff and landing. One notable example was the Quiet Short-Haul Research Aircraft Flight Research Program conducted by NASA Ames (Ref. 5-7). During spiraling takeoff trajectories, noise measurements showed a 90 EPNdB at a sideline of 500 ft, and an overall noise footprint much smaller than a comparable conventional jet transport. The Firefly is expected to have similar noise characteristics, putting it well below the maximum noise levels allowed by FAR part 36.

6 Stability and Control

The configuration and mission of the Firefly leads to significant stability and control challenges. The pitching moment and forces acting on the wing due to the USB system are designed to be much larger than a regular wing, requiring larger and more effective control surfaces to trim and control the aircraft. This problem is further complicated by the need to accommodate a possible engine failure.

6.1 Design Philosophy

A Fly-By-Light (FBL) flight control system was chosen for the Firefly, because of the weight savings and increased longevity and survivability for the secondary mission. This system also allows the aircraft to utilize a Stability Augmentation System (SAS), where a flight computer provides the necessary elevator deflections to keep the aircraft stable during cruise, and allows the aircraft to have “relaxed stability.” The Firefly is designed to have a low static margin, which actually becomes negative during some loading conditions and places the aircraft in a state of relaxed stability. With the low static margin, the elevator will not have to be deflected as much to balance the moments, resulting in a lower trim drag.

6.2 Tail Design

The T-tail configuration was selected primarily because of the advantages in terms of stability and control. The horizontal tail acts as an endplate, improving rudder effectiveness, and the horizontal tail is above the wake of the engine and wing. Initial sizing was done based on tail volume coefficients numbers from the YC-14 and C-17. More detailed sizing was done by evaluating the stability and control derivatives of the aircraft for different tail sizes and control surface chord lengths.

6.3 Control Surfaces

Historical guidelines and comparator aircraft served as the basis for the initial sizing of the control surface, namely: ailerons, elevator, and rudder. Analysis of the corresponding control derivatives provided more detailed design. The ailerons consist of the outer 14' of each wing, with a chord length of 25% of the wing. These relatively large ailerons were necessary to counteract the rolling moment that is generated when only one engine is being used for powered lift on one side of the aircraft.

The rudder chord length is 35% of the vertical tail chord length, and extends along 85% of the vertical tail. The rudder is double knuckled, similar to the design of the YC-14 and C-17. The knuckling allows for a larger range of control surface deflections, more effectiveness, and better control response.

The elevator is double hinged like the rudder, and extends along the outer 90% of the horizontal tail. The elevator chord length is 30% of the chord length of the horizontal tail.

6.4 Stability and Control Derivatives

Stability and control derivatives were found using a program JKayVLM, developed by Jacob Kay at Virginia Tech (Ref. 6-1). The code uses trapezoidal shapes to approximate the main lateral and longitudinal geometry of the aircraft. The aircraft was evaluated at cruise, takeoff, and landing conditions, as detailed in Table 6-1. The results for the different flight conditions are shown in Table 6-2.

Table 6-1: Flight Conditions for Stability and Control Evaluation

Flight Phase	Cruise	Takeoff	Landing
Altitude (ft)	38,500	50	50
Speed (knots)	425	65	65
CG location (% MAC)	15%	19%	8%

Table 6-2: Stability and Control Derivatives

FlightPhase	Cruise	Takeoff	Landing
$C_{L\alpha}$	6.18	6.24	6.24
$C_{m\alpha}$	-0.60	-0.37	-0.93
C_m / C_L	-0.09	-0.06	-0.15
C_{Lq}	12.15	11.74	12.84
C_{mq}	-15.78	-15.67	-16.24
$C_{L\delta\epsilon}$	0.82	0.82	0.82
$C_{m\delta\epsilon}$	-3.49	-3.46	-3.54
$C_{l\delta\alpha}$	-0.23	-0.23	-0.23
$C_{n\delta\alpha}$	-0.0024	-0.0024	-0.0024
$C_{Y\delta r}$	-0.38	-0.38	-0.38
$C_{l\delta r}$	-0.04	-0.04	-0.05
$C_{n\delta r}$	0.14	0.14	0.15
$C_{Y\beta}$	-0.56	-0.56	-0.56
$C_{n\beta}$	0.077	0.12	0.16
$C_{l\beta}$	-0.08	-0.08	-0.08
C_{Yr}	0.70	0.69	0.71
C_{nr}	-0.24	-0.24	-0.25
C_{lr}	0.06	0.06	0.07
C_{lp}	-0.57	-0.57	-0.57
C_{np}	-0.29	-0.28	-0.28

6.5 Dynamic Response and Handling Qualities

The handling qualities of the Firefly were computed using Roskam's methods, with the stability and control derivatives produced by JKayVLM. These values were evaluated against the MIL-F-8785C (Ref. 6-2) requirements, since the aircraft will be used for government missions as well as commercial flights. The aircraft will have to perform both terminal and non-terminal maneuvers, so both Class A and C Flight Categories were considered, in addition to Class B. Tables 6-3 and 6-4 show the results of this analysis. The Firefly is clearly within the Level 1 requirements for the short period, phugoid, and Dutch roll modes. However, in the landing and takeoff conditions, it struggles to meet the time-to-bank and roll mode time-constant values. This is primarily because the velocity and dynamic pressure at these conditions is very low, so it is difficult to quickly generate the required moments.

Table 6-3: Class A and C, Level 1 Handling Qualities

Class A and C Flight Categories	MIL-F-8785C Requirements		Takeoff	Landing
	Minimum	Maximum		
ζ_{SP}	0.35	1.3	0.45	0.46
ω_{SP}	0.28	3.6	1.35	1.44
ζ_{Ph}	0.04	-	0.40	0.41
ζ_{DR}	0.19	-	0.38	0.39
ω_{DR}	0.4	-	0.57	0.58
τ_r	-	1.4	1.0	1.08
t_{30deg}	-	1.4	1.38	1.45

Table 6-4: Class B, Level 1 Handling Qualities

Class B Flight Categories	MIL-F-8785C Requirements		Cruise
	Minimum	Maximum	
ζ_{SP}	0.3	2.0	1.54
ω_{SP}	0.085	3.6	1.10
ζ_{Ph}	0.04	-	0.08
ζ_{DR}	0.08	-	0.46
ω_{DR}	1.0	-	2.58
τ_r	-	1.4	0.55
t_{30deg}	-	1.9	0.85

6.6 SNI Approach

A primary motivation for this new design is the ability to conduct a simultaneous non-interfering (SNI) approach that utilizes currently unused airspace and runways at congested airports. This basic concept behind this approach trajectory is the aircraft flies over the airport above normal approach altitudes, and follows a spiral descent path down to the runway. The nominal trajectory defined in the RFP requires the aircraft arrive at the airport airspace at 5000 ft AGL, and follow a 1 nm diameter spiral, completing two loops. The aircraft breaks out of the spiral approach at 50 ft, the decision height, at a speed of 65-80 knots. Additionally, the aircraft must be able to complete the SNI approach in IMC Cat 3C conditions, and with one engine inoperative.

Curved, decelerating approaches such as the SNI approach received considerable attention in the early 1980's. However, the conclusion at the time was that the pilot workload was too great, as the pilot was required to control the aircraft's attitude with the ailerons, elevator, and rudder, while also varying the flap settings and possibly throttle if powered lift was used (Ref. 6-3). Some effort was put into developing a computer automated system which assisted the pilot, but computers at the time were not fast enough to provide full control. With today's technology, an automated system can be designed to fly the aircraft through the SNI approach all the way down to the landing. This will be achieved by a feedback control system similar to the system depicted in Figure 6-1. The system will require accurate knowledge of the aircraft's current position and orientation relative to the spiral trajectory. Position will be measured by inertial measurement units with updates from an onboard GPS system. The GPS system will utilize the FAA's "Local Area Augmentation System," (LAAS) which uses differential GPS to achieve accuracies of less than 1 meter (Ref. 6-4). This system will allow the aircraft to make the approach in IMC Cat 3 conditions (zero visibility). After the approach, a flare and landing automatic control can be used to land the plane automatically, if necessary.

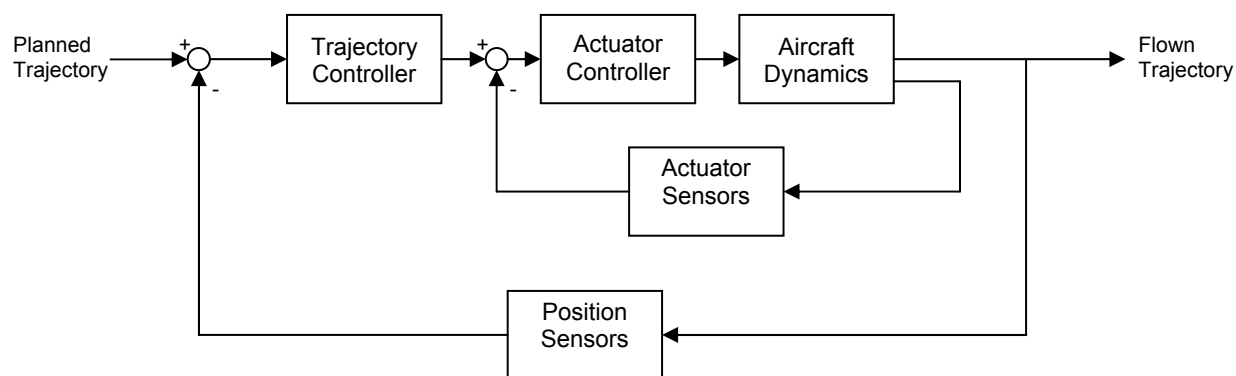


Figure 6-1: Feedback Control Loop

6.7 Engine Out and Crosswind

The RFP requires that the aircraft be capable of completing the SNI approach with one engine inoperative. Since the working engine will still be producing thrust, the rudder and aileron will have to be deflected to balance out the resulting moment. This is especially important since the powered lift system will be producing a lot more lift on one side of the aircraft than the other, creating a significant roll moment. The aircraft's ability to trim out these moments was evaluated at the end of the SNI approach, when dynamic pressure is the lowest, and the roll moment due to powered lift will be the largest. The approach speed is set to 80 knots, the upper limit of the RFP requirement, to meet this goal. The necessary control deflections at these conditions are given in Table 6-5.

For the secondary mission, the remote airfields will not always be lined up with the dominate wind, so the aircraft must be capable of landing in a strong crosswind, with a possible tail wind component. The RFP defines such a situation, with a 25 knot crosswind, with a 5 knot tailwind component. In these conditions, the rudder will provide most of the balancing force, with the ailerons deflected to balance the roll moments. The necessary control deflections are given in Table 6-5.

Table 6-5: Necessary Control Deflections

Situation	SNI Approach with Engine Out ($V_{APP} = 80$ knots)	25 knot Crosswind ($V_{APP} = 80$ knots)
Aileron Deflection (δ_a)	-26.94°	-26.85°
Rudder Deflection (δ_r)	26.85°	1.7°
Bank Angle (ϕ)	-	18.2°

6.8 Trim at C_{Lmax}

The Firefly utilizes upper-surface blowing to produce the lift necessary to meet the short takeoff and landings requirements. In addition to the large lifting force, this will tend to produce a large pitching moment, as shown in the NASA wind tunnel data presented in Figures 4-2 and 4-3. To verify that the Firefly can be trimmed at our desired C_{Lmax} of 8.5 at maximum throttle, C_M versus C_L was plotted for different elevator deflections in Figure 6-2. The data for this plot was based on the NASA wind tunnel data and the stability and control derivatives given in Table 6-2. From this analysis, an elevator deflection of 26° will provide the necessary trimming moment.

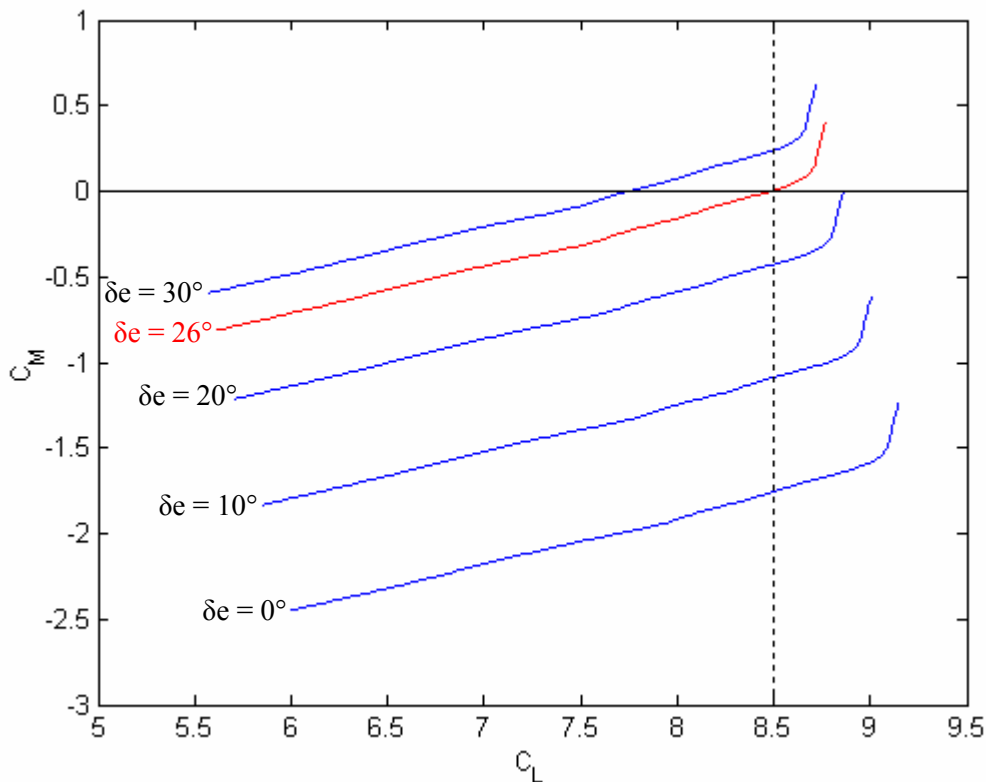


Figure 6-2: Elevator Deflection Required to Trim at C_{Lmax} at Max. Throttle

7 Performance

The methods used to analyze aircraft performance are outlined in *Airplane Design: Part VII* by Roskam (Ref 7-1) and *Aircraft Performance and Design* by John D. Anderson (Ref 7-2). Aircraft performance calculations are carried out with the aid of programs and functions written in MATLAB.

Several MATLAB codes required iterative techniques. Aircraft performance was analyzed for the requirements and constraints given in the RFP. Table 7.1 summarizes performance requirements for both the primary and secondary mission.

Table 7-1: Performance Requirements

Mission Segment	Primary Mission	Secondary Mission
Takeoff & Landing BFL	≤ 2500 ft	≤ 2000 ft
Take Off Velocity	≤ 65 knots	≤ 65 knots
Approach Speed	≤ 65 knots	≤ 65 knots
Cruise Speed	≥ 400 knots	≥ 400 knots
Block Range	≥ 1500 nmi	≥ 750 nmi x 2
Loiter Time	45 min	n/a
Diversion	150 nmi	n/a
Landing Speed	≤ 65 knots	≤ 65 knots

7.1 Takeoff and Landing Performance

Take off and landing requirements for both primary and secondary missions are key constraints in this design. For the primary mission, an airplane must be able to takeoff and land within a nominal balanced field length of 2,500 ft and also meet other FAR-25 requirements, such as clearing a 35 foot obstacle and achieving takeoff at a speed of $1.25-1.3V_{\text{stall}}$. In the secondary mission, an airplane must use a remote airfield defined as a blacktop with a useful area of 2,000 ft by 150 ft with obstacles 250 ft from either end of the runway. The nominal balanced field takeoff length at an altitude of 5,000 ft for different surfaces and weather conditions for both primary and secondary missions are shown in Table 7-2. Although the primary mission requirements were set for sea level conditions, the aircraft was evaluated at 5000 ft, recognizing that there are commercial airports at this altitude that the Firefly could serve.

Table 7-2: BFL Takeoff Length for different surfaces at 5000 ft

Ground Surface Type	Friction Coefficient (Ref 3.1.2)	Primary Mission BFL (ft)	Secondary Mission BFL (ft)
Icy Concrete/asphalt	0.02	2118	1747
Dry Concrete/asphalt	0.04	2204	1791
Hard Turf	0.05	n/a	1816
Soft Turf	0.07	n/a	1871
Wet Grass	0.08	n/a	1902
Long Grass	0.10	n/a	1974

The analysis of the landing performance of an airplane is similar to the analysis for takeoff. The landing includes clearing a 50 foot vertical obstacle. Total landing field length consists of final approach, flare distance and ground roll distance. The total landing distance must be less than 2,500 ft for the primary mission and less than 2,000 ft for the secondary mission. Table 7-3 shows landing field length for both missions for different surfaces and conditions.

Table 7-3: Landing Distance for different surfaces at 5000 ft

Ground Surface Type	Friction Coefficient (Ref 3.1.2)	Primary Mission Field Length (ft)	Secondary Mission Field Length (ft)
Icy Concrete/asphalt	0.02	1619	1511
Dry Concrete/asphalt	0.04	1490	1403
Hard Turf	0.05	n/a	1361
Soft Turf	0.07	n/a	1291
Wet Grass	0.08	n/a	1263
Long Grass	0.10	n/a	1214

7.2 Rate of Climb, Absolute & Service Ceiling and Time to Climb

Table 7-4 shows a brief summary of the aircraft's performance at maximum rate of climb and maximum climb angle. The significant difference in the rates of climb between missions is due to the weight difference. Complete solutions for climb angles and rates of climb at 5,000 ft for both the primary and secondary missions are presented graphically in the hodograph diagram in Figure 7-1. The primary mission solutions are presented in blue, and secondary mission solutions are presented in red. The lines tangential to the parabolic curves indicate conditions for maximum climb angle conditions. The highest peaks of the curves represent the maximum rate of climb.

Absolute ceiling and service ceiling per FAR 25 are estimated to be the altitude where rate of climb is approaching 0 and 500 fpm respectively as shown in Figure 7-2. Absolute ceiling is determined to be at 43,500 ft and service ceiling at 38,500 ft.

According to FAR 25, commercial airplanes must not exceed indicated speed of 250 knots during its first 10,000 ft of climb due to noise limitations. Climb requirements per FAR 25 fall between best velocity gradient conditions and best rate of climb conditions. After an aircraft passes 10,000 ft,

maximum climb rate conditions are assumed. Numerical integration was used to estimate the time to climb to best cruise altitude. This means that for every altitude change new maximum climb conditions were computed. The time to climb at the cruise altitude conditions at two climb conditions described above was estimated to be 18.3 minutes.

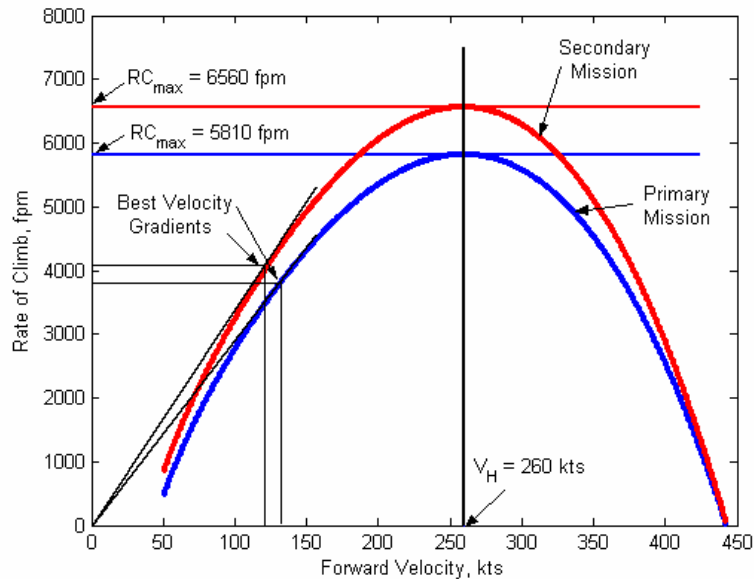


Figure 7-1: Hodograph Diagram

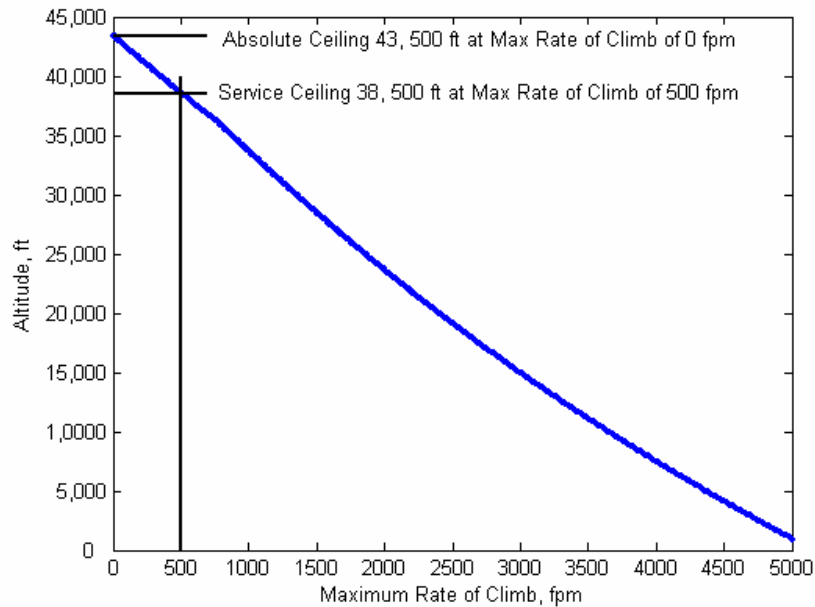


Figure 7-2: Absolute and Service Ceiling

Table 7-4: Maximum Rate of Climb and Climb Angle

Mission	Best Rate of Climb			Best Velocity Gradient		
	Rate of Climb	Angle	FWD Velocity	Angle	Rate of Climb	FWD Velocity
	ft/min	deg.	knots	deg.	ft/sec	knots
Primary	5,810	12.5	260.0	16.3	3,650	132.0
Secondary	6,560	14.0	259.4	18.6	4,250	126.0

7.3 Cruise Performance and Level Flight Envelope

The contributing factors in defining the cruise performance are the altitude and velocity for best range. The cruise speed of $V_{\text{cruise}} \geq 400$ knots and block range of 1,500 nautical miles are specified by the RFP. The maximum range needed for the primary mission is estimated to be 1650 nm, including a 150 nm diversion, and 1500 nm for the secondary mission, without a diversion.

To determine the best cruise altitude, the specific range (nm/lbs) is plotted as a function of Mach number for the both mission as show in Figures 7-3 and 7-4. The velocity for the best range is defined as the velocity that gives 99% of the maximum specific range. At 38,500 ft, this was computed to be Mach 0.74.

At cruise conditions of 38,500 ft and Mach 0.74 there was some excess thrust available. This shows that the aircraft could fly faster. The maximum Mach number was determined by setting total thrust equal to total drag, including wave drag. Maximum obtainable speed of the aircraft was determined to be 0.83. The best ways to present ranges of stall speed, ceilings, and maximum aircraft speed is in the form of a 1-g flight envelope as shown in Figure 7-5. The 1-g flight envelope shows all possible Mach numbers with altitude, drag, and thrust available.

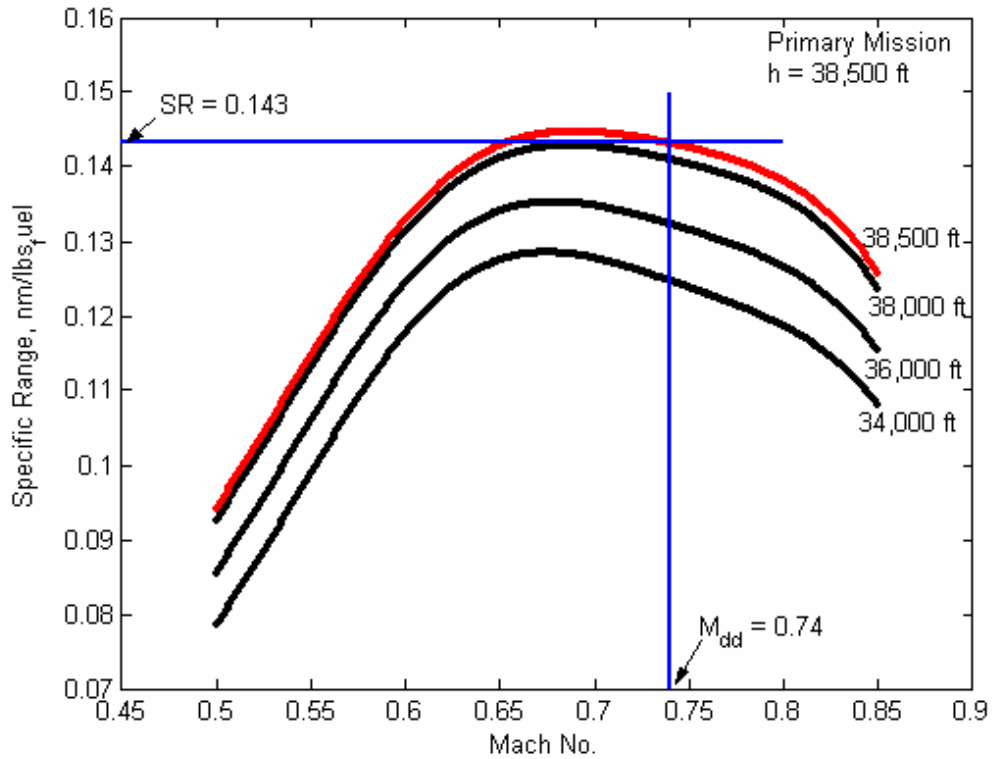


Figure 7-3: Specific Range at Various Altitudes for Primary Mission

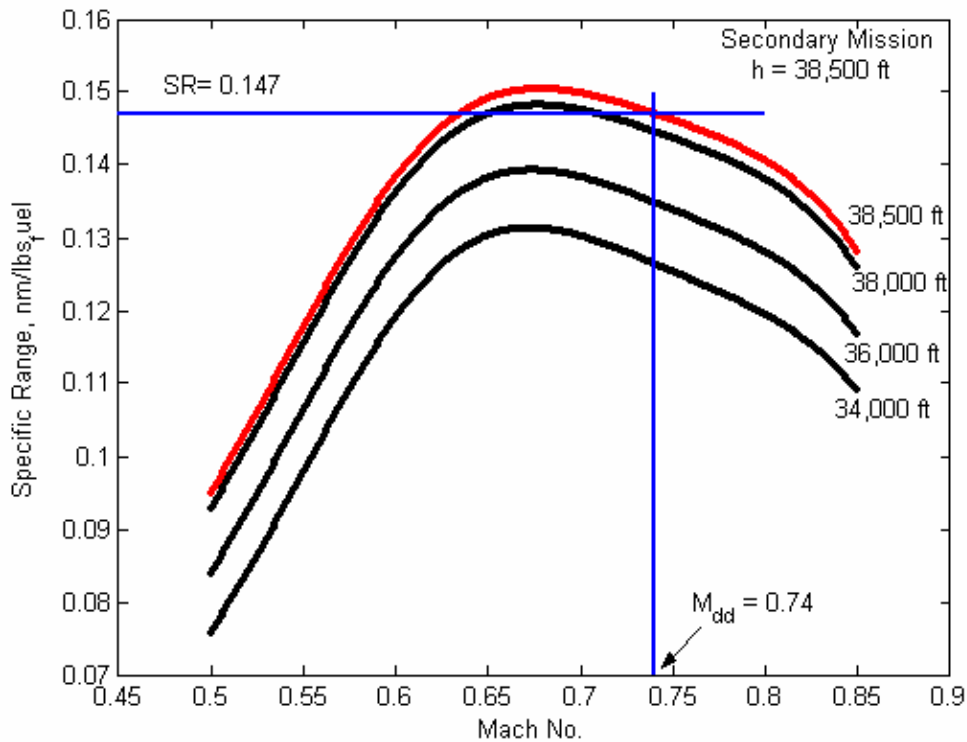
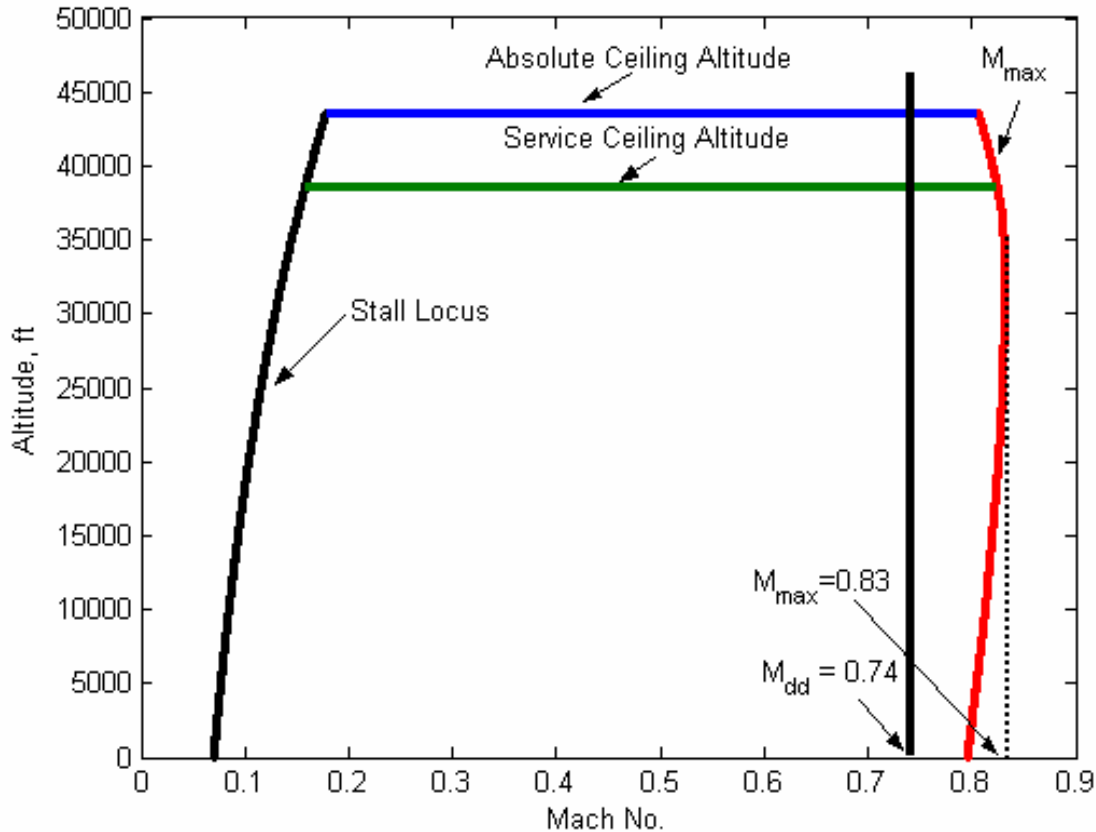


Figure 7-4: Specific Range at Various Altitudes for Secondary Mission

Table 7-5: Maximum Range and Optimum Cruise Speed

Constant Altitude Cruise Conditions		
Mission	Cruise Range	Optimum Cruise Speed
Primary	1,680 nm	Mach 0.74
Secondary	860 nm	Mach 0.74

**Figure 7-5: 1-g Operating Envelop**

7.4 Endurance and Loiter Endurance

The endurance is maximized by flying at maximum lift to drag ratio. Velocity at maximum lift to drag ratio is 166 knots at 5,000 ft. The RFP specifies a 45 min hold at 5,000 ft. Maximum endurance for the primary mission after 16,500 nm is estimated to 58.5 minutes.

8 Materials and Structures

8.1 Material Selections

The materials were chosen based on safety, strength, weight, cost, and practicality. Aluminum lithium alloys are used in the fuselage bulkheads and wing spars and ribs. Our concept also benefits from the use of advanced composites in the wing skin to counteract the effects of divergence and in the fuselage skin to reduce the number of bulkheads and increase fuselage strength. The use of upper surface blowing and the need for increased control when executing STOL operations at lower speeds will be more reliably executed with the use of composites for the wing and tail control surfaces. The landing gear and internal structures of the blister require titanium alloys because of the significant stresses in those areas. Al 7075 is the base material of our aircraft. It is used on the engine nacelles, struts, and blister skin.

Aluminum is a primary material in many aircraft because it becomes stronger, retains its ductility at subzero temperatures, and has a strong resistance to corrosion (Ref. 8-1). Aluminum is also less than one third the specific weight of steel, copper, or brass. Al 7075-T6 is a standard aluminum alloy that has been used on commercial and military aircraft since World War II. This alloy is used mainly for the engine nacelles, struts, and blister skin.

The aluminum-lithium based alloys have been used primarily by the Department of Defense for aerospace technology but are becoming more popular in the commercial industry for internal framework parts, fuselage bulkhead webs, and wing leading and trailing edges (Ref. 8-2). They have 10% lower density and more resistance to elastic deformation and crack propagation during long-term use than traditional aluminum alloys (Ref. 8-3). Disadvantages of Al-Li alloys include the need for cold work to attain peak properties and accelerated crack extension when cracks are structurally extremely small. They are also three to five times more expensive than conventional Al alloys (Ref. 8-4). The disadvantages and increased cost is outweighed by the advantages of using aluminum lithium alloys. Al 2091 is used for the bulkheads and wing spars and ribs.

Composites have a higher acquisition cost but require less individual parts to manufacture than metal alloys (Ref. 8-5). They have low weight, high stiffness and high strength, and can be customized for individual projects. Depending on the direction of the fibers, composites with unidirectional bending can be used to prevent divergence in the forward swept wing. The use of composites in our aircraft results in a decrease of 20% in the overall structural weight, compared to a similar aircraft using conventional materials. Some of the disadvantages of composites are: higher cost, complicated to fix and inspect for flaws, and difficult to make joints.

The most common composite used on aircraft is some variation of a carbon fiber composite. Our aircraft uses a carbon fiber/epoxy for the center wing box, horizontal and vertical tail structures, and the wing control surfaces. This creates immunity to corrosion and fatigue in these high loading and fatigue areas, and ultimately results in a saving in weight and fuel costs.

Glare is used on the fuselage skin and cabin floor panels. This is an alternating aluminum and glass-fiber reinforced adhesive that has been used for the fuselage of the ATR 72-500 and larger aircraft such as the A380. Glare is laid as a skin panel with curvature and stringers already in place. It can be up to 20% lighter and 25% stronger and more fire resistant than aluminum, while still being manufactured and repaired the same way as aluminum. The use of Glare on the fuselage makes the aircraft lighter and safer, especially in the secondary mission.

Titanium alloys have the best strength to weight ratio among the metals. Ti alloys combine high strength and low weight with excellent corrosion resistance, making it useful for landing gear and wing connecting structures. The kind of titanium alloy most suited for aircraft applications is an alpha-beta alloy. The aerospace industry uses wrought titanium alloy, rather than cast or sintered. The high strength titanium alloy chosen for our landing gear, interior blister structures, and engine connections is Ti6Al4V.

The properties of our chosen materials are compared to Al 7075-T6 in Table 8-1. The table includes density, ultimate tensile strength, Young's specific modulus (E/ρ) and shear specific modulus (G/ρ), and cost. The specific modulus is strength per unit mass value, which is used to compare strengths of different materials. The table shows the superiority of composites in density, tensile strength, and

Young's modulus, although aluminum alloys are a fraction of the cost of composites and more readily available. The placement of these materials is listed in Table 8-2 and pictured in Figure 8-1.

Table 8-1: Material Specifications (Ref. 8-6)

Property	Aluminum 7075-T6	Aluminum 2091	Ti6Al4V, Annealed	Carbon Fiber/Epoxy Sheet	Carbon Fiber/Epoxy Rod	Glare®*
Density, lb/in ³	0.102	0.0932	0.16	0.0580	0.0580	0.090
Ultimate Tensile Strength, ksi	83.0	62.4	138	87.0	217.6	
E, 10 ⁶ psi	10.4	10.9	16.5	10.2	18.9	12.9
G, 10 ⁶ psi	3.9	-	6.38	0.725	-	-
E/ρ, 10 ⁶	101.96	116.95	103.1	175.9	325.9	143.3
G/ρ, 10 ⁶	38.2	-	39.9	12.5	-	-
Cost, /lb	\$2-3	~\$9	\$27-50	~\$100	~\$100	-

* Limited data was available for Glare®; listed data represents general metal/ glass matrix

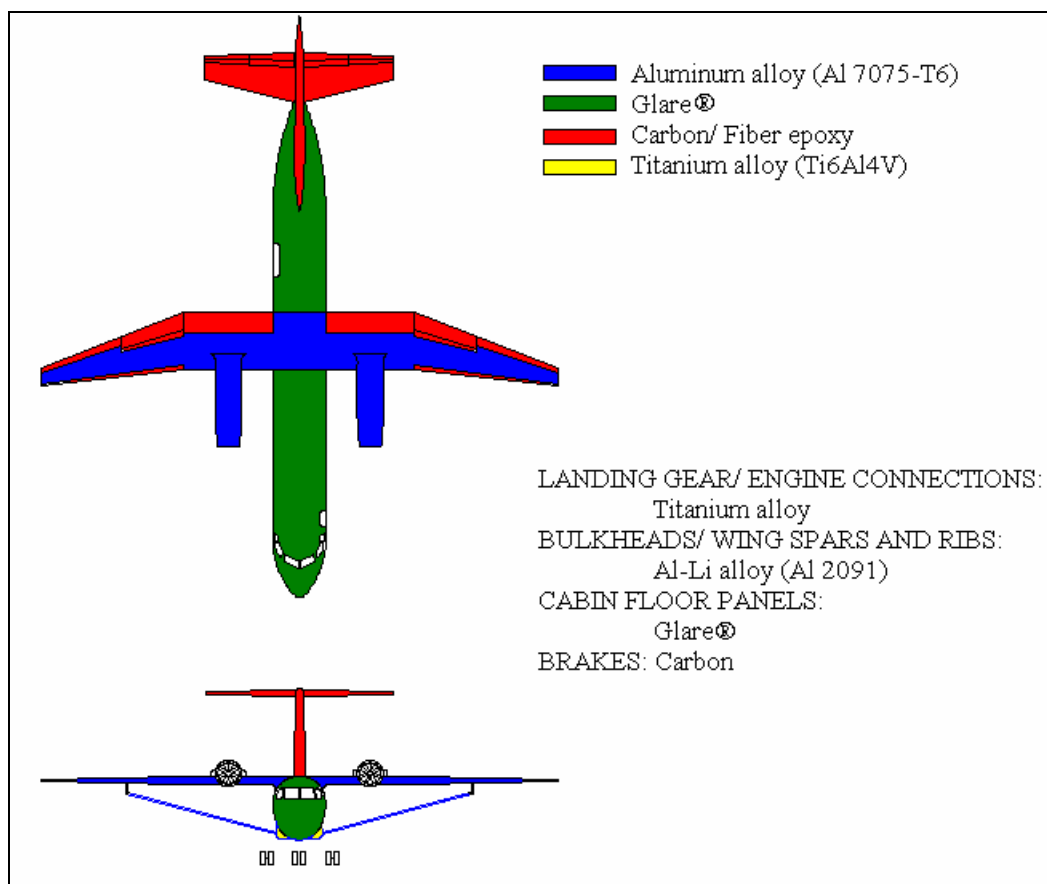


Figure 8-1: Material Distribution

Table 8-2: Material Placement

Material	Locations Of Use
Al 7075-T6	Engine nacelles, struts
Al 2091 (Al Li alloy)	Bulkheads, Wing spars and ribs
Carbon fiber/epoxy composites	Center wing box, Horizontal and vertical tail, Control surfaces on wing and tail (elevators, ailerons, rudders)
Glare	Fuselage skin, Cabin floor panels
Ti6Al4V	Landing Gear, Blister, Engine Connections
Carbon	Brakes

8.2 Structural Requirements

It is necessary to design the structures of an aircraft so that structural components are never stressed beyond their yield point when the limit load is applied. The FAR regulations require that the structure must be able to carry its ultimate loads without collapsing, even though the members may acquire permanent deformation. Typical maximum and minimum load factors for commercial transports are 2.5 g and -1 g. The minimum load factor is for inverted flight or down gusts.

A V-n diagram is a way to analyze the flight envelope of an aircraft when taking into account structural limits, aircraft performance (such as cruise and dive speeds, and the stall boundary), and gust conditions specified by FAR 25 regulations.

For the purposes of this analysis, cruise speed is set at 425 knots and dive speed is typically about 1.4 times the cruise speed. The following are the three gust conditions specified by FAR 25 for gusts in any direction:

Rough gust, $u = 66$ fps at turbulent gust penetration speed

High speed gust, $u = 50$ fps at cruise speed

Dive speed gust, $u = 25$ fps at dive speed

Wing loading is found to be 72 lbs/ft^2 , as determined in Section 3.4, and the lift maximum coefficient is assumed to be 8.5. The lift coefficient is based on NASA experimental wind tunnel data.

Under gust condition (1) the maximum and minimum load factors are found to be 1.45 and 0.55 at the stall boundary. For gust condition (2), maximum and minimum load factors are 3.28 and -1.28 at cruise

speed and 2.54 and -0.54 at dive speed for condition (3). These calculations can be visually interpreted by looking at Figure 8-2.

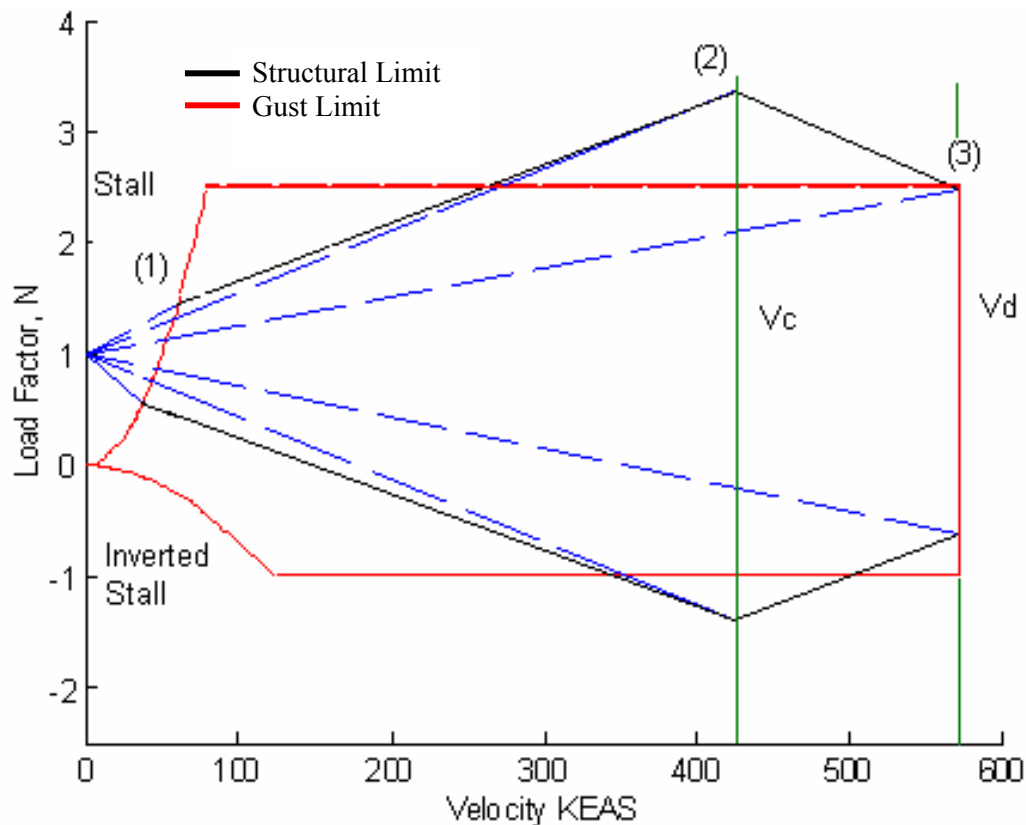
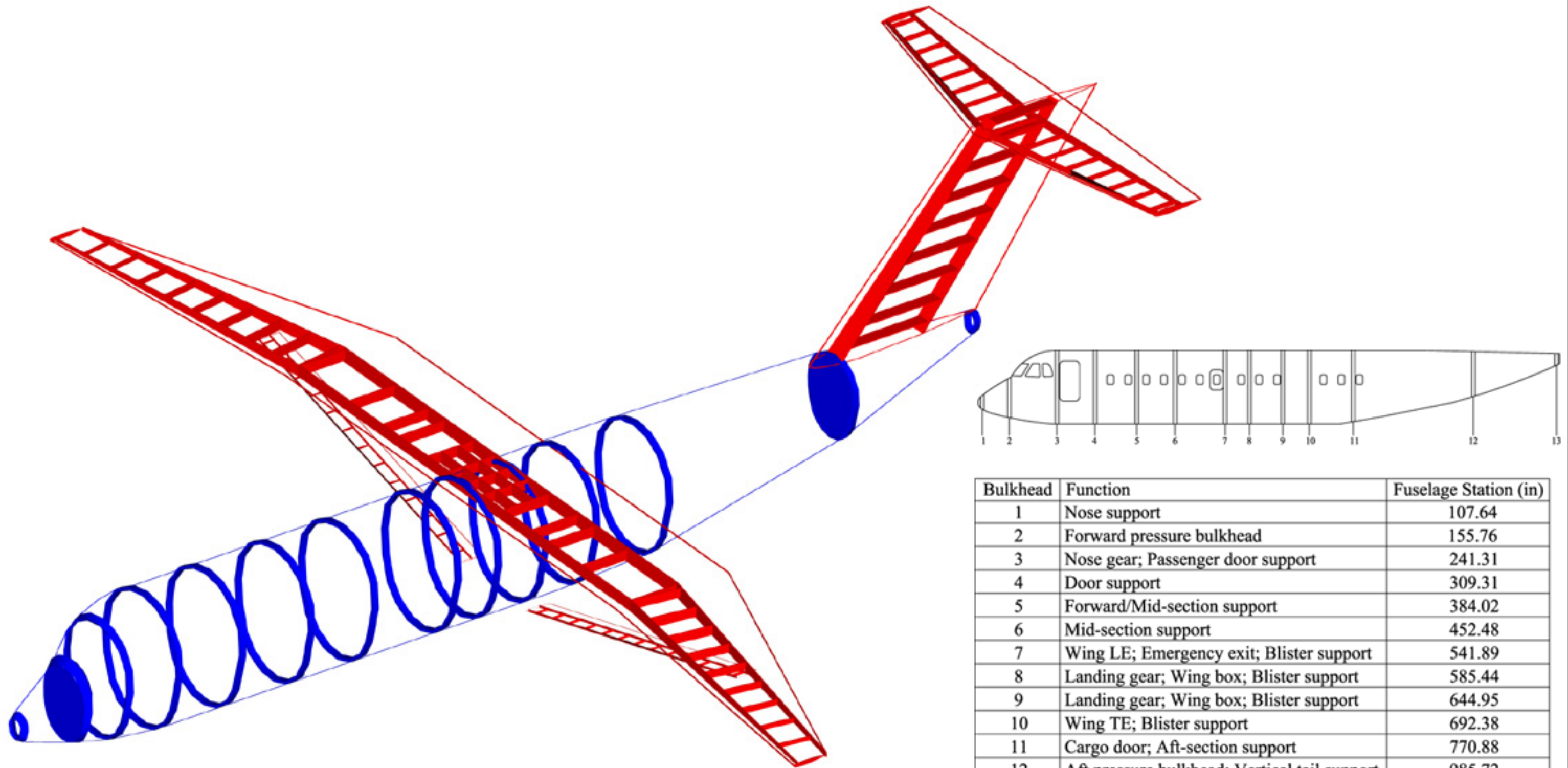


Figure 8-2: V-n Diagram

8.3 Structural Design

The aircraft structure must be able to withstand the cycle of forces such as landing, pressurization, and taxi loads associated with continual commercial flights, along with the stress of operation in “remote, high, hot areas with minimal runway length for take off and landing” as stated in the RFP. Upper surface blowing and a high mounted wing add heat and stress to the aircraft and dictate most of the fuselage and wing structural configuration, shown in Figure 8-3. Executing an SNI landing with one engine inoperative can increase the structural stresses on the control surfaces and landing gear during touchdown. These additional stresses will be absorbed by the dual tandem Jockey landing gear and associated shock absorbers and then transfer into the fuselage.



Bulkhead	Function	Fuselage Station (in)
1	Nose support	107.64
2	Forward pressure bulkhead	155.76
3	Nose gear; Passenger door support	241.31
4	Door support	309.31
5	Forward/Mid-section support	384.02
6	Mid-section support	452.48
7	Wing LE; Emergency exit; Blister support	541.89
8	Landing gear; Wing box; Blister support	585.44
9	Landing gear; Wing box; Blister support	644.95
10	Wing TE; Blister support	692.38
11	Cargo door; Aft-section support	770.88
12	Aft pressure bulkhead; Vertical tail support	985.72
13	Vertical tail; Fuselage tail support	1134.41

DRAWING TITLE:

FIREFLY 3D STRUCTURAL LAYOUT

DESIGNED BY:

TEAM VOLANT

DRAFTED BY:

MATT LONG

SCALE: **NTS**

DATE: **5/4/04**

DWG NO. **FIG. 8-3**

8.3.1 Wing Design

The wing structure consists of two spars located at 10% and 60% of the chord length. A third spar was considered unnecessary with the addition of a composite wing skin. There is an allowance of space between the trailing edge spar and the trailing edge control surfaces for associated electrical or mechanical parts. Eleven ribs are placed at varying intervals of approximately 3', beginning at the wing root. The ribs are placed closer together at locations of higher loading, such as engine and strut attachment. The strut is attached at 66% of the semi-span, measured from the wing root. The ribs join the spars and add support for the hinge attachments. Stringers run the length of the wing and are manufactured into the wing skin at 6 inch intervals. The combination of the wing skin, stringers, and the strut will resist torsion and divergence. The two spars, combined with the ribs and stringers, counteract the wing loads while minimizing weight. The rib and stringer spacing was configured using Niu, so the distances are slightly increased from conventional aircraft data due to the use of composite materials used throughout our structure (Ref. 8-7). A carry through wing box design includes the addition of two struts to strength the connection of the high mounted wing to the fuselage bulkheads.

8.3.2 Strut Design

The addition of a strut allows for a wing thickness of 12% by reducing the load to be carried by the wing spar, thus decreasing structural weight. Lower weight, decreased thickness, and increased span reduce induced drag and increase overall performance (Ref. 8-8). The strut will be in tension during flight and in compression during landing and taxi. The compression during landing could ultimately result in buckling, which is counteracted by the strut dampening system shown in Figure 8-4.

The strut is attached to the wing at 29.9' from the fuselage and is mounted to a 1.83' vertical pylon, as shown in Figure 3-5. At the end of the pylon there is an elbow that turns the strut 77° clockwise towards the fuselage. Each strut is 30.7' long, and is connected to a telescoping sleeve in the landing gear housing to prevent buckling during landing, similar to the system shown in Figure 8-4.

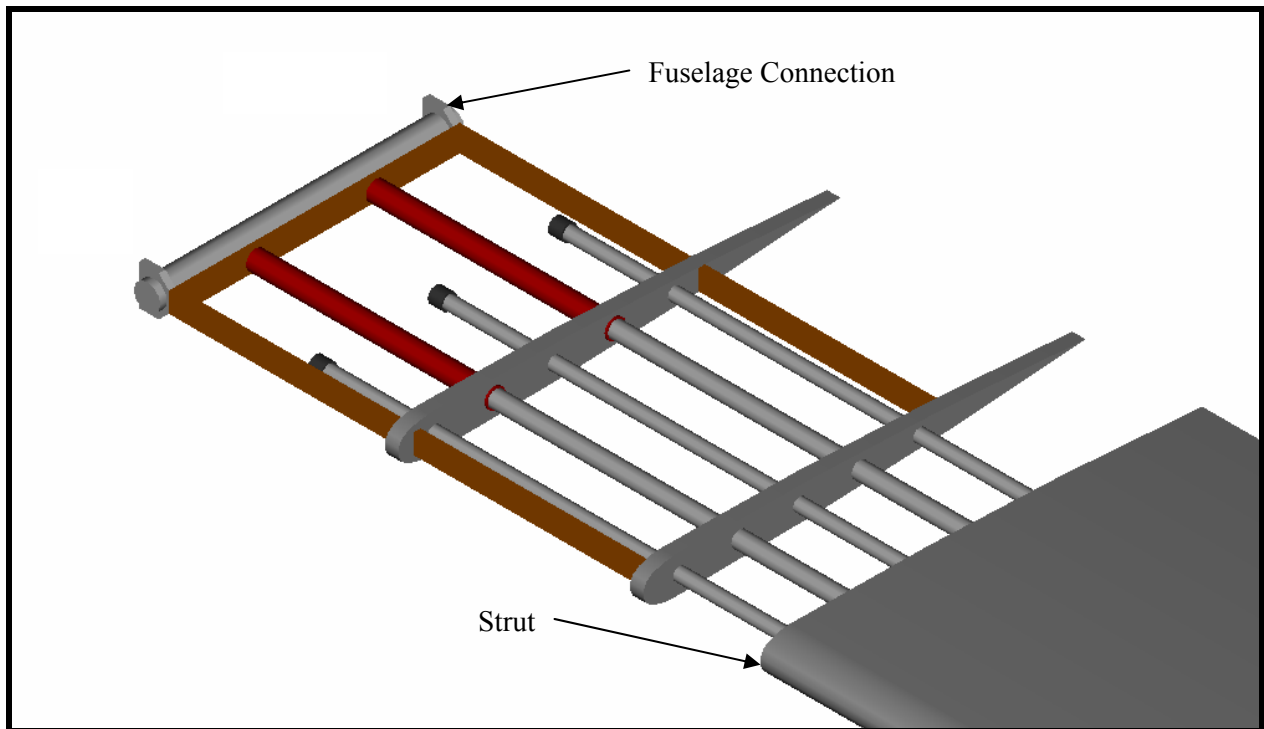


Figure 8-4: Strut Dampening System

8.3.3 Fuselage Design

The fuselage structure consists of thirteen bulkheads placed in locations of high loading, as pictured in Figure 8-3. Pressure bulkheads are placed near the nose and tail of the aircraft to seal the pressurized cabin while in flight. Bulkheads are also placed forward and aft of doors and throughout the center of the fuselage to support the landing gear, wing and strut. Glare skin panels make up the fuselage skin and cabin floor. The required floor strength is higher for cargo or military missions than for passenger missions; therefore, the use of Glare on the cabin floor negates the problem of different floor strengths for the primary and secondary missions (Ref. 8-7). Reinforced cabin floors and a stronger fuselage skin also allow for more spacing between the thirteen bulkheads.

8.3.4 Tail Design

The vertical and horizontal tail boxes have two spars each, located at 15% and 65% of the chord length. The spars on the vertical box are parallel to the leading and trailing edges of the tail. The ribs lie perpendicular to the spars at approximately 3' intervals. The ribs of the horizontal tail box are placed at

approximately 2' intervals, with the center rib connected to the vertical tail and lying parallel to the fuselage. The remaining ribs lie perpendicular to the rear spar.

8.3.5 Landing Gear

The “tricycle” landing gear arrangement is used for the Firefly. There are two main struts with four-main wheels each, which are located at 15° aft from the C.G. location and 25° off the centerline. More specifically, our aircraft uses the Messier “Jockey” twin wheel configuration for the main units, with a modification from tandem to dual tandem. This type of landing gear is used on the Breguet 941, Transall C-160, and An-22 and is suitable for high wing aircraft and STOL transports (Ref 8-7). The Jockey configuration couples two wheels in tandem and allows independent pivoting on trailing arms at each end of a double-acting shock absorber. The trailing arm allows a smooth ride over rough terrain for the secondary mission.

Larger tires combined with smaller wheel rim diameters will also create a smoother landing on uneven ground. The Firefly uses Type III 9.50-16 tires with a maximum width of 9.70” and a maximum diameter of 33.35”. These maximum values give an allowance of 7.0” between the landing gear tires in the stowed configuration. The wheels have a diameter of 16.0” and are made of forged aluminum alloy.

Coupling the wheels onto one shock absorber balances the shock forces in the gears, rather than the fuselage. The oleo-pneumatic shock absorbers of the dampening system have excellent energy dissipation with good rebound control and will absorb the high stresses associated with landing. Oleo-pneumatic shocks have an efficiency of 90%, compared to 50% for steel spring, 60% for rubber, and 75-90% for oil/liquid. (Ref 8-7)

A strut with twin nose-wheels is located at fuselage station 2. Aircraft weighing less than 50,000 lb would be sufficiently supported by a single main wheel per strut, but the double configuration will be better for safety and reliability in the secondary mission.

The landing gear will be retracted into separate gear pods located on the bottom sides of the fuselage. The maximum time for retraction or extension of the gear is 30 seconds. The pods have a higher drag coefficient but allow housing for the wing struts and landing gear. The landing gear, wing strut and associated shock absorbers are designed to handle the landing load and taxi bumps associated with both missions (Ref. 8-9).

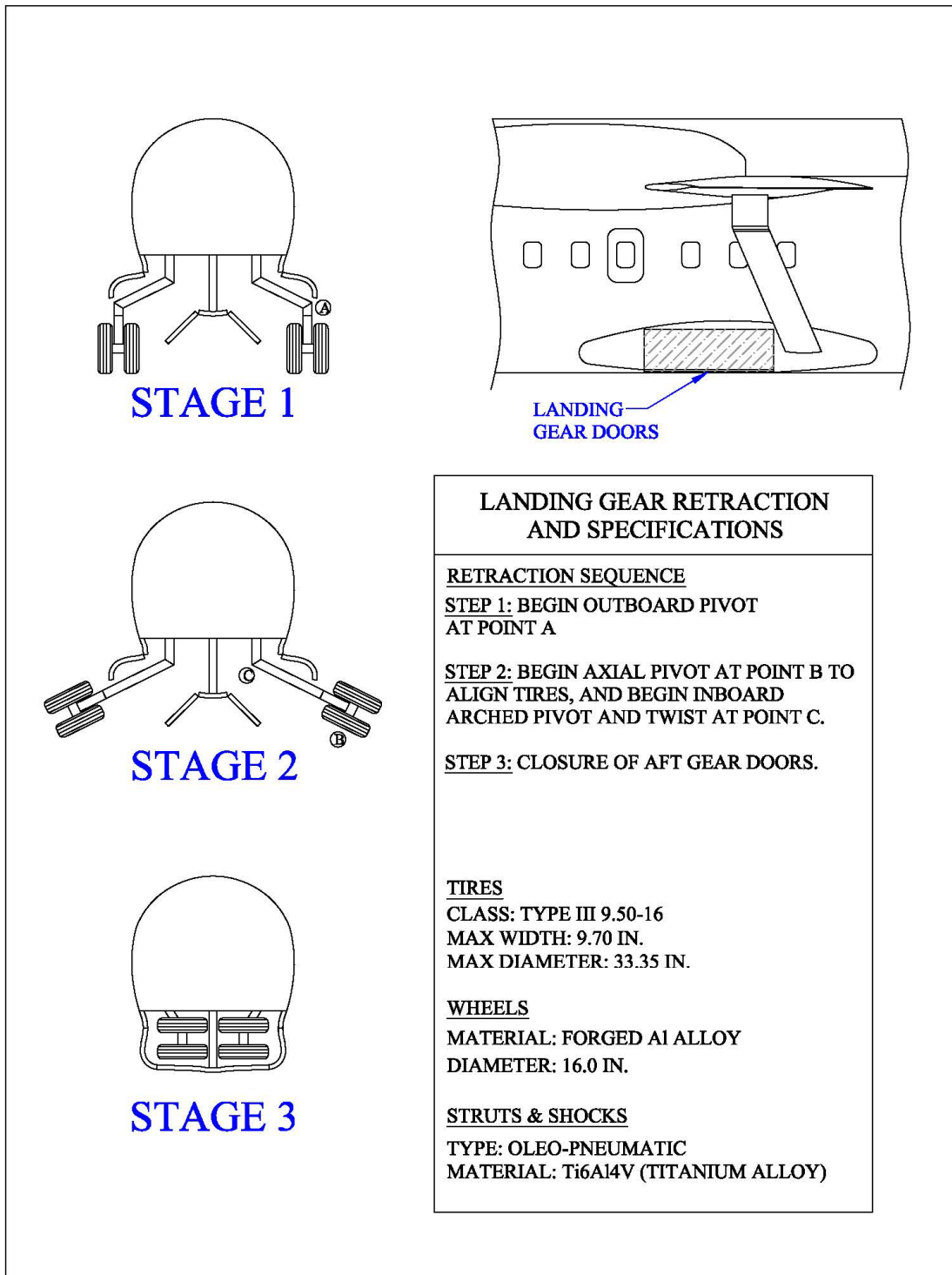


Figure 8-5: Landing Gear Retraction and Specifications

9 Systems

9.1 Basic Layout

Figure 9-1 is a layout of the systems and their location in the aircraft. The wiring represents the fly-by-light system used for the control surfaces, as discussed in section 9.3. Each of the systems discussed below contribute to the capability of the aircraft to complete its primary and secondary missions.

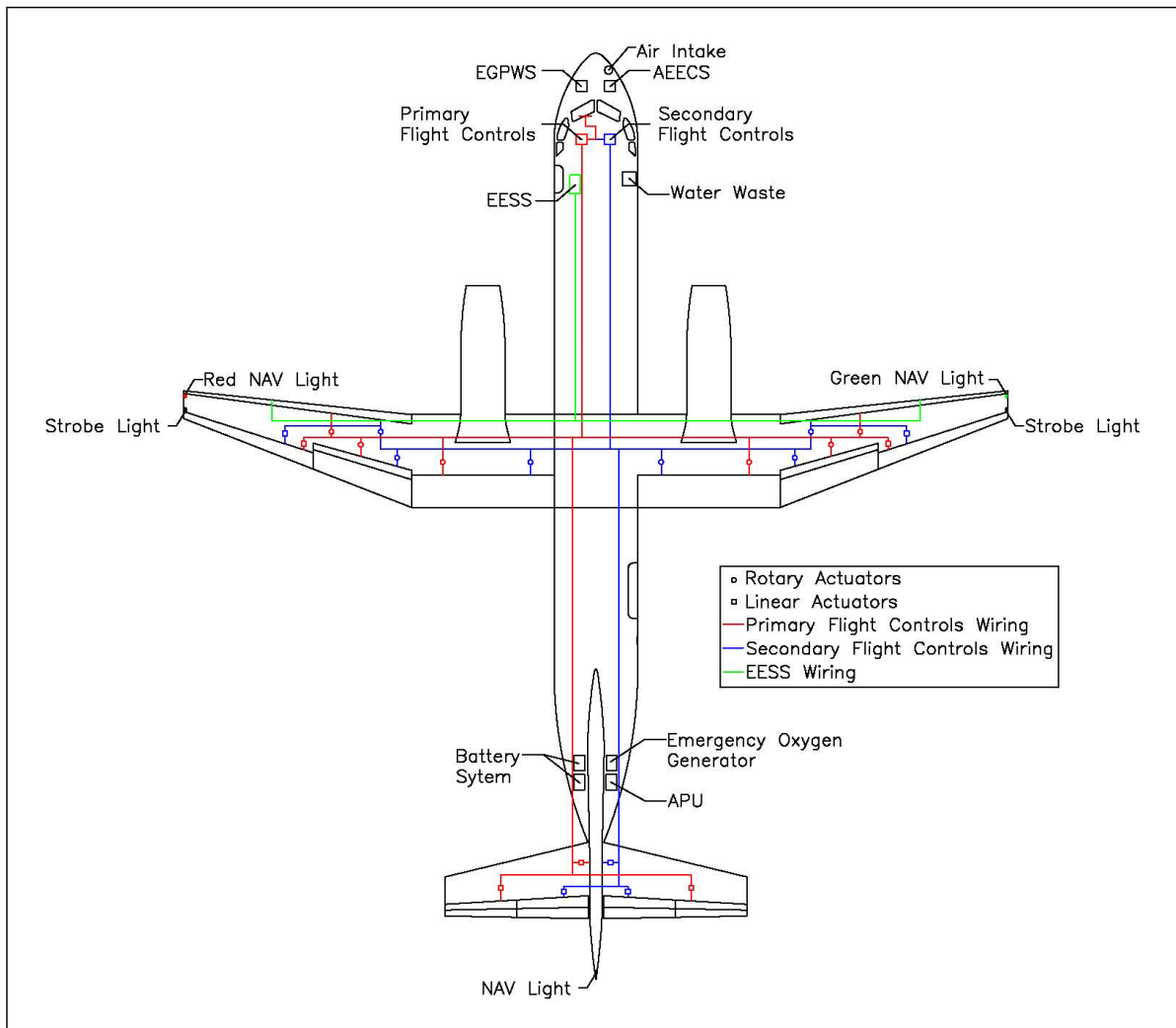
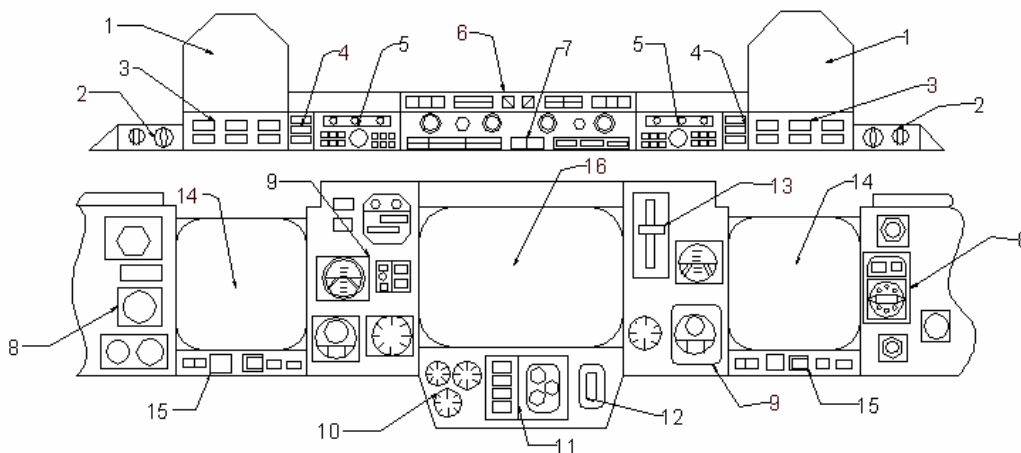


Figure 9-1: Aircraft Systems Layout

9.2 Cockpit

We investigated many of the existing systems and layouts used today to determine the most efficient and practical arrangement that could accomplish the necessary tasks for both missions. The Embraer ERJ-145 provides the basis for which systems would be needed to operate as a regional jet. The systems used in the C-17 were also taken into consideration since the plane would be under government control in the secondary mission. A sidestick configuration was considered, but since the aircraft will primarily be a commercial aircraft, a traditional yoke was chosen. As shown in Figure 9-2, the aircraft will have two HUDs. This will aid the pilots during STOL operations, including the SNI approach, and for military objectives in the government role. The integration of the Garmin G1000 with current systems found in the Embraer ERJ-145 and the C-17 created the most efficient set of avionics for the required missions.



1	Head-Up Displays	9	Standby Attitude/Airspeed Indicators & Total Fuel Indicator
2	Instrument Lighting Controls	10	Trim & Speedbrake Position Indicators
3	Head-Up Display Controls	11	Standby Engine Display
4	Warning Lights	12	Trim/Flap Position Indicators
5	Communications Navigation Control Panel	13	Landing Gear Extend/Retract Handle & Brake Pressure Indicator
6	Engine Fire Extinguisher Controls	14	Primary Flight Display
7	Automatic Flight System Control Panel	15	Primary Flight Display Controls
8	Clocks & Bearing Distance Heading Indicators	16	Multi-function Display

Figure 9-2: Cockpit Dash

As seen in Figure 9-2, the Garmin G1000 uses two-ten inch primary flight displays (one each for the pilot and co-pilot) which provide access to flight critical systems such as the horizontal situation indicator, air speed, altitude, and vertical speed. The Garmin G1000 also incorporates a fifteen inch multi-function display to present weather maps, traffic data, or other flight information (Ref. 9-1). The overhead panel and the center console, as seen in Figure 9-3 and 9-4, allow the public address system and the backup system controls and to be easily accessed by both the pilot and the copilot. Systems that will be used in the government aircraft role, such as countermeasures and Friend/Foe identification will be located in the center console. To ensure the safety of the passengers and flight crew in case of an electrical failure, backup controls were installed in the cockpit.

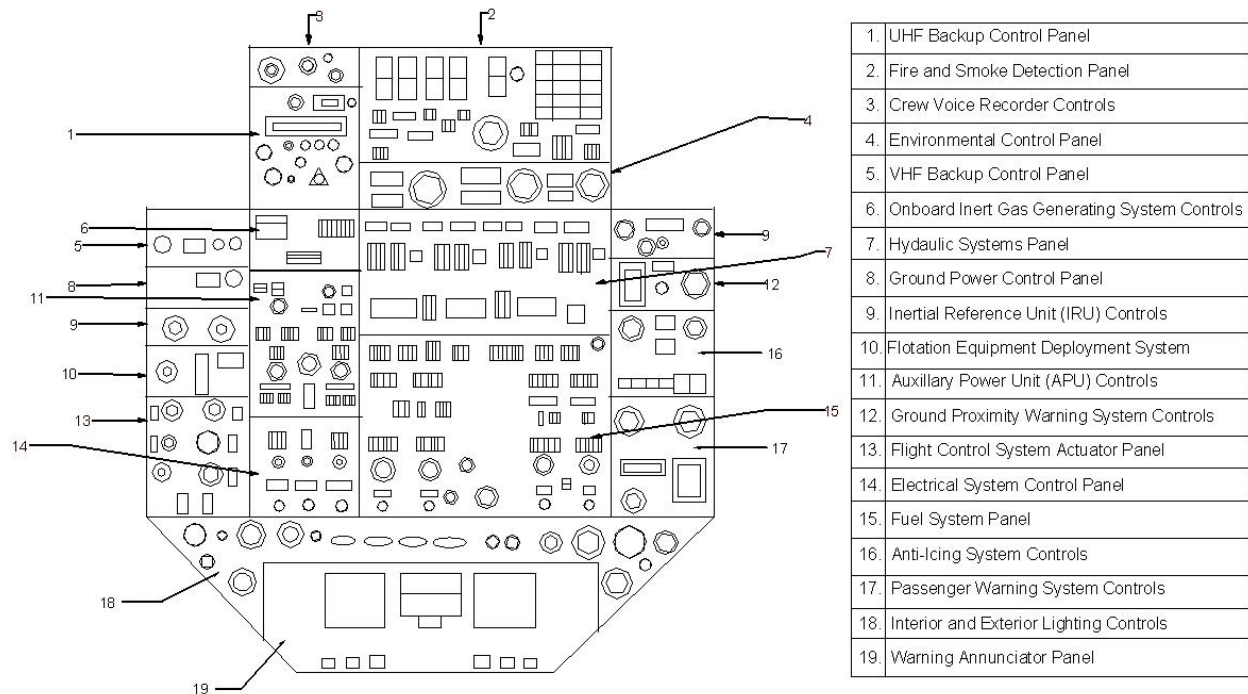


Figure 9-3: Overhead Panel

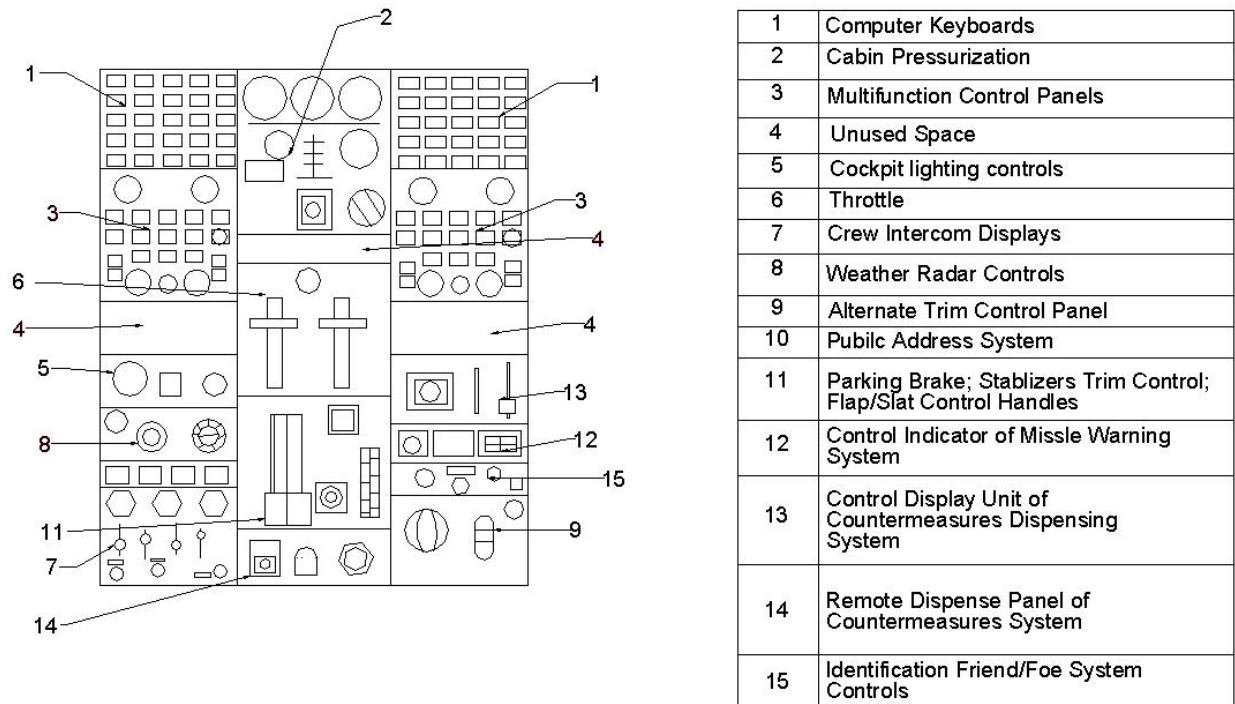


Figure 9-4: Center Console

9.3 Flight Controls

The aircraft uses a Fly-By-Light (FBL) system of fiber-optic cable in place of traditional fly-by-wire electrical wiring. This system allows for a safer, higher performance, lighter, more reliable and lower life cycle cost aircraft. The mechanical controls in regional jets are very heavy and require much more maintenance time and cost compared to a FBL system. This will accommodate the double-hinged rudder and elevator system. The FBL system is not affected by lightning or high energy radio frequency. An added benefit for use in the homeland security role will be its immunity to electromagnetic interference (EMI) and electromagnetic pulse (EMP) which could be used against the United States to knock out its electrical and computer systems. The FBL system allows for larger bandwidth data transfer, increased sensor multiplexing, high speed computing, and built-in fault detection and isolation capabilities (Ref. 9-2). This also provides easier maintenance and upgrading capability.

Electrically powered hydrostatic actuators will be used on all control surfaces on the aircraft. There is a primary and backup for each system. This system has the advantage of eliminating most of the

hydraulic lines that would run through the aircraft, had it been equipped with a traditional hydraulic system, and replacing them with fiber-optic cables. Hydraulic systems are heavy, high-maintenance items and replacing them with hydrostatic actuators would reduce the weight and maintenance requirements. This system improves safety and reliability in addition to lower acquisition and operational cost. Inside each actuator is a hydraulic reservoir with the only connector external to the actuator being the fiber-optic control input and power cables. To complete the required SNI approach, quick response control surfaces are needed. The traditional electrical motor actuators have a time delay while running through its gears. The electro-hydrostatic system eliminates most of this delay for near instantaneous control surface response. (Ref. 9-3) Force-feedback control yokes are used in place of the conventional hydraulic system to give the pilot more response to his control inputs.

There are two types of electro-hydrostatic actuators in the aircraft. Rotary actuators are geared for flap and slat movement. Linear actuators are piston driven for deflection of the rudder, elevators and ailerons. The hydraulic system used by each actuator is located internally, so the only necessary external connections are for control input and power. Independent electro-hydrostatic systems are used for backup as well as primary.

Our flight control computer is supplied by Honeywell in the form of a fail-operational, fail-passive integrated flight director/autopilot system with multiple sensor redundancy management. This allows for sensor data from both sides of the aircraft to be available to the flight computers for continued operation after sensor failure (Ref. 9-4). A schematic of the flight control system is show in Figure 9-1.

9.4 Aircraft Lighting and Deicing

The aircraft is equipped with a landing light on the nose gear strut and navigation lights on each wing tip; red on port and green on starboard. A navigation light is also located on the top leading edge of the vertical stabilizer; red on port and green on starboard. Strobe lights are also included on the wing tips to help prevent mid-air collisions.

An Electro Expulsive Separation System (EESS) is used for ice removal. It is capable of removing ice as thick as one inch. It consists of layers of conductors encased in materials which are bonded directly onto the airframe structure. When ice accumulation is detected, it sends an electrical current through the conductors, causing them to pulse. This causes them to move about twenty-thousandth of an inch in milliseconds. This system uses about one-thousandth the power of conventional ice removal systems and is about one-tenth the weight (Ref. 9-5).

9.5 Cabin environment

An All Electrical Environmental Control System (AEECS) is used for cabin pressurization and climate control. This system eliminates the need for heavy internal ducting to run bleed air from the engines to the pressurization unit and lowers specific fuel consumption, allowing the engines to run more efficiently. The air is drawn in below and in front of the cockpit.

9.6 Altitude Warning

The aircraft is equipped with an EGPWS, Enhanced Ground Proximity Warning System. This will allow the aircraft to operate at low altitude during its secondary mission with greater security from running into terrain. This is especially important during the wildfire mission, where the aircraft will be flying through low visibility smoke clouds in the mountains. This system is equipped with altitude callouts, obstacle alert, windshear detection, terrain awareness display, bank angle callout, and many other features (9-6).

9.7 Electrical System

For primary electrical power, turbine generators are run from each engine. These provide AC power which is converted to DC for use by the aircraft's systems. An Allied Signals APU is used for auxiliary power to start the engines without ground equipment, which will not be available during the secondary missions. DC lead acid batteries provide power for APU and avionics startup, as well as emergency in-flight power in case of engine failure.

9.8 Fuel System

All of the fuel needed to complete the required mission is located in the wings in self-sealing bladders extending 33.57 ft from the centerline of the fuselage. The bladder prevents leaks if the tank is punctured. This is especially important for the government role, when the aircraft may be fired upon by hostile forces. Given the low thickness to chord ratio of our wing, approximately 75% of the wing is responsible for storing fuel as shown in Figure 9-4. Each wing holds 117.18 ft³ or 876.59 gallons U.S. of fuel inside the wing box. This equates to 234.37 ft³ and 1753.19 gallons U.S. of fuel for the entire wing, including the portion of the wing through the fuselage. The placement of the inboard fuel tanks allows for structural support of the engines to continue through the wing box between the tanks.

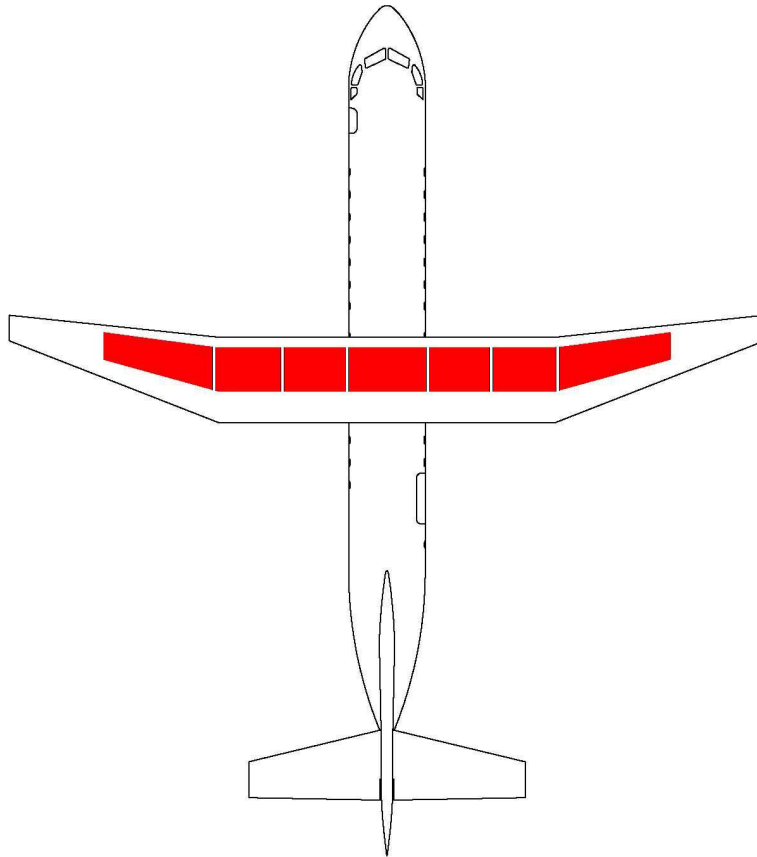


Figure 9-5: Fuel Tank Locations

10 Aircraft Weight Analysis

The aircraft weight estimation went through two phase. An initial phase, the preliminary weight estimation, was done using methods outlined in *Roskam's Airplane Design: Part 1* (Ref. 10-1). Class I methods by Roskam were used to determine take off gross weight, W_{TOGW} , empty weight, W_o , fuel weight, W_{fuel} and payload weight. Payload weight, $W_{payload}$ is defined in the RFP. For phase two, the detailed weight estimation, *Roskam's Airplane Design: Part 5* (Ref. 10-2) methods were used to determine aircraft component weights.

10.1 Aircraft Component Weight

The method used to estimate aircraft component weights utilized statistical algorithms based upon sophisticated regression analysis of airplanes. Weights of other components such as payload, crew and cargo were given in the RFP. The component weights summary for both primary and secondary missions are shown in Table 10-1. Variation in the take off weights between primary and secondary mission is due to the different payloads. Some of the equipment carried on the aircraft is only designed for the government's use, but will have to be carried on the airplane at all times, such as in-flight refueling equipment, counter measures, and a radar that meets military requirements. This additional weight is factored into the government's operational cost subsidy, as discussed in Chapter 11.

Table 10-1: Weights and CG for Primary and Secondary Mission

#	Component	Primary (lbs)	Secondary (lbs)	CG-x (ft)	CG-y (ft)
STRUCTURE					
1	Fuselage	7191.4	7191.4	39.6	5.8
2	Wing	2571.9	2571.9	42.8	10.0
3	Vertical Tail	768.9	768.9	83.1	17.9
4	Horizontal Tail	797.5	797.5	90.5	25.3
5	Nacelles	780.0	780.0	32.5	11.5
6	Main Landing Gear	1349.3	1349.3	42.3	1.1
7	Nose Landing Gear	578.3	578.3	11.8	1.2
FIXED EQUIPMENT					
8	Flight Control Sys.	869.4	869.4	56.6	8.0
9	Hydraulic & Pneumatic Sys	450.6	450.6	48.7	10.0
10	Electrical Sys	1812.1	1812.1	41.6	8.0
11	Avionics Sys	1015.5	1015.5	9.0	3.0
12	AC, Pressure, and De-Ice Sys.	807.4	807.4	70.5	5.0
13	Oxygen Sys.	88.8	88.8	74.3	5.0
14	APU Sys.	425.6	425.6	82.0	9.0
15	Paint	200.3	200.3	38.2	5.8
16	Fuel Dumping Sys.	32.0	32.0	49.5	10.3
17	Furnishing & Lavatory Sys.	2832.4	-	42.0	5.2
17	Furnishing & Lavatory Sys.	-	457.4	13.0	5.2
FIXED EQUIPMENT FOR GOVERNMENT MISSION					
18	In-flight Refueling Probe Sys.	230.7	230.7	20.6	10.5
19	Counter Measures Sys.	325.9	325.9	82.3	2.0
20	Military Spec. Radar Sys.	455.3	455.3	4.0	2.0
POWERPLANT					
21	Engine (2)	4505.6	4505.6	32.5	11.5
22	Fuel Sys.	491.0	491.0	38.2	10.3
23	Propulsion Sys.	108.7	108.7	37.0	11.0
FUEL					
24	Mission Fuel	11687.0	11687.0	42.5	10.3
24	Trapped Fuel	746.0	746.0	42.5	10.3
PAYLOAD					
26	Pilot (2)	370.0	370.0	7.5	5.8
27	Crew (1)	185.0	185.0	16.8	5.8
28	Passengers (49)	9065.0	-	38.0	5.8
28	Passengers (20)	-	6180.0	35.6	5.8
29	Baggage	2340.0	-	26.0	1.5
29	Fire Suppressant	-	2000.0	54.0	4.6
TOTAL - PRIMARY MISSION		53082.0		40.42	7.82
TOTAL - SECONDARY MISSION			47482.0	41.18	8.25

10.2 Aircraft Center of Gravity

Table 10-1 also gives CG locations for the aircraft components. These locations are illustrated in Figure 10-1. Moments of inertia were estimated based on this data and are given in Table 10-2.

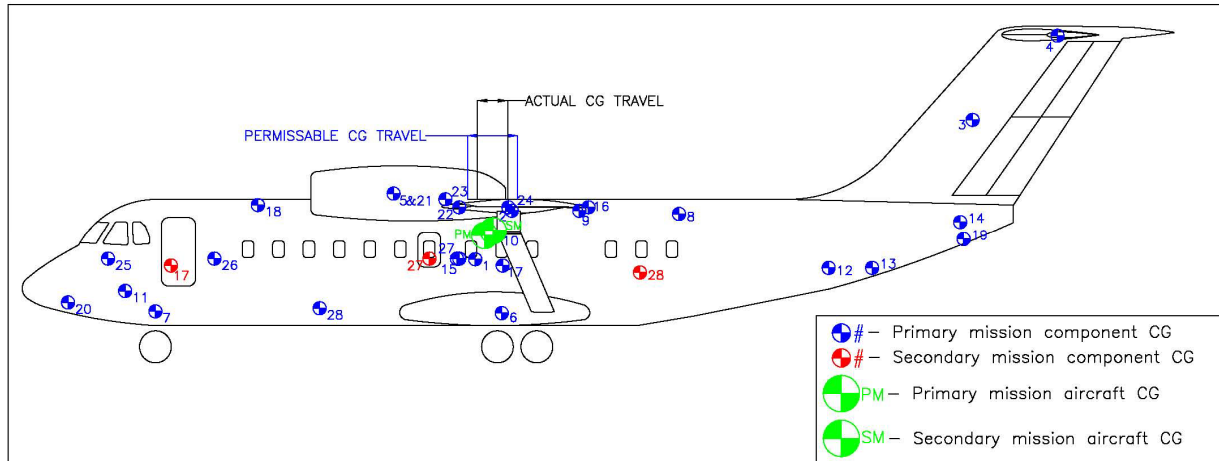


Figure 10-1: CG Locations

Table 10-2: Estimated Moments of Inertia

I_{XX}	244,264 slug-ft ²
I_{YY}	341,357 slug-ft ²
I_{ZZ}	412,671 slug-ft ²

Figure 10-2 and 10-3 show how the CG travels for the primary and secondary mission, respectively. The neutral point was found to be at 26% MAC. As shown in Figures 10-2 and 10-3, under certain loading conditions, the aircraft will be unstable, so a stability augmentation system will be required to keep the aircraft stable, as discussed in Chapter 6. The curved, dotted lines in Figures 10-2 and 10-3 represent cases where the passengers board the aircraft either starting with the last row, or starting with the first row. These curves show that under certain passenger loadings, the aircraft will not be within the CG limits. This is a common problem with regional jets and requires seating restrictions during partially full flights.

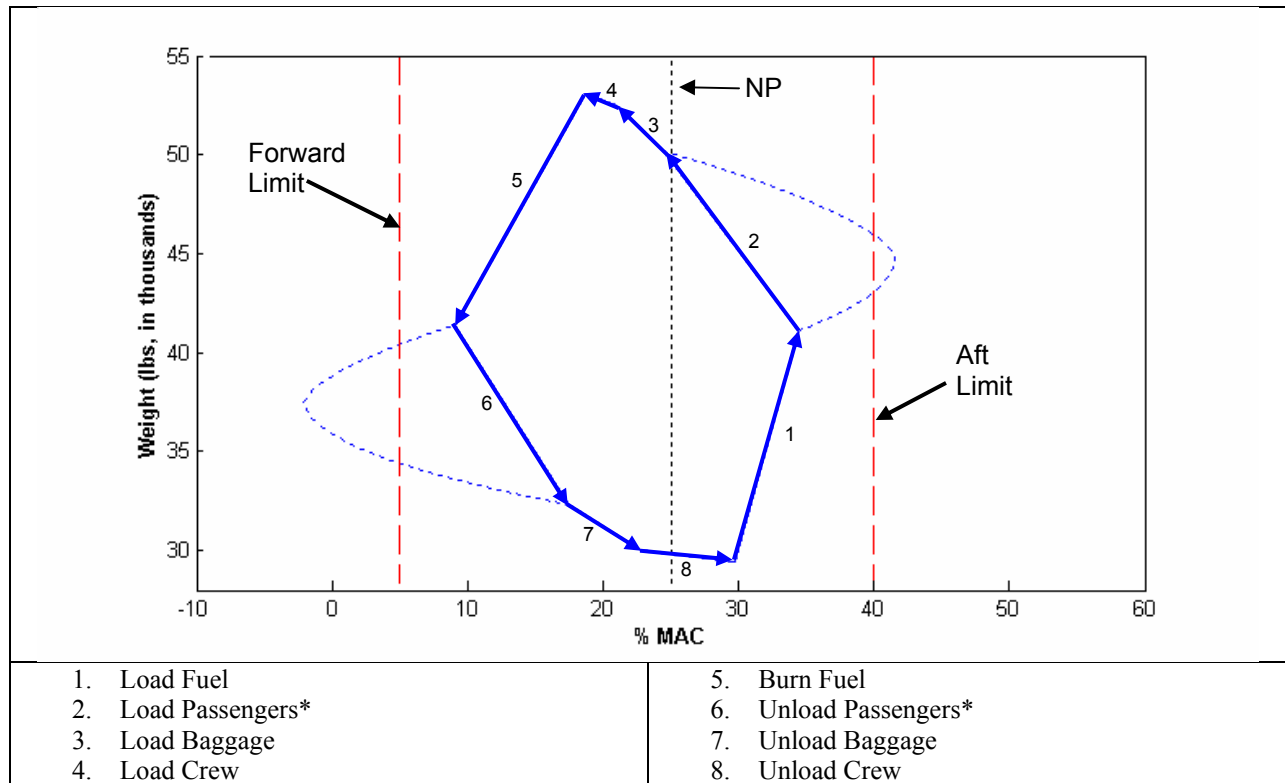


Figure 10-2: CG Travel for Primary Mission

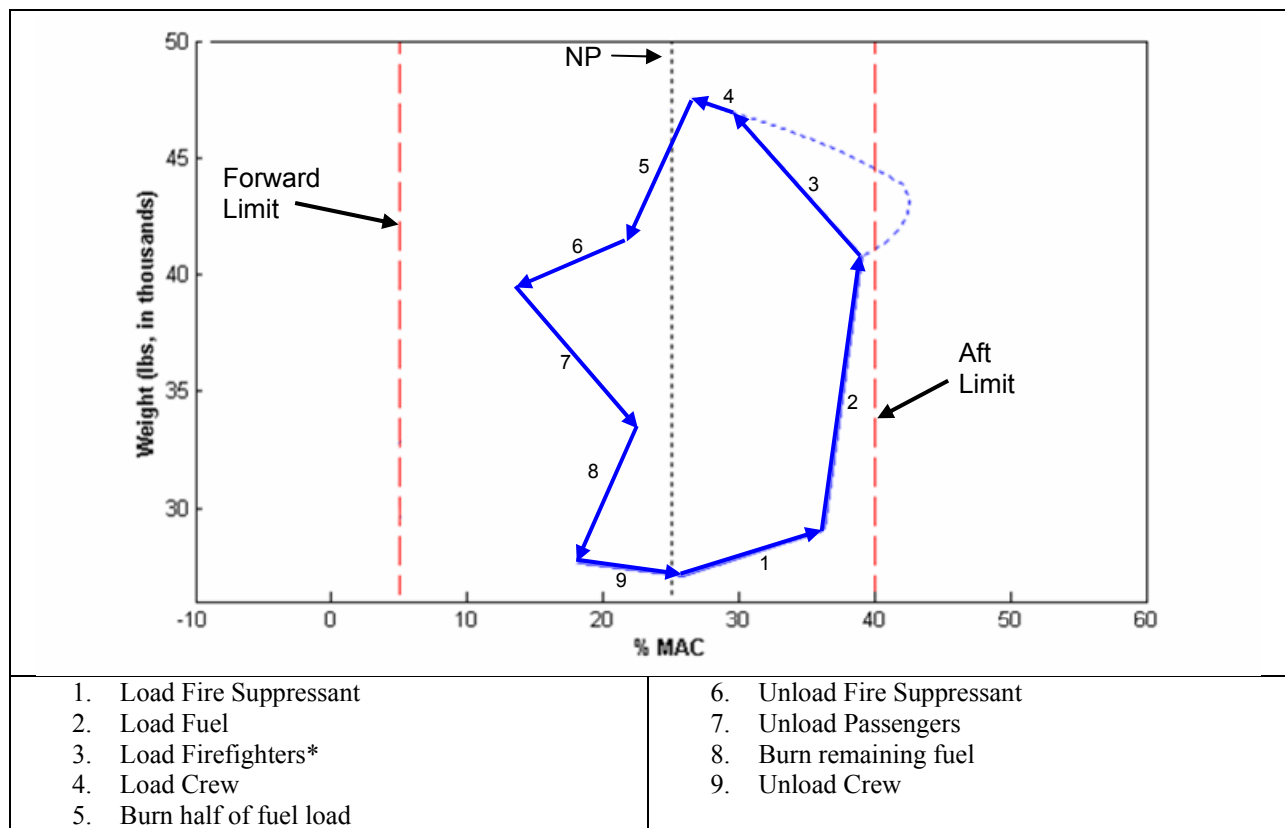


Figure 10-3: CG Travel for Secondary Mission

11 Aircraft Cost Analysis

Meeting the RFP's performance requirements is not the only characteristic of a winning design. The government subsidy for flyaway and operational cost due to the secondary mission requirements is also one of the major decision criteria. Outstanding design, great ingenuity, and engineering come at the lowest and most affordable price.

The RFP states that flyaway and direct operation cost requirements are to be estimated for the production of 150, 500 and 1500 aircraft units. The methods used to estimate costs are outlined in *Airplane Design: Part VIII* by Roskam (Ref. 11-1) and *Aircraft Design: A Conceptual Approach* by Raymer (Ref 11-2).

11.1 Aircraft Cost Method and Cost Breakdown

The aircraft costs are broken down into four sections: Research, Development, Test and Evaluation (RDT&E) Cost, Manufacturing Cost, Acquisition Cost and Direct Operation Cost. Five flight test airplanes and three static test airplanes are included in all aircraft production cost estimates. All cost estimates are based on the 2004 dollar value.

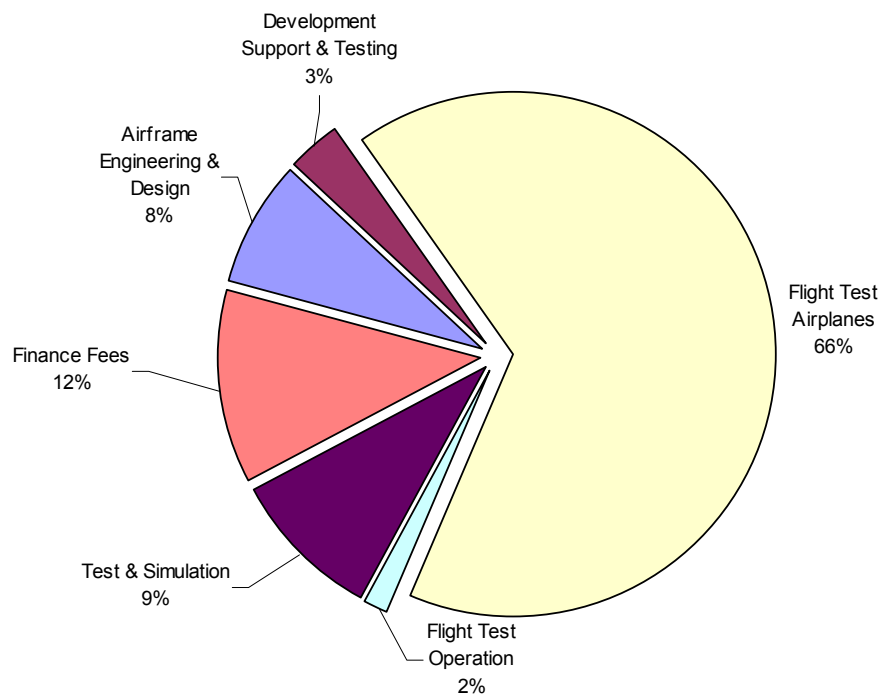
11.2 Research, Development, Test and Evaluation Cost

The RDT&E cost includes: Airframe Engineering & Design Cost, Development Support & Testing Cost, Flight Test Airplane Cost, Flight Operation Cost, Test & Simulations Cost and Cost of Finance for the RDT&E phase.

The parameters used to determine RDT&E cost are TOGW, empty weight, maximum airspeed, engine and avionics costs, number of passengers, and the total number of units being produced. The RDT&E cost breakdowns are shown in Table 11-1. Figure 11-1 is a pie chart showing the cost breakdown in percentage of cost per phase. The RDT&E cost for any number of units within the aircraft families is going to be the same in this phase of the design because only the total number of airplanes is used.

Table 11-1: RDT&E Cost Breakdown (in millions of year 2004 USD)

RDT&E Category	Cost
Airframe Engineering & Design	\$153.96
Development Support & Testing	\$64.74
Flight Test Airplanes	\$1,312.49
Flight Test Operation	\$30.16
Test & Simulation	\$187.36
Finance Fees	\$234.20
Total RDTE Cost =	\$1,982.91

**Figure 11-1: RDT&E Cost Percentage**

11.3 Manufacturing Cost

Manufacturing cost is further broken down into the following sections: Airframe Engineering & Design, Airplane Production, Production Flight Test Operation Cost, and Cost of Financing Manufacturing phase.

Manufacturing cost was determined using the parameters from the RDT&E phase, the total number of airplanes produced, and the airplane production rate. A detailed summary of the manufacturing cost is shown in Table 11-2.

Table 11-2: Manufacturing Cost (in millions of year 2004 USD)

Manufacturing Category	150 Units	500 Units	1500 Units
Airframe Engineering & Design	\$111.80	\$175.13	\$247.63
Airplane Production	\$4,095.69	\$9,519.17	\$20,855.09
Production Flight Test Operation	\$11.37	\$37.90	\$113.70
Financing Fees	\$632.83	\$1,459.83	\$3,182.46
Total Manufacturing Cost =	\$4,851.69	\$11,192.02	\$24,398.88

11.4 Total Flyaway Cost

The acquisition cost, or flyaway cost, is the amount of capital required to purchase an entire production run. The acquisition cost consists of three parts: RDT&E Cost, Manufacturing cost and profits. Table 11-3 shows acquisition cost for an entire production run of 150, 500, and 1500 aircraft.

Table 11-3: Flyaway Cost (in millions of year 2004 USD)

Flyaway Category	150 Units	500 Units	1500 Units
RDTE	\$1,982.91	\$1,982.91	\$1,982.91
RDTE Profits	\$312.27	\$312.27	\$312.27
Manufacturing	\$4,851.69	\$11,192.02	\$24,398.88
Manufacturing Profits	\$843.77	\$1,946.44	\$4,243.28
Total Flyaway Cost =	\$7,990.65	\$15,433.65	\$30,937.35

11.5 Differentiating Consumer and Government Cost

Unit cost is divided into two parts: airline cost and direct government cost. A weight-cost method was developed to determine the government's contribution towards each aircraft purchase. The weight-cost method determined the cost of one pound of aircraft. Then, the government contribution is found as a function of weight added or removed from the aircraft plus additional labor costs.

Secondary mission tailored parts such as larger than regular landing gear, cargo door, countermeasures and the avionics are installed during original equipment manufacturing (OEM). This is what constitutes direct government cost. Table 11-4 shows the acquisition cost break up between the

airline and the government for -100 series. The secondary mission capable aircraft is designed only for the -100 series.

Table 11-4: Government and Airline Acquisition Costs per Unit (in millions of year 2004 USD)

	150 Units	500 Units	1500 Units
Government	\$3.42	\$2.01	\$1.34
Costumer	\$53.25	\$30.86	\$20.62
<i>Total Acquisition Cost =</i>	\$56.67	\$32.87	\$21.96

The increase in flyaway cost and direct operating cost that is incurred by designing for the secondary mission will be subsidized by the government with the understanding that the government may commandeer the aircraft when necessary. Table 11-5 shows direct operational cost breakdown for customer and government.

Table 11-5: Breakdown of Operational Costs between Airline and Government (in year 2004 USD)

Operational Cost Category	Airline	Government
Crew Cost	\$352.21	n/a
Fuel, Oil and Lubrication Cost	\$661.02	\$42.19
Insurance Cost	\$41.21	\$2.63
Maintenance Cost	\$461.92	\$29.48
Interest Cost	\$434.32	n/a
Miscellaneous Cost	\$127.13	\$8.11
Total DOC	\$2,077.81	\$82.42
Total IOC	\$1,246.68	\$49.45
<i>Total Operation Cost =</i>	\$3,324.49	\$131.88

12 Conclusion

Firefly's design meets and exceeds the RFP requirements set out by the AIAA. Firefly's 1-2-3 combination is unprecedented: Upper Surface Blowing allows for extremely short takeoffs and landings; the strut allows for a more efficient wing at cruise, and the forward swept wings provide better control during slow speeds. Easy conversion between primary and secondary missions makes the Firefly an attractive option for both commercial and government customers.

Table 12-1 lists major RFP requirements, broken down between the primary and secondary mission, with a reference to where the requirements are addressed in this report.

Table 12-1: Major RFP Requirements

Requirement	Met?	Page #
Primary Mission		
Takeoff and Landing Balanced Field Length $\leq 2,500$ ft	YES	52
Cruise Speed ≥ 400 knots to 1500 nm block range	YES	55
Conduct SNI approach with Engine out and in IMC Cat 3C conditions	YES	48
Meet FAR 36 Noise Limits	YES	44
Design for future expansion to 65 and 81 passenger models	YES	26
Secondary Mission		
Convertible from regional jet to government use model	YES	23
Takeoff and Landing Balanced Field Length $< 2,000$ ft	YES	52
Cruise Speed ≥ 400 knots to 750 nm block range, with return flight	YES	55
Land in a 25 knot crosswind with 5 knot tailwind component	YES	49

References

- 1-1. Babikian, R., S. P. Lukachko and I. A. Waitz, "The Historical Fuel Efficiency Characteristics of Regional Aircraft from Technological, Operational, and Cost Perspectives," MIT, Department of Aeronautics and Astronautics.
- 1-2. American Institute of Aeronautics and Astronautics. 2003/2004 AIAA Foundation: Undergraduate Team Aircraft Design Competition. *Request for Proposal*. <http://www.aiaa.org/>.
- 1-3. "Jones Four Star Arrival." American Institute of Aeronautics and Astronautics. <http://www.aiaa.org/education/students/Jonez.pdf>.
- 2-1. Aerospace Technology, 2004. <http://www.aerospace-technology.com>.
- 2-2. Raymer, Daniel P. *Aircraft Design: A Conceptual Approach*, Chapter 5. AIAA. 1999.
- 2-3. Nicolai, Leland, *Fundamentals of Aircraft Design*, METS, Inc. San Jose, CA. 1975.
- 3-1. Filippone, A. "Aerodynamic Database," 2004. <http://aerodyn.org/HighLift/tables.html>.
- 3-2. Bertin, J.J. and Smith, M.L. *Aerodynamics for Engineers*. 4th ed. Prentice Hall. 2001.
- 3-3. Raymer, Daniel P. *Aircraft Design: A Conceptual Approach*, Chapter 4. AIAA. 1999.
- 3-4. RAM Aircraft, Waco Texas. <http://www.ramaircraft.com/PricePages/Winglets/winglets.htm>.
- 3-5. Nicolai, Leland, *Fundamentals of Aircraft Design*, METS, Inc. San Jose, CA. 1975.
- 3-6. Wimpess, John K. and Conrad F. Newberry, *The YC-14 STOL Prototype: Its Design, Development, and Flight Test*, AIAA, 1998.
- 3-7. Cochrane, John A, Riddle, Dennis W., Stevens, Victor C, and Shovlin, Michael D. "Selected Results from the Quiet Short-Haul Research Aircraft Flight Research Program" AIAA paper 81-2625R.
- 3-8. Japan Aerospace Exploration Agency, 2003. <http://www.nal.go.jp/flight/eng/Museum/ASKA/aska.html>.
- 3-9. Kamofov, Vladimir. Aviation International News, August 2001. http://www.ainonline.com/issues/08_01/08_01_antonovan74pg65.html.
- 3-10. Grasmeyer, J.M., Naghshineh_Pour, A., Tetrault, P.-A., Grossman, B., Haftka, R.T., Kapania, R.K., Mason, W.H., Schetz, J.A., "Multidisciplinary Design Optimization of a Strut-Braced Wing Aircraft with Tip-Mounted Engines," MAD 98-01-01, 1998.
- 3-11. Redeker, G., Wichmann, G., "Forward sweep - A favourable concept for a laminar flow wing," AIAA Design, Systems and Operations Meeting, Sept. 7-9, 1988, AIAA paper 88-4418.
- 3-12. Aerospace Technology, 2004. <http://www.aerospace-technology.com>.

- 4-1. Sleeman, William C. Jr, and Hohlweg, William C. "Low-Speed Wind-Tunnel Investigation of a Four-Engine Upper Surface Blown Model Having a Swept Wing and Rectangular and D-Shaped Exhaust Nozzles" NASA TN D-8061, Dec. 1975.
- 4-2. Cochrane, John A, Riddle, Dennis W., Stevens, Victor C, and Shovlin, Michael D. "Selected Results from the Quiet Short-Haul Research Aircraft Flight Research Program" AIAA paper 81-2625R.
- 4-3. Mason, W.H., *Configuration Aerodynamics*, Chapter 7.
http://www.aoe.vt.edu/~mason/Mason_f/ConfigAero.html.
- 4-4. Ko, Andy, Mason, William H., and Grossman, Bernard. "Transonic Aerodynamics of a Wing/Pylon/Strut Juncture." AIAA paper 2003-4062.
- 4-5. Mark Drela, MIT Computational Aerospace Sciences Laboratory
- 4-6. Raymer, Daniel P. *Aircraft Design: A Conceptual Approach*. Chapter 18.
- 4-7. Roskam, Jan, *Airplane Design Part IV*. DARCorporation. 1999.
- 5-1. General Electric Company, 2004. <http://www.geae.com/engines/commercial/cf34/cf34-10.html>.
- 5-2. General Electric Company, 2004. <http://www.geae.com/engines/commercial/cfm56/index.html>.
- 5-3. Honeywell, 2002. http://www.honeywellaerospaceservices.com/tfe_after/prod_specs.html.
- 5-4. Rolls-Royce, 2004. <http://www.rollsroyce.com/civil/products/turbofans/ae3007/Default.htm>.
- 5-5. Pratt and Whitney Canada Corp. 2003. http://www.pwc.ca/en/3_0/3_0_2/3_0_2_3_1.asp.
- 5-6. Sleeman, William C. Jr, and Hohlweg, William C. "Low-Speed Wind-Tunnel Investigation of a Four-Engine Upper Surface Blown Model Having a Swept Wing and Rectangular and D-Shaped Exhaust Nozzles" NASA TN D-8061, Dec. 1975.
- 5-7. Cochrane, John A, Riddle, Dennis W., Stevens, Victor C, and Shovlin, Michael D. "Selected Results from the Quiet Short-Haul Research Aircraft Flight Research Program" AIAA paper 81-2625R.
- 6-1. Kay, J. et. al. , "Control Authority Issues in Aircraft Conceptual Design," VPI-Aero-200, 1993.
- 6-2. *Military Specification: Flying Qualities of Piloted Aircraft*. MIL-F-8785C
- 6-3. Hindson, W. S., Hardy, G. H., Innis, R. C., "Flight-Test Evaluation of STOL Control and Flight Director Concepts in a Powered Lift Aircraft Flying Curved Decelerating Approaches." NASA TP 1641, March 1981.
- 6-4. "All about GPS." Trimble. <http://www.trimble.com/gps>.
- 7-1. Roskam, Jan. *Airplane Design Part VII*. DARCorporation. 1999.
- 7-2. Anderson, John. *Aircraft Performance and Design*. McGraw Hill, 1999.

- 8-1. Efundu, 2004. <http://www.efunda.com/materials/alloys/aluminum/aluminum.cfm>
- 8-2. Reade Advanced Materials, 1997. www.reade.com. Last updated 28 Dec 2003.
- 8-3. Katz, Joshua. "Emerging Aerospace Materials: Aluminum Lithium." Presentation. 11 Nov 2001.
- 8-4. MEE433B Aluminum-Lithium Alloys. Queens University. <http://me.queensu.ca/courses/mech412/Notes/aluminum-lithium.doc>
- 8-5. http://www.centennialofflight.gov/essay/Evolution_of_Technology/composites
- 8-6. MatWeb Material Property Data, 2004. www.matweb.com
- 8-7. Niu, Michael C.Y. *Airframe Structural Design*. Conmilit Press Ltd, 1988. Burbank, California.
- 8-8. Gundlach IV, J., Tetrault, P., Gern, F., Nagshineh-Pour, A., Ko, A., Schetz, J., Mason, W., Kapania, R., Grossman, B., and Haftka, R. (2000) Multidisciplinary Design Optimization of a Strut Braced Wing Transonic Transport. AIAA 2000-0420.
- 8-9. Raymer, Daniel P. *Aircraft Design: A Conceptual Approach*. Chapter 15. AIAA. 1999.
- 9-1. Garmin G1000. Garmin Ltd. 2004. <http://www.garmin.com/products/g1000>
- 9-2. Thompson, D.B.. Fly-by-Light II. <http://www.spie.org/web/meetings/calls/denver/thompson.html>
- 9-3. Brown, Alan. Actuator Research Complete. NASA Dryden X-Press. <http://www.dfrc.nasa.gov/Newsroom/X-Press/1999/Jan15/actuator.html>
- 9-4. Honeywell Advanced Flight Controls
:<http://www.cas.honeywell.com/ats/products/flightcontrol.cfm>
- 9-5. "A Cool Tool for Deicing Planes." <http://www.nasatech.com/Spinoff/spinoff2001/ps5.html>.
- 9-6. Enhanced Ground Proximity Warning System. <http://www.egpws.com/>.
- 10-1. Roskam, Jan. *Airplane Design Part I*. DARCorporation. 1999.
- 10-2. Roskam, Jan. *Airplane Design Part V*. DARCorporation. 1999.
- 11-1. Roskam, Jan. *Airplane Design Part VII*. DARCorporation. 1999..
- 11-2. Raymer, Daniel P. *Aircraft Design: A Conceptual Approach*. Chapter 18. AIAA. 1999.